Journal of Systematic Palaeontology, Vol. 10, Issue 4, December 2012, 679–723

Taylor & Francis
Taylor & Francis Group

A systematic revision of the Upper Ordovician trilobite genus *Bumastoides* (Illaenidae), with new species from Oklahoma, Virginia and Missouri

Jesse R. Carlucci[a]*, Stephen R. Westrop[a], Lisa Amati[b], Jonathan M. Adrain[c] and Robert E. Swisher[a]

[a]*Oklahoma Museum of Natural History and School of Geology, University of Oklahoma, Norman, OK 73072, USA;* [b]*Department of Geology, State University of New York at Potsdam, Potsdam, New York 13676, USA;* [c]*Department of Geoscience, University of Iowa, 121 Trowbridge Hall, Iowa City, Iowa 52242, USA*

(Received 28 March 2011; accepted 13 July 2011; printed 5 December 2012)

Species of the Ordovician illaenid trilobite genus *Bumastoides* Whittington, 1954, have been notoriously difficult to classify because of their high degree of exoskeletal effacement. New species from Oklahoma (*B. graffhami* sp. nov), Virginia (*B. moundensis* sp. nov) and Missouri (*B. kimmswickensis* sp. nov) provide more data for a phylogenetic analysis of the genus. Continuous characters were analysed with finite mixture coding in two separate parsimony analyses. A strict consensus tree of eight equally most parsimonious trees, and a weighted best-fit tree both indicate that many species previously assigned to *Bumastoides* should be removed from the genus. Both methods yielded a tree with similar topology, supporting the removal of three *Stenopareia*-like species from *Bumastoides*. Based on the optimized character distribution, the supporting synapomorphies for *Bumastoides* are: weak to effaced cranidial axial furrow and lack of glabellar differentiation even by change in convexity, dicuspid inner margin of pygidial doublure, subtrapezoidal pygidium, undifferentiated or minimally expressed pygidial axis, long pygidial doublure, and maximum pygidial width at half-length. The pygidial outline shape, length of pygidial doublure, and degree of independent convexity on the cranidium are characters that may be useful in separating species of *Stenopareia* and *Bumastoides*.

Keywords: *Bumastoides*; *Stenopareia*; systematics; cladistics; continuous characters; Ordovician

Introduction

The Ordovician (Darriwilian–Hirnantian) illaenid trilobite genus *Bumastoides* was originally erected by Whittington (1954) as a subgenus of *Bumastus* Murchison, 1839. The former has, among other characters, fainter axial furrows, a distinctive lunette, proportionally smaller palpebral lobes, and 8–10 segments in the thorax. Ludvigsen & Chatterton (1980) elevated *Bumastoides* to full generic status, and placed the genus in the Illaeninae. Later workers (e.g. Whittington 1997a) cited thoracic morphology to reiterate that *Bumastoides* is an illaenid, rather than a styginid (as is *Bumastus*). Although the taxonomic position of *Bumastoides* itself is currently well constrained, recognizing taxonomic divisions within the genus has been problematic. The extremely high level of exoskeletal effacement makes discrete differences difficult to identify, resulting in species diagnoses that are not truly diagnostic. Shape differences that describe variation along a curve, for instance, are often relative, and not easily binned into discrete character states. Chatterton & Ludvigsen (1976, p. 35) considered imperceptible axial furrows, prominent lunettes, a steeply curved anterior cephalic profile, absence of a median pustule, and an ovate to rounded subpentagonal pygidium to be diagnostic characters of *Bumastoides lenzi*. While undoubtedly characteristic of *B. lenzi*, the same combination of characters can also be used to describe other *Bumastoides* species. The vague diagnoses of illanid genera closely related to *Bumastoides* (e.g. *Stenopareia* Holm, 1886; the most recent diagnosis is given by Curtis & Lane 1997, p. 18) further exacerbates the problem of distinguishing between the taxa. Certain species could be placed in either *Bumastoides* or *Stenopareia* according to current diagnoses. These issues, combined with new species data from the Sandbian–Katian interval, demonstrate the need for a systematic revision of *Bumastoides*. Ideally, any revision of the genus should effectively deal with the difficulties inherent in diagnosing species, and that is the approach taken here.

A cladistic analysis allows the relationships of ingroup *Bumastoides* to be explored, and character optimization provides discrete apomorphies with which to construct new diagnoses. Finite mixture coding (FMC) (Strait *et al*. 1996) allows for subtle differences in quantitative characteristics to be binned into discrete states, and is contrasted with a method that treats continuous characters as such (Goloboff *et al.* 2006). The optimized character distribution is

*Corresponding author. Email: jesse.r.carlucci-1@ou.edu

ISSN 1477-2019 print / 1478-0941 online

http://dx.doi.org/10.1080/14772019.2011.637518
http://www.tandfonline.com

synthesized with descriptions and diagnoses of previously documented *Bumastoides* species (including types) and new material from the Upper Ordovician (Sandbian–Katian) of Oklahoma, Virginia and Missouri.

Geologic setting of new material

Oklahoma

The Bromide Formation (Ulrich 1911) is an Upper Ordovician (Sandbian; Turinian) carbonate-dominated succession that is the youngest unit of the Simpson Group (Cooper 1956; Harris 1957). It is exposed throughout the Arbuckle Mountains and Criner Hills region of south-central Oklahoma (see Fay *et al*. 1982, fig. 77; Carlucci *et al*. 2010, fig. 1), and was deposited along a depth gradient from the Arbuckle Platform up-ramp, to the subsiding Southern Oklahoma aulacogen down-ramp (Longman 1982a, b) (Fig. 1A). Siliclastic material is common in the stratigraphically lower Mountain Lake Member (Cooper 1956), often forming metre-scale cyclic packages with bryozoan- and pelmatozoan-rich wackestone, packstone and grainstone. Cycle tops are commonly mineralized, starved surfaces, often associated with bryozoan rudstone horizons. Up-ramp, the younger Pooleville Member is characterized by massive to thickly bedded carbonate mudstone, wackestone and grainstone, with reworked tempestites commonplace. A thin cap of peritidal carbonate is referred to as the Corbin Ranch Submember (Harris 1957; Amsden & Sweet 1983). Down-ramp, the Pooleville is composed of fine-grained, thickly bedded, laminated carbonate mudstone, and resembles the overlying Viola Formation. Shaw (1974) and Carlucci *et al.* (2010) present discussions of the trilobite fauna of the Bromide.

Three localities in the Bromide Formation yielded material of *Bumastoides graffhami* sp. nov. Tyson's Quarry (TQ) is a private quarry approximately 8 km south-west of Ardmore (Fig. 1A) in the Criner Hills region of Carter County (Carlucci *et al.* 2010). The type specimen of *B. graffhami* was collected from the upper Pooleville Member, in an interval of rudstone pavements (interpreted here as tempesites) that top blue massive carbonate wackestone (see Carlucci *et al.* 2010, fig. 2 for a measured section and approximate collection levels). Shaw (1974) assigned this material to the nearby Rudd Quarry, but the original label specifies the "upper" quarry (TQ here, formerly the Dunn quarry). The Daube Ranch (DRa) (formerly the Johnston Ranch) locality (Fig. 1A) exposes the Bromide Formation along Spring Creek, below the dam forming the upper Humbolt Lake in Murray County. The *B. graffhami* material was collected 21.3 m below the Viola contact, in a light tan, thinly bedded wackestone (with localized packstone) that alternates with fissile tan shale (see Fay *et al.* 1982, p. 336 for a detailed measured section). The final locality is a roadcut along US Highway 177 at its intersection with Goddard Youth Road (Fig. 1A), approximately 13 km

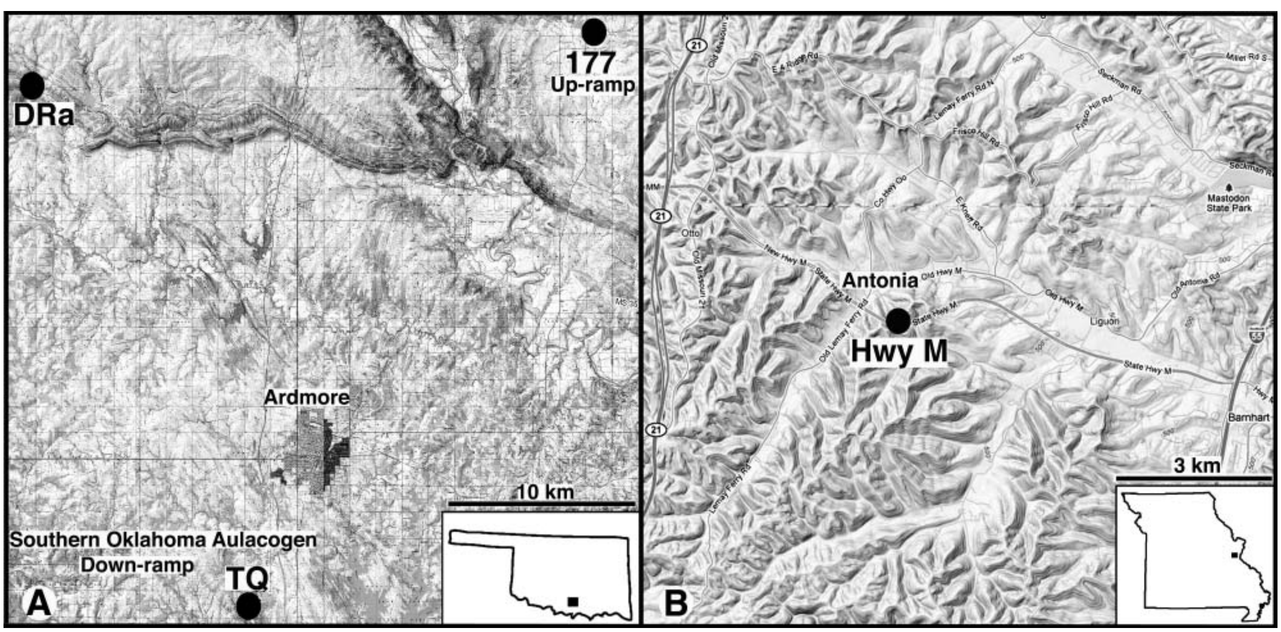

Figure 1. A, Oklahoma locality map, 177, 34.405 lat, 96.950 long, UTM NAD27 14S 0688414, 3808808, Daube (Johnston) Ranch (DRa), 34.377 lat, 97.321 long, UTM NAD27 14S 0654400, 380508085, coordinates for Tyson's Quarry (TQ) are withheld at the request of the quarry owner. **B,** Missouri locality map, Hwy M, 38.359 lat, 90.465 long, UTM NAD27 15S 0721533 4248502. Virginia localities are not shown as they have been illustrated elsewhere (Read 1982, fig. 1; Carlucci *et al.* 2010, fig. 3–2). The coordinates for I-77 are 37.745 lat, 79.513 long, UTM NAD27 17S 630905, 4178443, PQ is 36.878 lat, 81.681 long, UTM NAD27 17S 439250, 4081420.

south of the town of Sulphur, Murray County. The material of *B. graffhami* was collected at two levels (Fig. 2). The lower collection is from thinly interbedded marly shale and wackestone. The shale layers thin very slightly upwards, and the percentage of bioclasts increases upwards in the wackestone. The upper collection is from an interbedded laminated carbonate mudstone, and brachiopod-rich fossiliferous wackestone. Rudstone pavements often cap the wackestone beds, and are likely coeval with the pavements at TQ from which the type specimen was collected.

Sclerites assigned to *Bumastoides* cf. *milleri* (Billings, 1859) were collected from the Viola Springs Formation (Viola Group; Upper Ordovician, Katian) at the Highway 99 section, near Fittstown, south-central Oklahoma (Amati & Westrop 2004, fig. 1, 2006, figs 3 and 7). They occur in a bryozoan grainstone-to rudstone facies (Amati & Westrop 2006, p. 521) between 18 and 34 m above the base of the Viola Springs Formation.

Virginia

All material of *Bumastoides moundensis* sp. nov is from either the Effna Formation or the Botetourt limestone (Cooper & Cooper 1946) in the Valley and Ridge Province of Virginia (Read 1982, fig. 1). The Effna Formation was deposited in downslope carbonate mud-mound buildups that are composed of a series of biohermal pods flanked by grainstone (see Read 1998, fig. 4). These buildups form primarily by marine cementation and baffling of carbonate fines by bryozoans and pelmatazoans, with frame building organisms of little importance (Read 1982; King 1986). The first (often-pod surrounding) unit of the Effna is a biostromal grainstone, which formed as debris was shed from the mudstone pods (Sabol 1958; Ruppel & Walker 1977; Read 1982). The other unit is the biohermal mudstone of the buildups, which is the primary constituent of the pod facies. Both units are highly fossiliferous; Carlucci *et al.* (2010) provided a list of trilobite genera commonly found in the Effna. The Botetourt limestone is a dark, shaly, nodular wackestone, packstone and grainstone that flanks, interfingers with, and overlies the Effna. The Botetourt is considered to be transitional between the Effna and the basinal Liberty Hall facies (Read 1982).

Two localities provided new material of *Bumastoides moundensis*. Porterfield Quarry (PQ) is an abandoned facility located 7 km south-west of Saltville, in Smyth County. The quarry is exposed approximately 1 km down an unlabelled service road off VA 610 (see Carlucci *et al.* 2010, fig. 3-2 for a locality map). The PQ collections (Carlucci *et al.* 2010, fig. 3-1) are from boulders of biohermal mudstone left behind when the quarry ceased operation. The mudstone is massive and very fine grained with bryozoans locally forming boundstone. Additional *B. moundensis* material was collected from a roadcut along Interstate 77 near the town

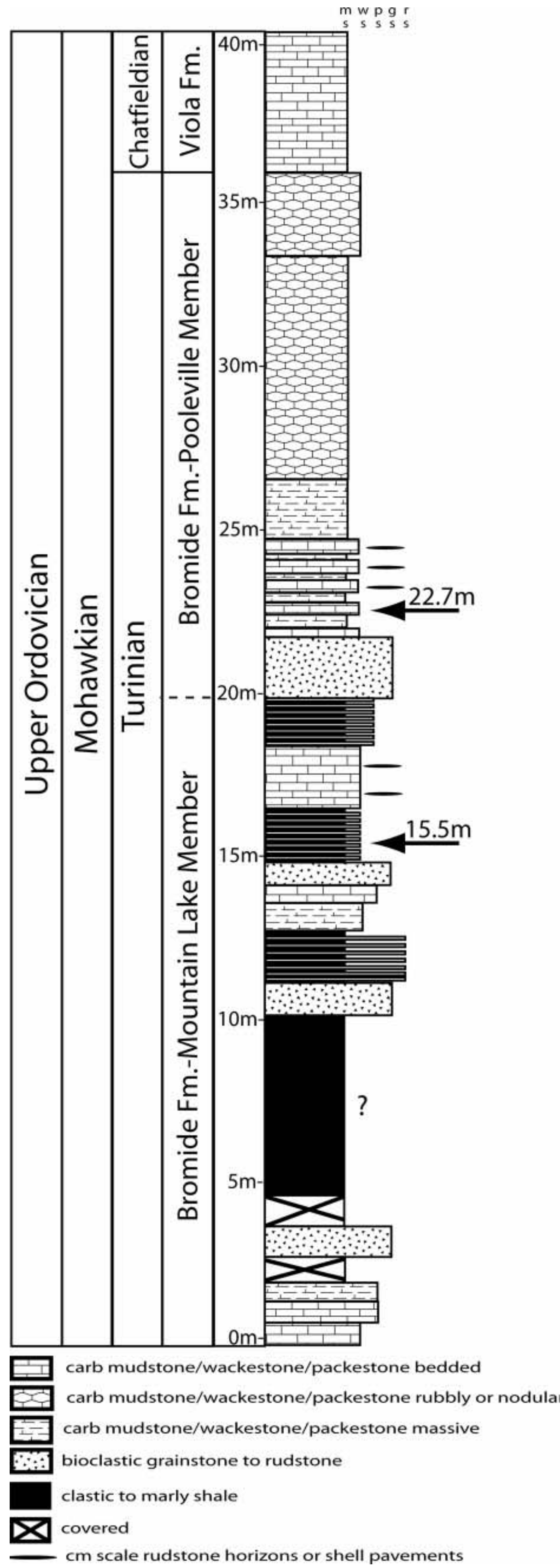

of Bland in Bland County. The roadcut is less than 1 km north of the Big Walker Mountain Tunnel exit. The material was collected from 1 metre above the Effna/Botetourt contact in a black, nodular wackestone. See Read (1982, fig. 7A) for a facies mosaic; 'nodular, shaly skeletal limestone' is here referred to as the Botetourt.

Missouri and Illinois

Archival material from Missouri that was described by Bradley (1930) and assigned here to *B. billingsi* (Raymond & Narraway, 1908) was collected from the Upper Ordovician (Katian) 'Kimmswick Limestone' (now Dunleith Formation of the Kimmswick Subgroup; Templeton & Willman 1963) along the Mississippi River at Batchtown, Illinois, and Glen Park, Missouri (Bradley 1925). New material of *B. kimmswickensis* sp. nov. is from a previously undocumented roadcut along Missouri State Highway M, 0.5 km south of Antonia and about 6 km west of its intersection with Interstate 55 at Barnhart (Fig. 1B). The trilobite occurs at a single horizon 90 cm above the base of the Dunleith Formation, within a 44 cm thick interval of grey shale with bioclastic packstone lenses and lime mudstone nodules; the House Springs Bentonite (Kolata *et al.* 1998, figs 5, 8) forms the basal 8 cm of this interval.

Phylogenetic analysis

Taxonomic notes

The analysis used 16 ingroup species and one outgroup species, of which 15 have been classified previously as *Bumastoides*, and two as *Stenopareia* Holm, 1886. *Stenopareia* is an illaenid genus that is considered to be closely related to *Bumastoides* because it also exhibits a high degree of exoskeletal effacement, has prominent lunettes, and an inflated, highly convex cranidium with the eyes positioned just forward of the posterior border. The type species of *Stenopareia*, *S. linnarssoni* Holm, 1882, was chosen as the outgroup taxon because its morphology has been well documented and it occupies a relatively basal position within *Stenopareia*. The pygidia of species of *Stenopareia* are clearly distinct from those of *Bumastoides* (subsemicircular, with faint expression of the axis), and they possess more pronounced axial furrows over all three tagmata.

Whiteley *et al.* (2002) treated *Bumastus globosus* Billings, 1859 as a species of *Bumastoides*, though it has never formally been placed in the genus. Based on evaluation of the lectotype (GSC1090b; Shaw 1968, pl. 17, figs 20–22, 24) and hypotypes, this species does not belong to *Bumastoides*, and was not used in our analysis. The deeply incised axial furrows (Shaw 1968, pl. 17, fig. 15), wide cephalic axis, and highly convex thoracic axis are unlike any species of *Bumastoides*, and Westrop & Ludvigsen (1983) placed it in *Stenopareia*. All species formally named as *Bumastoides* were considered for inclusion, but some were omitted from the analysis because the known material is too incomplete to code properly (e.g. *B. scoticus* Tripp, 1965; *B. fornax* Tripp, 1980; *B. tricuspidatus* Edgecombe *et al*., 2006). *Bumastoides rivilus* was the only Scottish species included. The types of other Scottish species placed in *Bumastoides* (*B. fornax* Tripp, 1980, pl. 1, figs 6–10; *B. scoticus* Tripp, 1965) were borrowed by us, but both were far too damaged and incomplete to code for the parsimony analysis. The type material of *B. fornax* is so badly damaged that we would hesitate to identify it to genus level. *Bumastus lioderma* Raymond, 1925 may belong to *Bumastoides*, but is only known from a partial cranidium, so it cannot be adequately assessed phylogenetically.

Characters and coding

The dataset includes 20 unordered characters (10 binary, 10 multistate) with a total of 52 states (see Online Supplementary Material Appendix 1). These characters code morphological features of the cranidium (seven characters), thorax (two characters) and pygidium (11 characters). All characters were binned into their states based on clearly discrete differences or statistically defined bins (see Finite Mixture Coding below). Characters that could not reliably be placed into discrete categories, parsimony uninformative characters, or those that dramatically covary with each other were removed in the initial analysis. A second analysis (20 discrete, six measured) retained continuous characters (Online Supplementary Material Appendix 2) that could not be discretized (Goloboff *et al.* 2006). There is some small degree of covariation in the pygidial characters. For example, the location of maximum (tr) width has some bearing on the overall pygidial shape, but is only one component of a more complex feature. In all such instances the characters code differently from each other. Characters with inapplicable states for some species were coded using

←

Figure 2. Stratigraphical section of the 177 locality showing the upper Mountain Lake and Pooleville Members (lower Mountain Lake not shown) of the Bromide Formation. Arrows denote collection levels. Question mark (?) indicates uncertainty associated with the continuity of the shale. Key to abbreviations: ms, mudstone; ws, wackestone; ps, packestone; gs, grainstone; rs, rudstone.

→

Figure 3. Results of the finite mixture coding (FMC). Each model number refers to the number of normal distributions being evaluated (e.g. model one is one normal distribution). The relative AIC score is the goodness of fit of that model using Aikake Information Criterion (Akaike 1974). The weight is the probability of that model being correct relative to the other models. The *x*-axis is the percentile result of that ratio character; the *y*-axis is the number of taxa. The program FMCBox (Sheets 2003) was used for all calculations. See text for explanation of the characters.

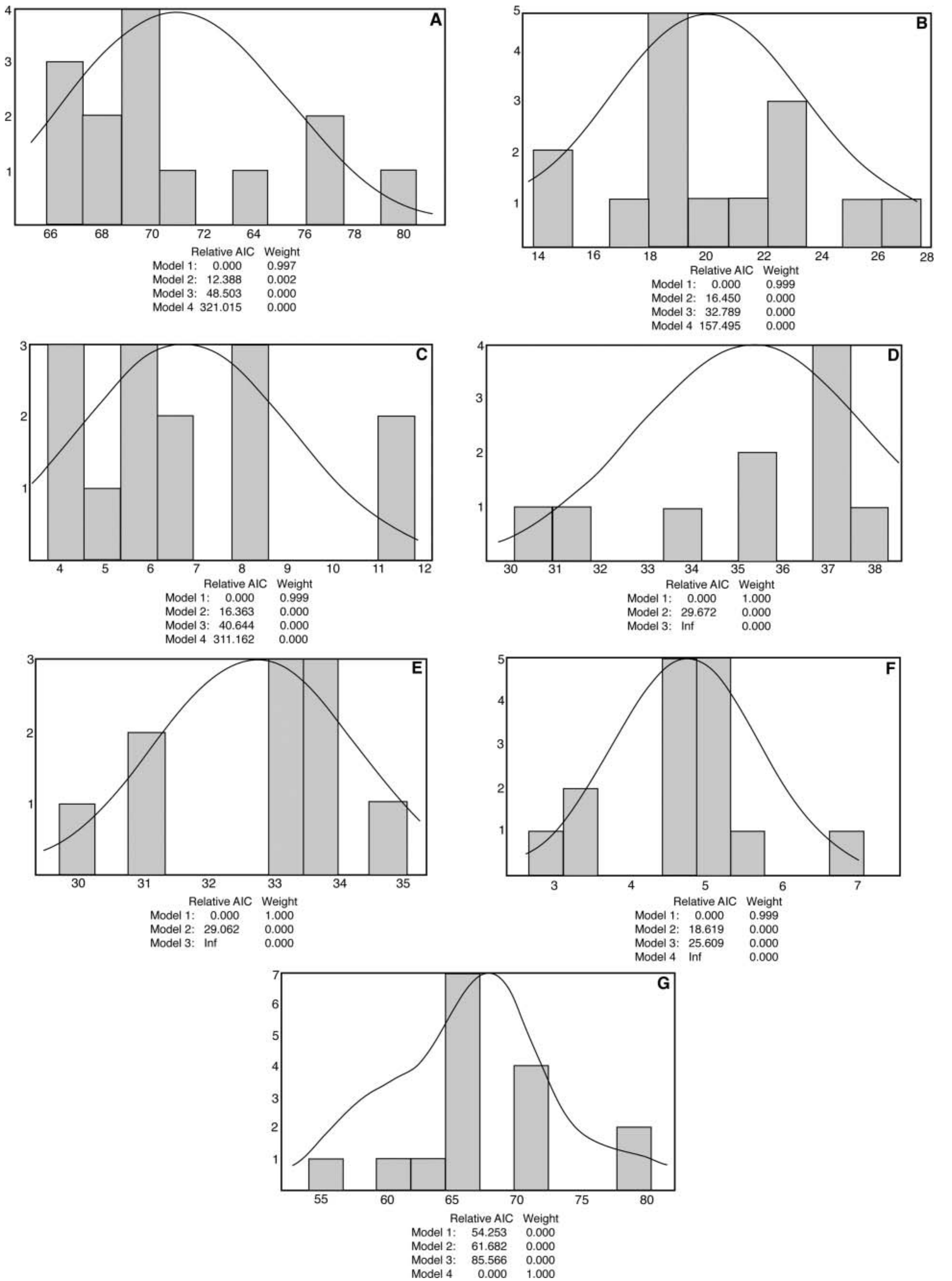
A
Relative AIC Weight
Model 1: 0.000 0.997
Model 2: 12.388 0.002
Model 3: 48.503 0.000
Model 4 321.015 0.000
B
Relative AIC Weight
Model 1: 0.000 0.999
Model 2: 16.450 0.000
Model 3: 32.789 0.000
Model 4 157.495 0.000
C
Relative AIC Weight
Model 1: 0.000 0.999
Model 2: 16.363 0.000
Model 3: 40.644 0.000
Model 4 311.162 0.000
D
Relative AIC Weight
Model 1: 0.000 1.000
Model 2: 29.672 0.000
Model 3: Inf 0.000
E
Relative AIC Weight
Model 1: 0.000 1.000
Model 2: 29.062 0.000
Model 3: Inf 0.000
F
Relative AIC Weight
Model 1: 0.000 0.999
Model 2: 18.619 0.000
Model 3: 25.609 0.000
Model 4 Inf 0.000
G
Relative AIC Weight
Model 1: 54.253 0.000
Model 2: 61.682 0.000
Model 3: 85.566 0.000
Model 4 0.000 1.000

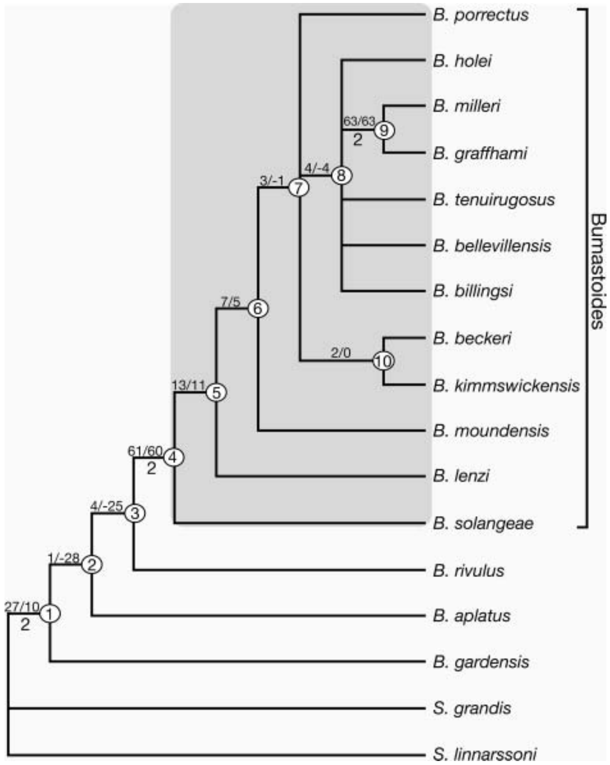

Figure 4. Strict consensus tree of the eight MPTs retained from the first parsimony analysis, with recommended taxonomy of *Bumastoides*; *B. rivulus*, *B. aplatus* and *B. gardensis* are here placed in *Stenopareia sensu lato*. Tree length is 56 steps, CI is 0.57, RI is 0.69, and RC is 0.40. The first number displayed on the top of branches is the symmetric resampling support value for the successive node; the second number is the GC value. The numbers on the bottom of the branches are the Bremer Support (if greater than one) value for the successive node. Nodes are numbered for easy reference within the text.

reductive coding (Strong & Lipscomb 1999) (e.g. species with a completely effaced axial furrow in character 1 were not coded again in character 5); inapplicable states were coded as '?'. In *Bumastoides*, sculptural characters of the cranidium and pygidium are often decoupled (e.g. terrace lines on the cranidium are not always associated with lines on the pygdium, and vice versa), so similar sculptural characters (e.g. terrace lines) were coded independently on the two tagmata. Finally, some characters were omitted simply because the variation in preservation made it impossible to detect discrete states where they may have existed (e.g. the presence or absence of a pygidial articulating facet border, or the number of terrace lines on the thoracic articulating facets).

The simple morphology and furrow effacement in *Bumastoides* makes the use of continuous measured characters an attractive option. Some measured character data were taken from literature sources (*Bumastoides tenuirugosus* Troedsson, 1928; Westrop & Ludvigsen 1983; *Bumastoides lenzi* Chatterton & Ludvigsen, 1976; *Bumastoides solangeae* Hunda *et al*., 2003; *Stenopareia linnarssoni* Holm, 1882; Warburg 1925; *Stenopareia grandis* Billings, 1859; Chatterton & Ludvigsen 2004). Literature illustrations were only used if the orientation of the specimens was comparable to those used in our figures (Figs 6–26). The majority of measured data are taken from the material illustrated here and non-illustrated material of the same species in our collections. The proportions we used are those that can be confidently measured in a majority of species included in the analysis. To avoid large amounts of missing data, some measured features used in the systematic descriptions were not used in the analysis (e.g. proportion of eye length in lateral view). Material that has obviously been flattened (e.g. Fig. 19E) was not measured.

Finite mixture coding. We follow the approach developed in Strait *et al.* (1996), automated by the program FMC Box (Sheets 2003). This method identifies a number of possible normal distribution models that best describe the character data, and then uses the Aikake Information Criterion (AIC, Akaike 1974) to assess the goodness of fit for each model. The model with the lowest AIC score and the highest weight (probability of that model being correct compared to the others) is the optimal distribution for binning character states. Characters that show a high relative probability of a one-model distribution were removed from the analysis; others were binned into their respective distribution by a group probability assignment based on the magnitude of the normal function at the specimen value. Finite mixture coding (FMC) is a particularly good approach for binning measured character states here because it potentially allows for the isolation of discrete character data from a genus which otherwise has very few ingroup apomorphies. In six of the seven measured ratio characters, a one-distribution model was clearly best supported (Fig. 3A–F have AIC values of 0, and relative probability of a one distribution model being correct of > 99.7%). These characters were removed from the first analysis because their values cannot confidently be assigned to discrete bins: cranidial length (sag.) in proportion to width (tr.) across palpebral lobes (Fig.

Figure 5. A, optimized character distribution showing character states that change unambiguously on one of the eight MPTs from the first analysis. Black circles show synapomorphic character states, and white circles indicate homoplastic character states. Optimization was performed in PAUP* version 4.0b10 (Swofford 2002), and checked in TNT (Goloboff *et al*. 2008). **B,** the best tree found from a second parsimony analysis (implicit enumeration in TNT) that treated continuous characters as such. Implied weighting with a concavity constant (k) of three scaled characters contributions to branch length. The first number displayed to the left of branches is the symmetric resampling support value for the successive node; the second number is the GC value. Best-fit value is 8.47, CI is 0.53, RI is 0.62, and RC is 0.33 (excluding continuous data).

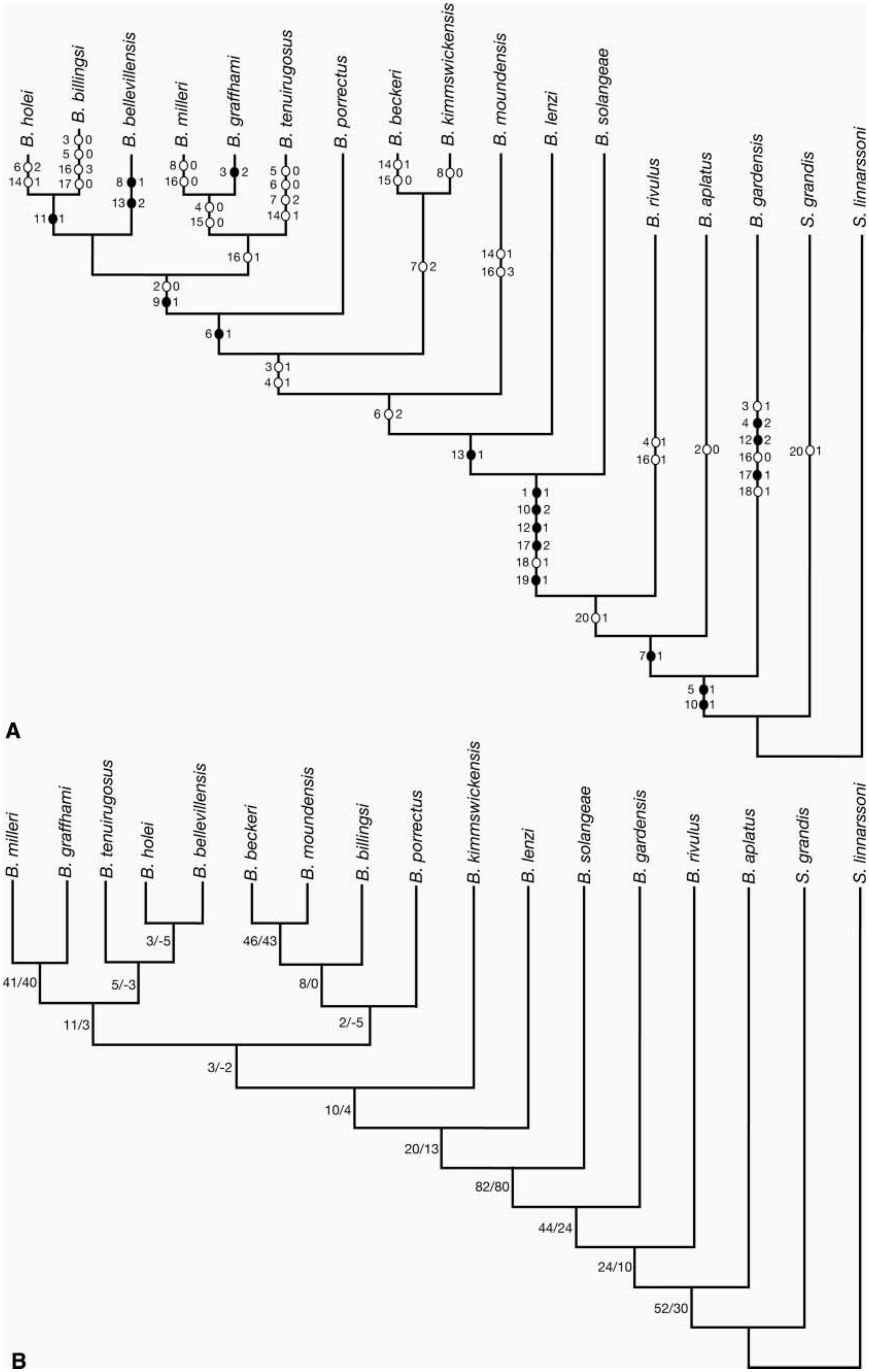
A
B. holei
B. billingsi
B. bellevillensis
B. milleri
B. graffhami
B. tenuirugosus
B. porrectus
B. beckeri
B. kimmswickensis
B. moundensis
B. lenzi
B. solangeae
B. rivulus
B. aplatus
B. gardensis
S. grandis
S. linnarssoni
B
B. milleri
B. graffhami
B. tenuirugosus
B. holei
B. bellevillensis
B. beckeri
B. moundensis
B. billingsi
B. porrectus
B. kimmswickensis
B. lenzi
B. solangeae
B. gardensis
B. rivulus
B. aplatus
S. grandis
S. linnarssoni
41/40
3/-5
5/-3
46/43
8/0
11/3
2/-5
3/-2
10/4
20/13
82/80
44/24
24/10
52/30

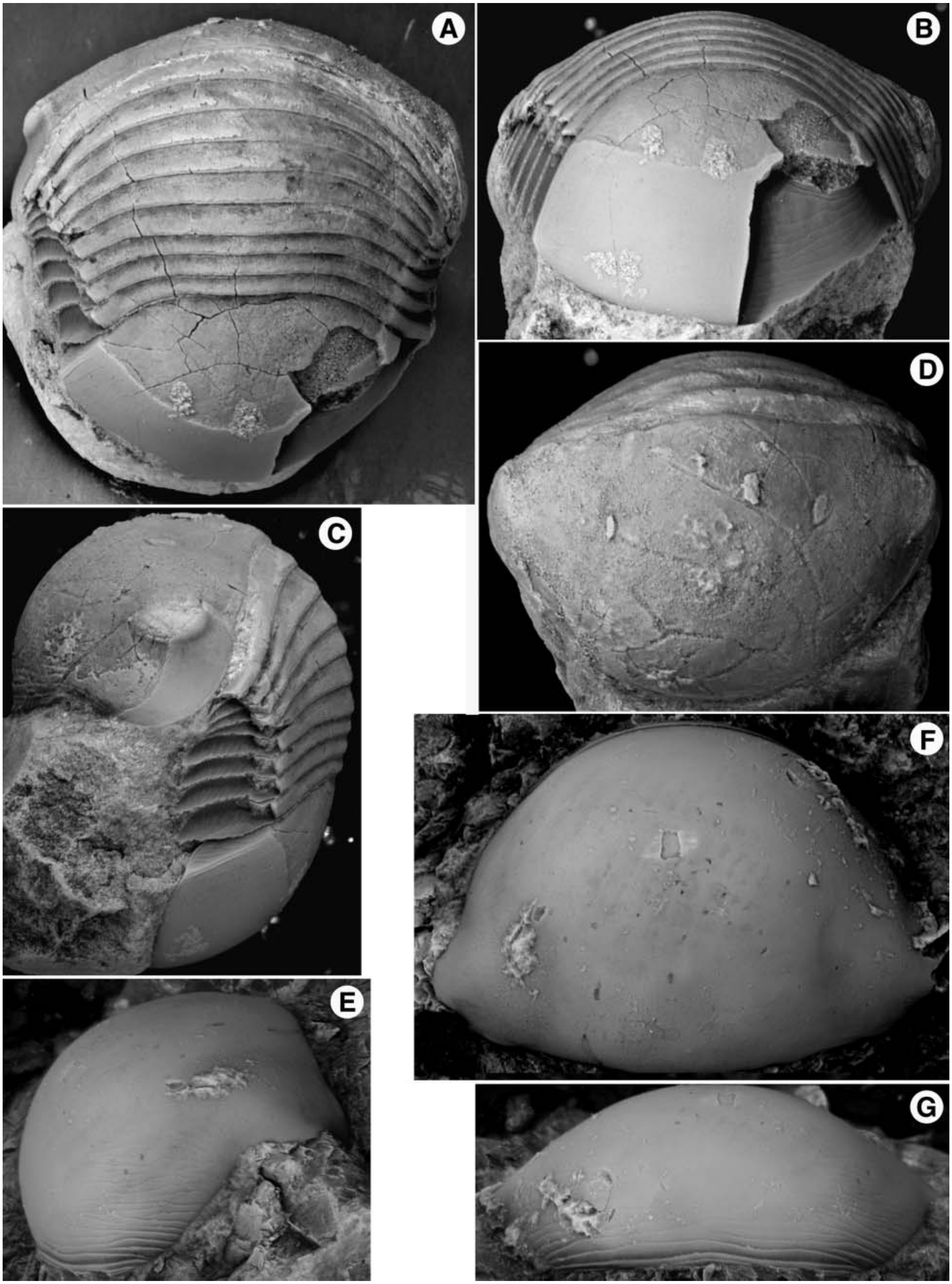
A
B
C
D
E
F
G

3A); maximum length (sag.) of lunettes in proportion to cranidial length (exsag.) in dorsal view (Fig. 3B); maximum width (tr.) of one lunette in proportion to width (tr.) across palpebral lobes (Fig. 3C); percentage of total exoskeletal length occupied by the cranidium (in lateral view) (Fig. 3D); percentage of total exoskeletal length occupied by the pygidium (in lateral view) (Fig. 3E); and width of one palpebral lobe as a percentage of cranidial width across palpebral lobes (Fig. 3F). The maximum length/width ratio of the pygidium best fits a four-distribution model (Fig. 3G) and it was retained for the first phylogenetic analysis. The inability of FMC to bin measured characters into more than one discrete state highlights the difficulty of diagnosing new species of *Bumastoides* with concrete, unequivocal evidence. We suggest that vague references to character proportions be omitted from diagnoses of new species (e.g. lunettes proportionally wide, long, etc.), and instead only be used for pairwise comparisons (e.g. *B. holei* has proportionally wider lunettes than *B. moundensis*). These data also show that measured characters with clear gaps in their distribution still best fit a one-bin model, suggesting that some workers may be overestimating the utility of measured characters (unless they are treated as such).

Continuous characters coded as such. Goloboff *et al.* (2006) suggested analysing continuous characters as such, rather than applying methods that make the data discrete. The characters that were removed based on the results of the FMC analysis were retained in a second analysis that treated them as additive characters with terminal ranges from −1/+1 standard error (SE). Following Goloboff *et al.* (2006), scaling problems associated with increased branch-lengths were controlled by using implied weights (Goloboff 1993) with a concavity constant (k) of three. The implied weight ratio is less than the ratio implied by the difference of scale, and is one method of balancing the contributions of the characters, making them more even.

Measured characters are identified with an asterisk (*) in the list below.

Cranidium

1. Axial furrow: (0) well defined and with glabella expressed by independent convexity (e.g. *S. aplatus*, Fig. 26F); (1) weak or effaced and glabella not differentiated even by change in convexity (e.g. ‘B.’ *graffhami*, Fig. 19B).

Figure 6. *Bumastoides milleri* (Billings, 1859). **A**–**D,** holotype, exfoliated dorsal exoskeleton (GSC 1319b); Upper Ordovician, Selby Formation, near Ottawa, Ontario, × 3 (Billings 1859, p. 375, fig. 10); **A,** dorsal view; **B,** posterior view; **C,** lateral view; **D,** anterior view. **E**–**G,** testate cranidium (MCZ 145734); Upper Ordovician, Trenton Group, Herkimer County, New York, × 3.5; **E,** lateral view; **F,** dorsal view; **G,** anterior views.

2. Path of posterior branch of facial suture: (0) nearly straight backwards to posterior margin (no posterolateral projection) (e.g. *B. holei*, Fig. 14E); (1) backwards and outwards, forming a small subtriangular posterolateral projection (e.g. *B. kimmswickensis*, Fig. 23E).
3. Median tubercle near posterior margin: (0) absent (e.g. *B. moundensis*, Fig. 20C); (1) present-circular (e.g. *B. bellevillensis*, Fig. 10A); (2) present-elliptical (e.g. *B. graffhami*, Fig. 19E).
4. Predominant shape of lunette: (0) crescentic; deeply incised adaxially, shallowing dramatically abaxially (e.g. *B. moundensis*, Fig. 21B); (1) elliptical; relatively consistent impression (e.g. *B. holei*, Fig. 13C); (2) lunettes absent (e.g. ‘S.’ *gardensis*, Fig. 26G).
5. Path of the axial furrow: (0) straight (e.g. *S. grandis*, Chatteron & Ludvigsen 2004, pl. 2, fig. 10); (1) converging inwards (e.g. *B. bellevillensis*, Fig. 10A).
6. Pitting on internal mould: (0) absent (e.g. ‘S.’ *aplatus*, Fig. 26C); (1) present and widely spaced (e.g. *B. graffhami*, Fig. 19C); (2) present; densely distributed (e.g. *B. moundensis*, Fig. 21A).
7. Cranidial terrace lines: (0) absent (e.g. *S. linnarssoni*, Warburg 1925, pl. 2, fig. 17); (1) only present anteriorly and ventrally (e.g. *B. graffhami*, Fig. 19B); (2) present on most of cranidial exoskeletal surface (e.g. *B. beckeri*, Fig. 11A).

Thorax

8. Number of thoracic segments: (0) nine (e.g. *B. milleri*, Fig. 7H); (1) eight (e.g. *B. bellevillensis,* Fig. 10D.); (2) 10 (e.g. *B. porrectus*, Fig. 16E).
9. Dorsal extent of the articulating facet: (0) below the axial furrow (e.g. *B. porrectus*, Fig. 15D); (1) to the axial furrow (e.g. *B. graffhami*, Fig. 18B).

Pygidium

10. Number of cusps on dorsal inner margin of doublure: (0) one (e.g. *S. linnarssoni*, Jaanusson 1954, fig. 10F); (1) none (e.g. ‘S.’ *rivulus*, Fig. 26A); (2) two (e.g. *B. kimmswickensis*, Fig. 22H).
11. Large paired pygidial muscle scars on exfoliated material: (0) absent (e.g. *B. tenuirugosus*, Fig. 17A); (1) present (e.g. *B. billingsi*, Fig. 8B).
12. Shape in outline: (0) semicircular (e.g. ‘S.’ *rivulus*, Fig. 26A); (1) subtrapezoidal to rounded subtrapezoidal (e.g. *B.* cf. *porrectus*, Fig. 15G); (2) elliptical (e.g. *B. gardensis*, Fig. 26H).
13. Median depression on dorsal surface (ventral ridge) of doublure inner margin: (0) absent (e.g. *Bumastoides solangeae*, Hunda *et al.* 2003, pl. 1 fig. 2); (1) complete (e.g. *B. kimmswickensis*, Fig. 23H); (2) effaced posteriorly (e.g. *B. bellevillensis*, Fig. 10E).
14. Concentric terrace lines on dorsal exoskeleton: (0) absent (e.g. *B. kimmswickensis*, Fig. 22D); (1) present (e.g. *B. holei*, Fig. 14D)

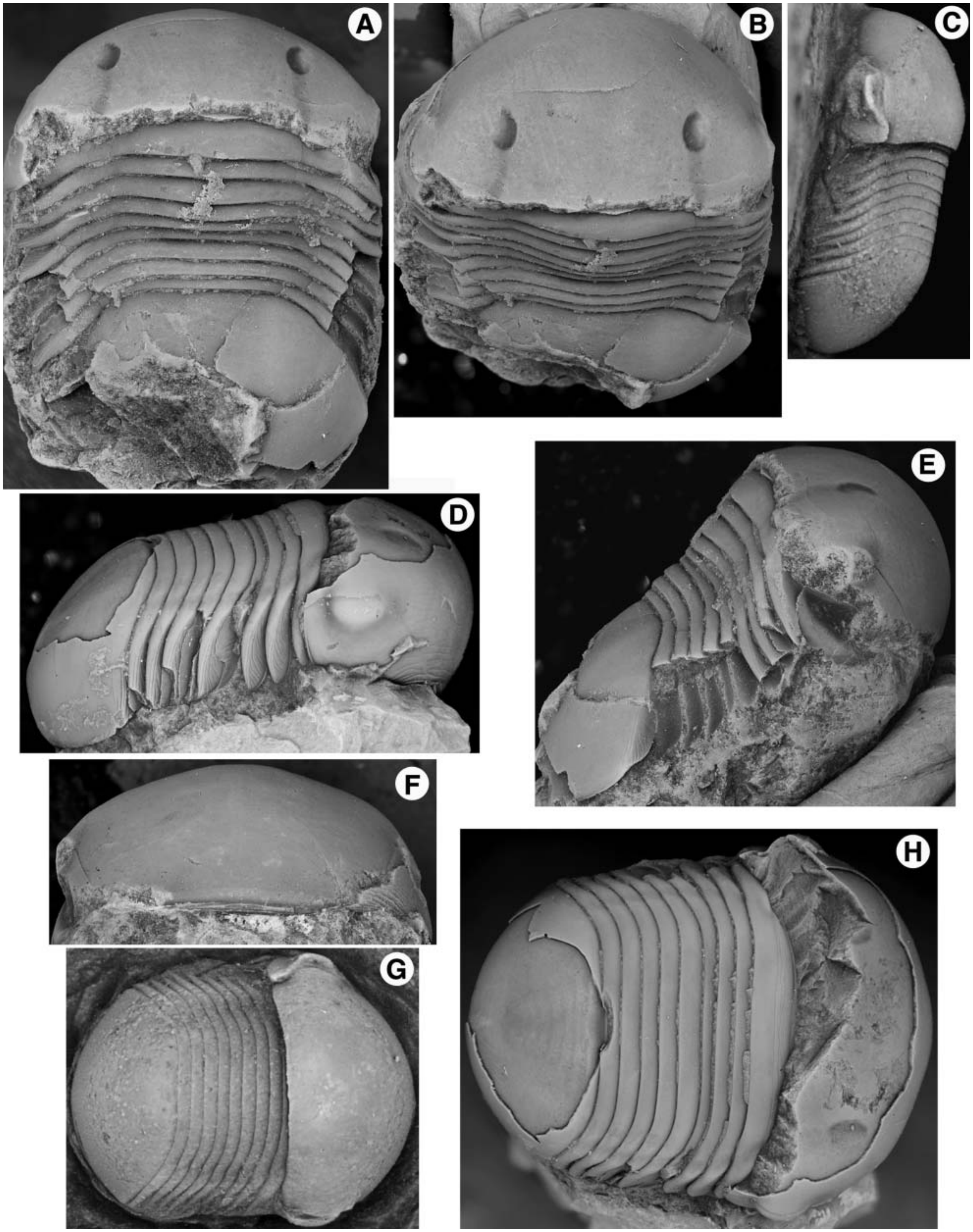

Figure 7. *Bumastoides milleri* (Billings, 1859) **A, B, E, F,** exfoliated, partial dorsal exoskeleton (NYSM 10757); Upper Ordovician, 'Rockland Formation' (Trenton Group), Hamilton County, New York, × 1.8 (Fisher 1957, pl. 16, fig. 9); **A,** dorsal view; **B,** cranidial dorsal view; **E,** lateral view; **F,** anterior view. **C, G,** dorsal exoskeleton (SUI 125988); Upper Ordovician Maquoketa Formation of Iowa, × 3; **C,** lateral view; **G,** dorsal view. **D, H,** partially exfoliated, dorsal exoskeleton, (SUI 125975); Upper Ordovician, Platteville Formation, Iowa, × 1.2; **D,** lateral view; **H,** dorsal view.

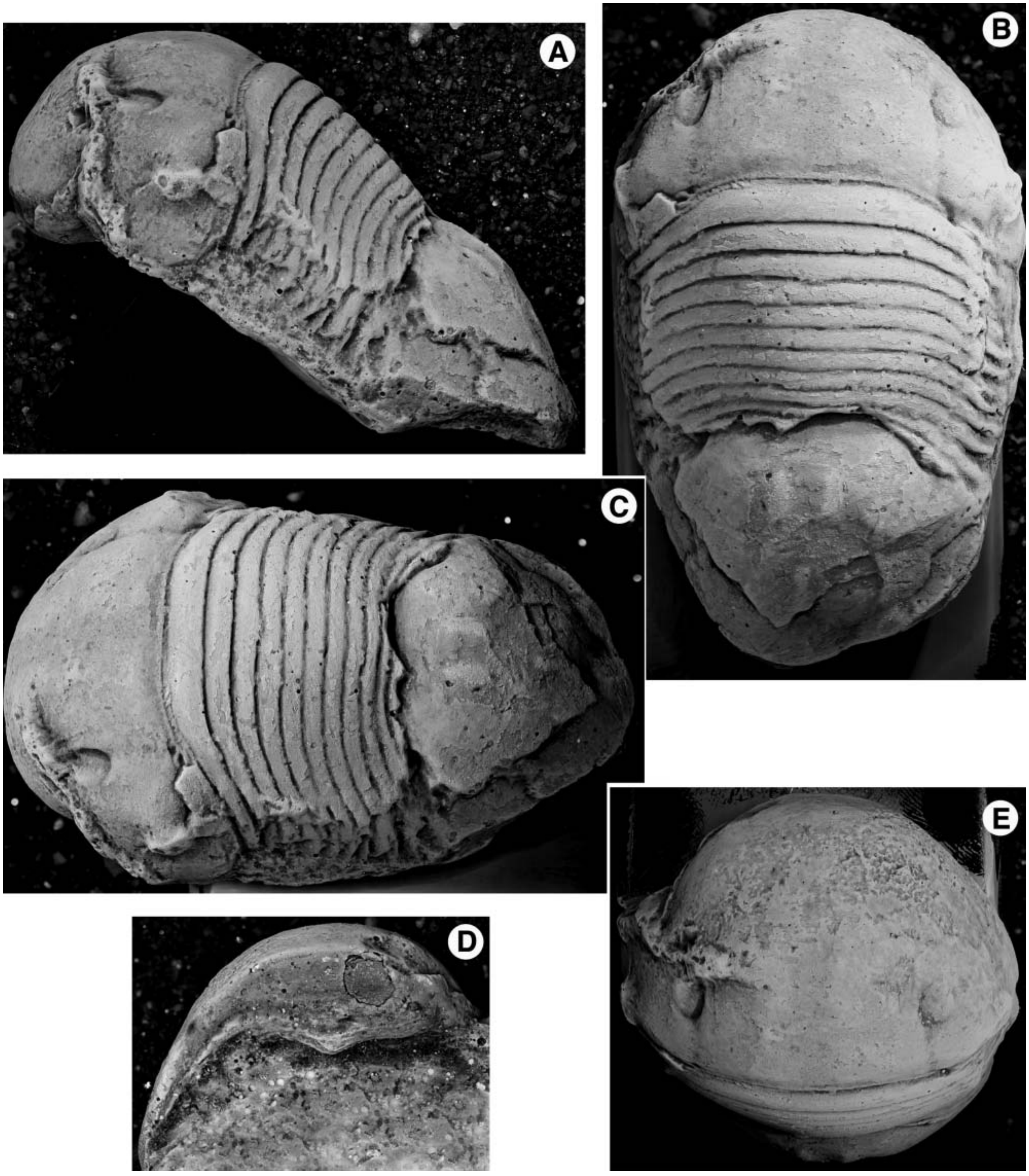

Figure 8. *Bumastoides billingsi* (Raymond & Narraway, 1908), plastotype, exfoliated dorsal exoskeleton (CM 5472); Upper Ordovician, Trenton Group, Hull, Quebec, × 0.95 (Raymond & Narraway 1908, pl. 62, figs 1, 2): **A,** lateral view; **B,** dorsal view; **C,** oblique lateral view; **D,** anterior view; **E,** cranidial dorsal view.

15. Undulating terrace lines directed inward from lateral margins on dorsal exoskeleton: (0) present (e.g. *B*. *graffhami*, Fig. 18C); (1) absent (e.g. *B*. *porrectus*, Fig. 16D).

16. *Ratio of max pygidial length (sag.) to max pygidial width (tr.): (0) (e.g. 'S.' *gardensis*, Fig. 26H); (1) (e.g. *B*. *graffhami*, Fig. 18F); (2) (e.g. *B*. *porrectus*, Fig. 15A); (3) (e.g. *B*. *moundensis*, Fig. 20F).

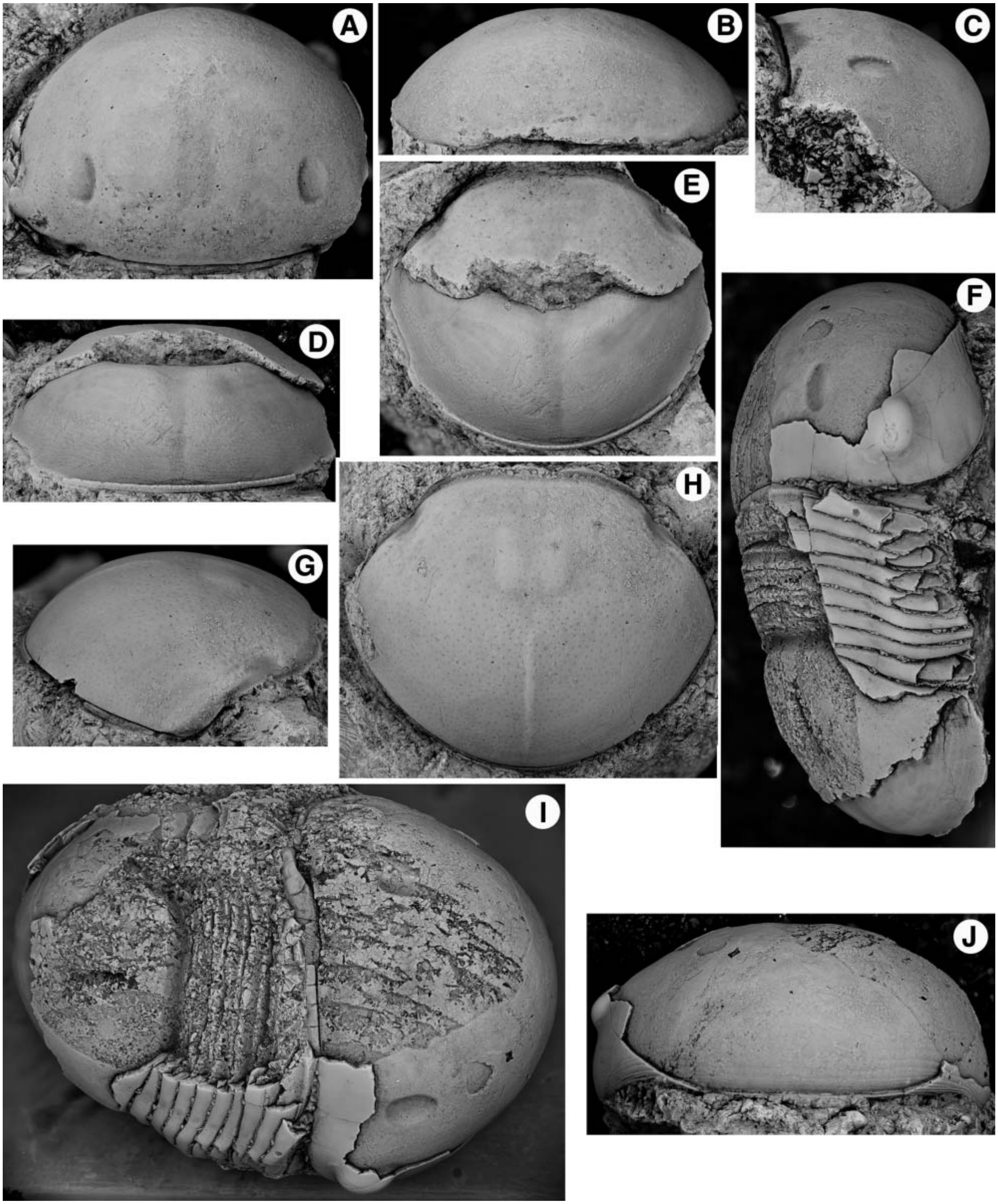

Figure 9. *Bumastoides billingsi* (Raymond & Narraway, 1908). **A**–**C,** exfoliated cranidium (UC 20700a); Upper Ordovician, Kimmswick Limestone, Batchtown, Illinois, × 1.5 (Bradley 1930, pl. 28, fig. 1): **A,** dorsal view; **B,** anterior view; **C,** lateral view. **D**–**I,** Kimmswick Limestone of Glen Park, Missouri; **D, E,** exfoliated pygidium (UC20710a), × 1.5 (Bradley 1930, pl. 28, fig. 2); **D,** posterior view; **E,** dorsal view. **G, H,** exfoliated pygidium **(**UC 20710b), × 1.6 (Bradley 1930, pl. 28, fig. 3); **G,** lateral view; **H,** dorsal view. **F, I, J,** exfoliated dorsal exoskeleton (UC 10776), × 1.4 (Bradley 1930, pl. 28, figs 6, 7); **F,** lateral view; **I,** dorsal view; **J,** anterior view.

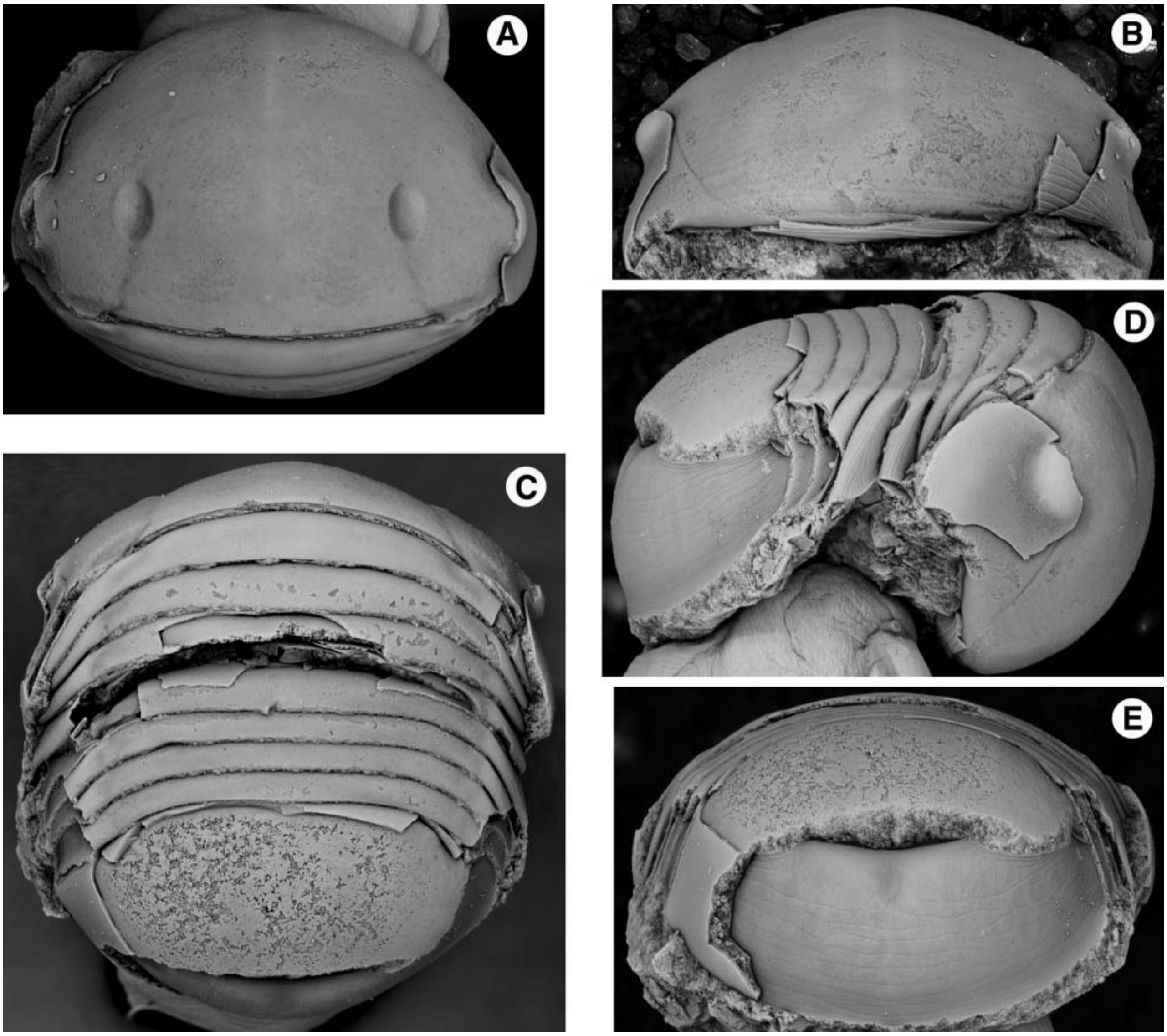

Figure 10. *Bumastoides bellevillensis* (Raymond & Narraway, 1908), holotype, partially exfoliated dorsal exoskeleton (CM 1900); Upper Ordovician, Verulam Formation (Trenton Group), Belleville, Ontario, × 2.6 (Raymond & Narraway 1908, pl. 61, figs 6, 7). **A,** cranidial dorsal view; **B,** anterior view; **C,** dorsal view; **D,** lateral view; **E,** posterior view.

17. Expression of axial furrow: (0) minor lateral notches that flank medial anterior margin (e.g. 'S.' *aplatus*, Fig. 26D); (1) present; outline a convex and well-defined axis (e.g. 'S.' *gardensis*, Fig. 26H); (2) completely effaced (e.g. *B*. *beckeri*, Fig. 11F).
18. Location of pygidial maximum width (tr.): (0) at or near the anterior end (e.g. 'S.' *rivulus*, Fig. 26A); (1) at half-length (sag.) (e.g. *B*. *kimmswickensis*, Fig. 22D).
19. Length (sag.) of doublure: (0) short, approximately 30% of pygidial length (e.g. 'S.' *rivulus*, Fig. 26A); (1) long, approximately 60% of pygidial length (e.g. *B*. *billingsi*, Fig. 9E).
20. Pitting on pygidial dorsal exoskeleton: (0) present (e.g. 'S.' *gardensis*, Fig. 26H); (1) absent (e.g. *B*. *porrectus*, Fig. 16B).

Results

Parsimony analysis

The data matrix was constructed in MacClade 4.08 OS X (Maddison & Maddison 2005), and parsimony and related analyses were conducted in PAUP* version 4.0b10 (Swofford 2002), and checked in TNT (Goloboff *et al.* 2008; implicit enumeration). A branch and bound search algorithm was used with the following settings: the initial upper bound was computed heuristically; addition sequence was furthest; zero length branches were not collapsed; topological constraints were not enforced; and trees were treated as unrooted. All characters were unordered, weighted equally and parsimony informative. PAUP* retained eight equally most parsimonious trees (MPTs) with a tree length of 56 steps, consistency index (CI) of 0.57, retention index (RI)

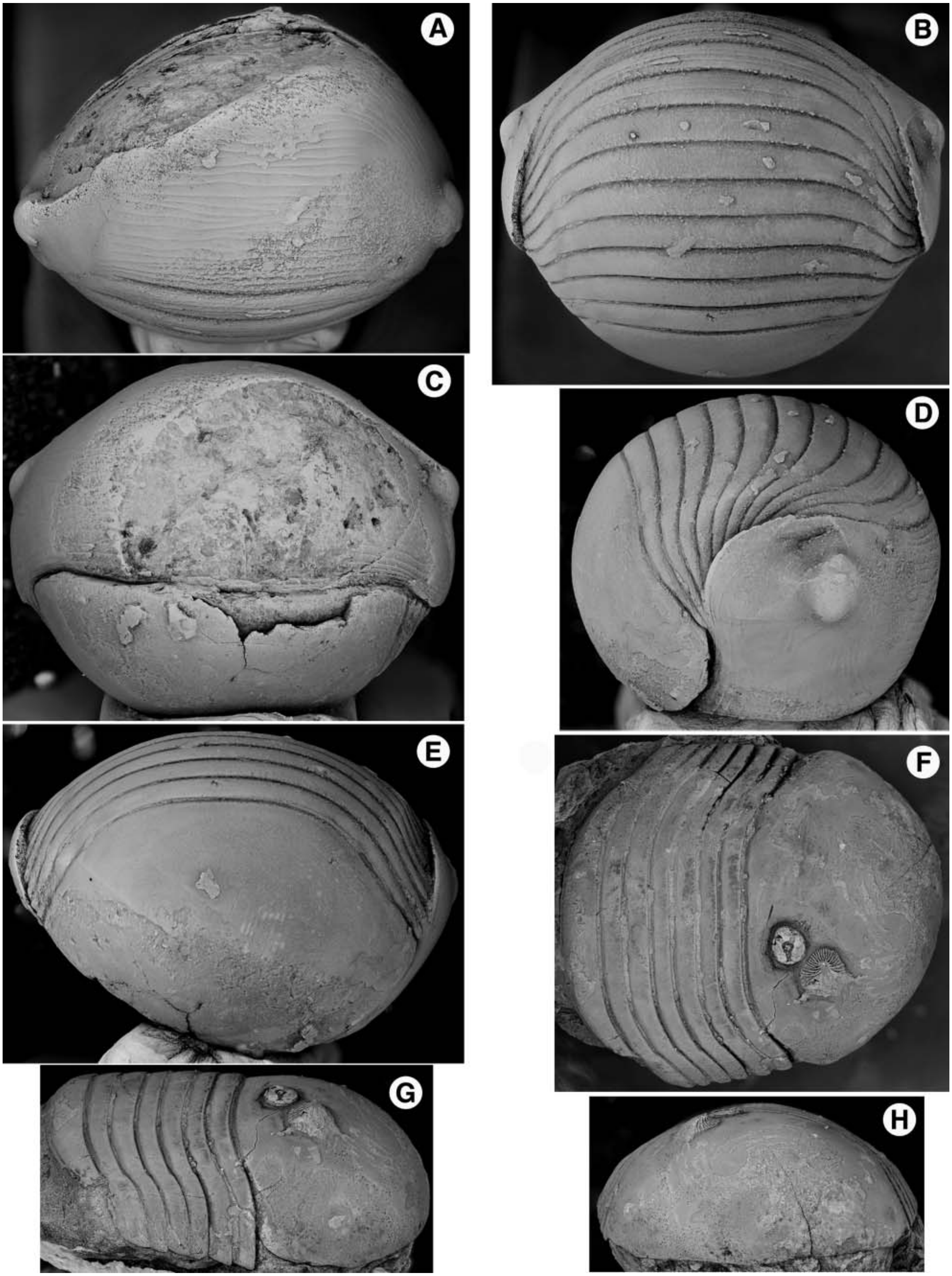
A
B
C
D
E
F
G
H

of 0.69, and rescaled consistency index (RC) of 0.40; the strict consensus tree is shown in Fig. 4, and one of the eight MPTs in Fig. 5A (chosen because it retains some relationships that are present in multiple MPTs, e.g. *Bumastoides holei* and *B. billingsi* as sister taxa). Calculation of a tree length distribution of 10,000 equally sampled random trees (with the same settings as the parsimony analysis) resulted in a mean tree length of 91.5 steps, with no retained trees approaching 56 steps. The probability of obtaining a tree of 56 steps at random is less than 0.0001. Symmetric resampling (33% probability) group support (see Fig. 4) and GC values (frequency differences, see Goloboff *et al.* 2005) were calculated by a 1000 replicate implicit enumeration algorithm, with two clades (nodes 4 and 9) appearing in at least 50% of the replicates. Bremer support values (Bremer 1994) were calculated by continually keeping trees with length values of N + 1 in PAUP* (checked in TNT), where N = the tree length of the strict consensus tree. Three clades have Bremer support values (Bremer 1994) of higher than 1 (nodes 1, 4 and 9: see Fig. 4).

A second analysis (continuous characters as such) used the same search algorithm (implicit enumeration) and settings in TNT as the first, with the exception of the implied weights. One tree (Fig. 5B) with a best-fit value of 8.47 was retained. Symmetric resampling group support of greater than 50% is present on the equivalents of node 2 and 4 (Fig. 4). *Bumastoides milleri* and *B. graffhami* (node 9) still have relatively high support, as does an arrangement not found in the initial analysis (*B. beckeri* and *B. moundensis*). In general, the support values are higher on the more basal nodes in the second analysis (compare Fig. 4 to Fig. 5B), but much of the resolved portions of the *Bumastoides* clade have contradictory (i.e. negative) GC values. The second tree also has more homoplasy in the optimization of the discrete characters (CI 0.53; RI 0.62; RC 0.33). The broad topology of the second tree is similar to the first, with high support (82/80 in the former, 61/60 in the latter) for the same *Bumastoides* clade that excludes *B. rivulus*, *B. aplatus* and *B. gardensis*. These data indicate that changing the treatment of continuous characters has little effect on the most important question here: what taxa belong in *Bumastoides*? The second analysis retains some other arrangements not found in the first (e.g. *B. holei* and *B. bellevillensis* as sister taxa), but this relationship is not well supported and has little bearing on the overall goals of revision. We think it is best to use the FMC driven results (Fig. 4) as the basis of the taxonomy because the strict consensus tree conservatively collapses much of the poorly supported in-group *Bumastoides*, and in general contains fewer assumptions than the second analysis.

The strict consensus tree (Fig. 4) is partially pectinate, and demonstrates a well-supported monophyletic group (*Bumastoides*) at node 4. *B. aplatus* Raymond, 1925, *B. rivulus* Ingham & Tripp, 1991, and *B. gardensis* Shaw, 1968 are excluded from *Bumastoides* because of the clade support and high number of apomorphies at node 4 (Fig. 5A). Nearly all of the pygidial characteristics shared by *Bumastoides* (characters 10, 12, 17, 18, 19) and one cranidial characteristic (character 1) exclude these three taxa, all of which generally share more features with *Stenopareia*. These three taxa (nodes 1–3 on Fig. 4) appear to render *Stenopareia* paraphyletic in the context of this analysis, but the species included here are inadequate to assess the monophyly of the genus as a whole (an option beyond the scope of this study). In the absence of an updated systematic revision of *Stenopareia*, we chose to provisionally regard these taxa as *Stenopareia sensu lato*. In this way, no new superfluous genera are formed within the Illaenidae, and the placement is consistent with the assessment of later authors who doubted the original assignment of *B. gardensis* and *B. aplatus* to *Bumastoides* (Chatterton & Ludvigsen 1976; Westrop & Ludvigsen 1983). Whittington (1954) also expressed concern about his placement of *B. aplatus* in *Bumastoides*, suggesting that the pygidial attributes of the species were not characteristic of the rest of the genus. Similarly, Shaw (1968) hesitantly placed *B. gardensis* in *Bumastoides* because of its similarity with *B. aplatus*, and Ingham & Tripp (1991) referred to their new species as '*Bumastoides*? *rivulus*'.

Character optimization

Fig. 5A is a character state optimization of unambiguous state changes (those present at the same node under both the assumptions of ACCTRAN and DELTRAN optimization) on one of the eight MPTs. *Stenopareia grandis* is the most basal ingroup taxon. The rest of the ingroup is united at node 1 based on converging inward axial furrows (character 5, state 1) and the loss of one cusp on the pygidial doublure (character 10, state 1). At node 2, cranidial terrace lines are present only anteriorly and ventrally (character 7, state 1), and at node 3, pitting on the pygidial dorsal exoskeleton is lost (character 20, state 1). *Bumastoides* species are united at node 4 by their shared axial furrow impression (character 1, state 1), two cusps on the doublure (character 10, state

←

Figure 11. *Bumastoides beckeri* (Slocom, 1913), Upper Ordovician, Maquoketa Formation, Fayette County, Iowa. **A**–**E,** holotype, enrolled dorsal exoskeleton (UC 41154), × 1.4 (Slocom 1913, pl. 14, figs 1–3); **A,** cranidial dorsal view; **B,** dorsal view; **C,** anterior view; **D,** lateral view; **E,** posterior view. **F**–**H,** thoracopygon (P16708), × 1.6 (Slocom 1913, pl. 14, fig. 4); **F,** dorsal view; **G,** lateral view; **H,** posterior view.

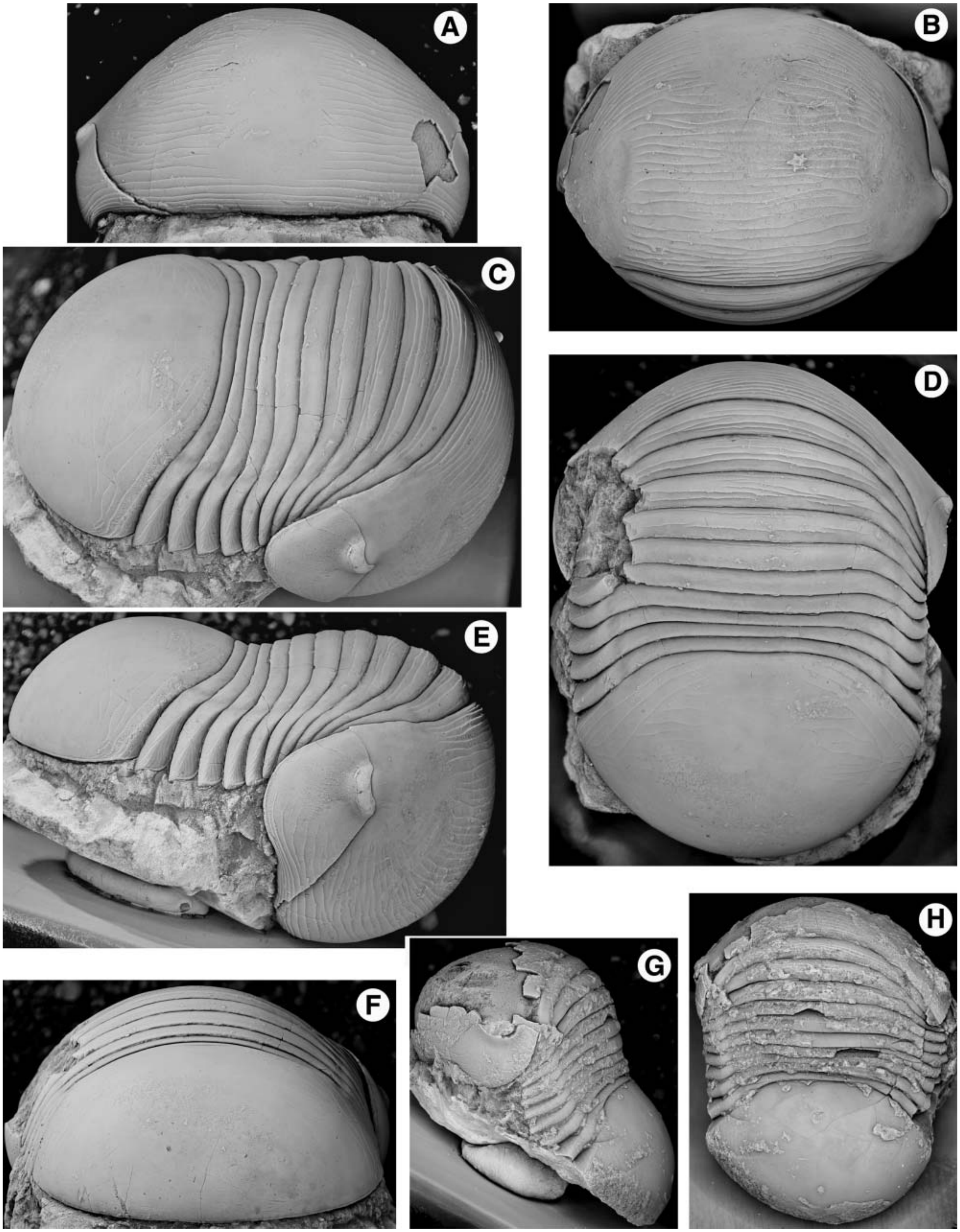

Figure 12. *Bumastoides beckeri* (Slocom, 1913), Upper Ordovician, Maquoketa Formation, Fayette County, Iowa, × 0.85. **A–F,** dorsal exoskeleton (SUI 125973); **A,** anterior view; **B,** cranidial dorsal view; **C**, oblique lateral view; **D,** dorsal view; **E,** lateral view; **F,** posterior view. **G, H,** partially exfoliated dorsal exoskeleton (SUI 125984); **G,** lateral view; **H,** dorsal view.

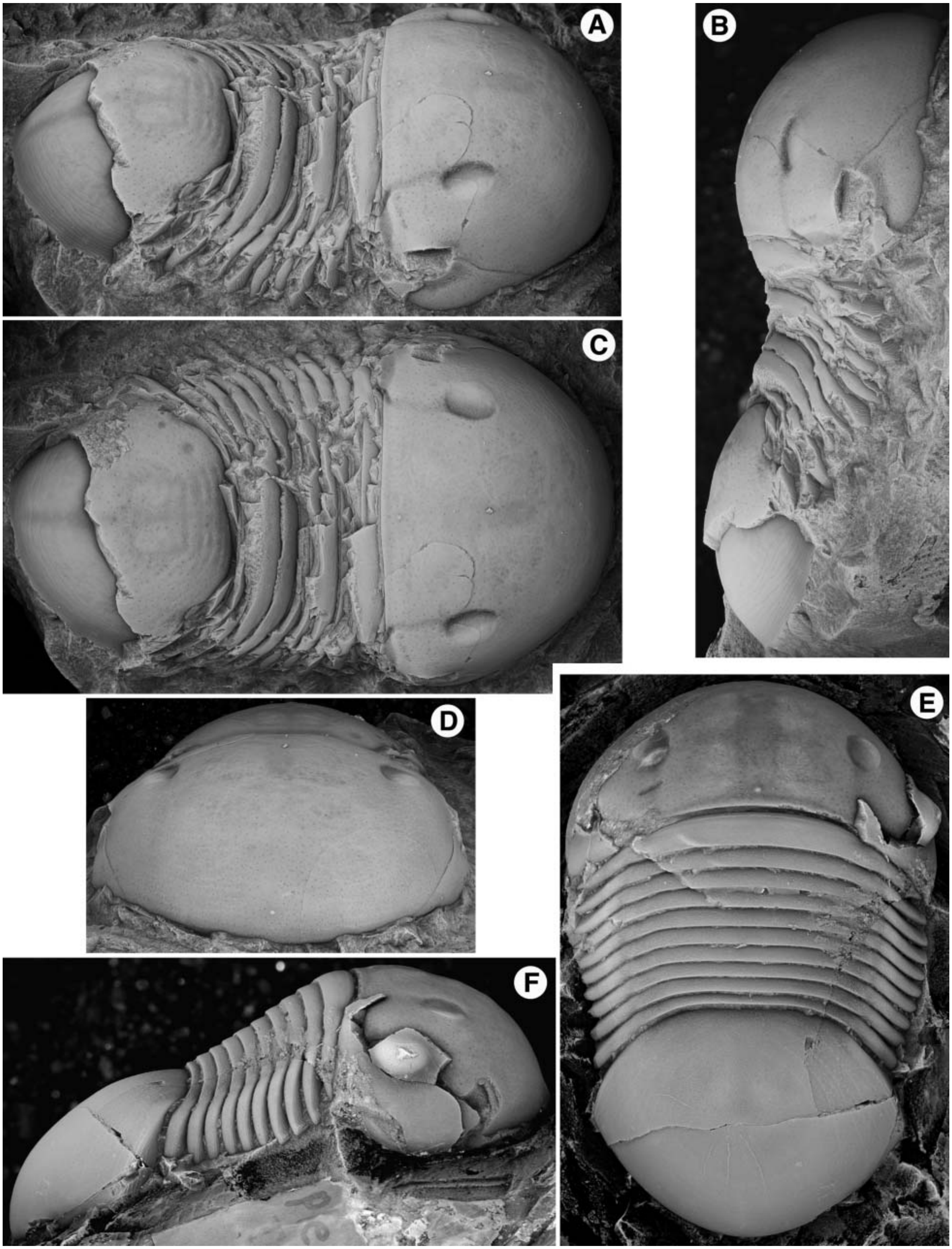

Figure 13. *Bumastoides holei* (Foerste, 1920), Upper Ordovician, Rust Formation (Trenton Group), Trenton Falls, Oneida County, New York. **A**–**D,** plesiotype, exfoliated dorsal exoskeleton (MCZ 101148), × 1.2 (Raymond 1925, pl. 8, figs 5, 6, intentionally exfoliated since the Raymond illustrations?); **A,** oblique lateral view; **B,** lateral view; **C,** dorsal view; **D,** anterior view. **E, F,** partially exfoliated dorsal exoskeleton (MCZ 144798), × 1.5; **E,** dorsal view; **F,** lateral view.

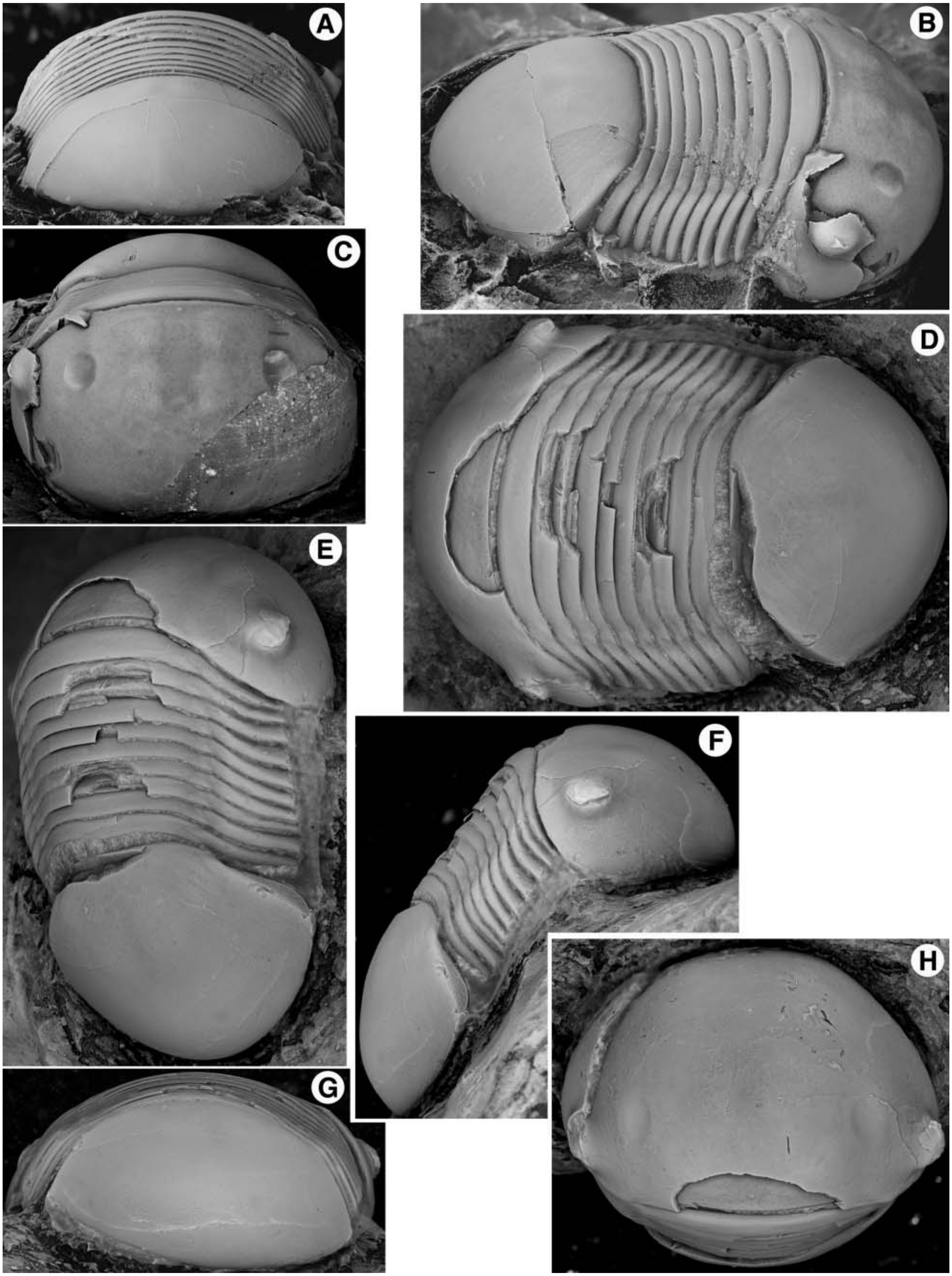
A
B
C
D
E
F
G
H

2), subtrapezoidal pygidial shape (character 12, state 1), lack of axis expression (character 17, state 2), half-length location of maximum pygidial width (character 18, state 1), and long length of doublure (character 19, state 1). The pygidial median depression (ventral ridge) is complete at node 5 (character 13, state 1). At node 6, the pitting on the cranidial internal mould changes to densely distributed (character 6, state 2), and at node 7 the median posterior tubercle is present (character 3, state 1), and the shape of the lunette is elliptical (character 4, state 1). The pitting on the cranidial internal mould changes from densely to loosely distributed at node 8 (character 6, state 1). *B. milleri* and *B. graffhami* are sister taxa at node 9, based on a predominantly crescentic lunette (character 4, state 0) and pygidial undulating terrace lines (character 15, state 0). *B. beckeri* and *B. kimmswickensis* are sister taxa at node 10 based on terrace lines covering the entire cranidial exoskeleton (character 7, state 2).

Systematic palaeontology

Material and methods

Illustrated material was photographed at 1 mm intervals with a Canon E05 5D camera equipped with 65, 80 or 120 mm lenses. Images were stacked using Helicon Focus 4.04 Pro Multiprocessor (Helicon Soft Lutd., Kharkov, Ukraine). References to length are in the sagittal direction, and width in transverse, unless otherwise noted. Outline shapes (e.g. crescentic) refer to dorsal view, unless specified otherwise. For the standard cranidial dorsal view, the midpoint of the lunette is approximately opposite the top of the palpebral lobe. The palpebral lobe (or eye if preserved) was oriented horizontal for the standard lateral view. Diagnostic characters which do not reference a character from the cladistic analysis are autapomorphies of that species, and are separated from the rest of the characters with a semicolon. Systematic diagnoses are based primarily on unambiguous state changes in Fig. 5A, although ambiguous states (e.g. number of thoracic segments) and autapomorphies are also used to create a complete (and unique) character assemblage for each species. The clade definitions (de Queiroz & Gauthier 1990; de Queiroz 2007) for *Bumastoides* are based on the strict consensus tree. We use a Linnean classification with named ranks, so the clade definitions are not the basis of the formal taxonomy, but additional information that specifies the clades exact location on the consensus tree.

Institutional abbreviations

Repository acronyms are as follows: **OU**, Sam Noble Oklahoma Museum of Natural History; **NYSM**, New York State Museum, Albany; **GLAHM**; Hunterian Museum and Art Gallery, Glasgow; **MCZ**, Museum of Comparative Zoology, Harvard University; **CM**, Carnegie Museum of Natural History, Pittsburgh; **GSC**, Geological Survey of Canada, Ottawa; **SUI**, University of Iowa Paleontology Repository, Iowa City; **UC, P**, Field Museum of Natural History, Chicago.

Class **Trilobita** Walch, 1771
Order **Corynexochida** Kobayashi, 1935
Suborder **Illaenina** Jaanusson, 1959
Family **Illaenidae** Hawle & Corda, 1847
Genus ***Bumastoides*** Whittington, 1954

Type species. *Illaneus milleri*, Billings, 1859 from the Trenton Group of Ontario, by original designation.

Definition. The clade *Bumastoides* is the common ancestor of *B. porrectus* and *B. solangea* and all of its descendants (Fig. 4, node 4). To underscore the importance of character 1, an apomorphy-based definition may also be useful: *Bumastoides* is the clade stemming from the first ancestor to possess an axial furrow that is weak or effaced and glabella not differentiated even by change in convexity from the rest of the cranidium.

Diagnosis. Cranidial axial furrow weak or effaced and glabella not differentiated even by change in convexity from the rest of the cranidium (character 1, state 1), dicuspid inner margin of pygidial doublure (character 10, state 2), pygidia subtrapezoidal or rounded subtrapezoidal (character 12, state 1), pygidial axis expression is undifferentiated or minimally expressed (character 17, states 0, 2), location of maximum pygidial width is at half-length (sag.) (character 18, state 1), pygidial doublure length (sag.) is long (character 19, state 1).

Remarks. Raymond (1916) and Troedsson (1928) recognized that Ordovician species referred to as *Bumastus* were a distinct group from Silurian bumastids, but did not propose a new taxonomic group to describe them. In his work on a trilobite fauna from Baffin Island, Whittington (1954) erected *Bumastoides* as a subgenus of *Bumastus* based on the following differences: axial furrows are faint or absent, the lunette is distinctive, the palpebral lobe is smaller and placed farther back from the midline, there are 8–10 segments in the thorax, and the maximum width of the pygidium is at half length (sag.). He originally placed *B. milleri*, *B. bellevillensis*, *B. beckeri*, *B. billingsi*,

←

Figure 14. *Bumastoides holei* (Foerste, 1920), Upper Ordovician, Rust Formation (Trenton Group), Trenton Falls, Oneida County, New York. **A**–**C**, partially exfoliated dorsal exoskeleton (MCZ 144798), × 1.5; **A**, posterior view; **B**, oblique lateral view; **C**, anterior view. **D**–**H**, dorsal exoskeleton (MCZ 115909), × 1.5 (Brett *et al*. 1999, pl. 7, fig. 4); **D**, dorsal view; **E**, oblique lateral view; **F**, lateral view; **G**, posterior view; **H**, cranidial dorsal view.

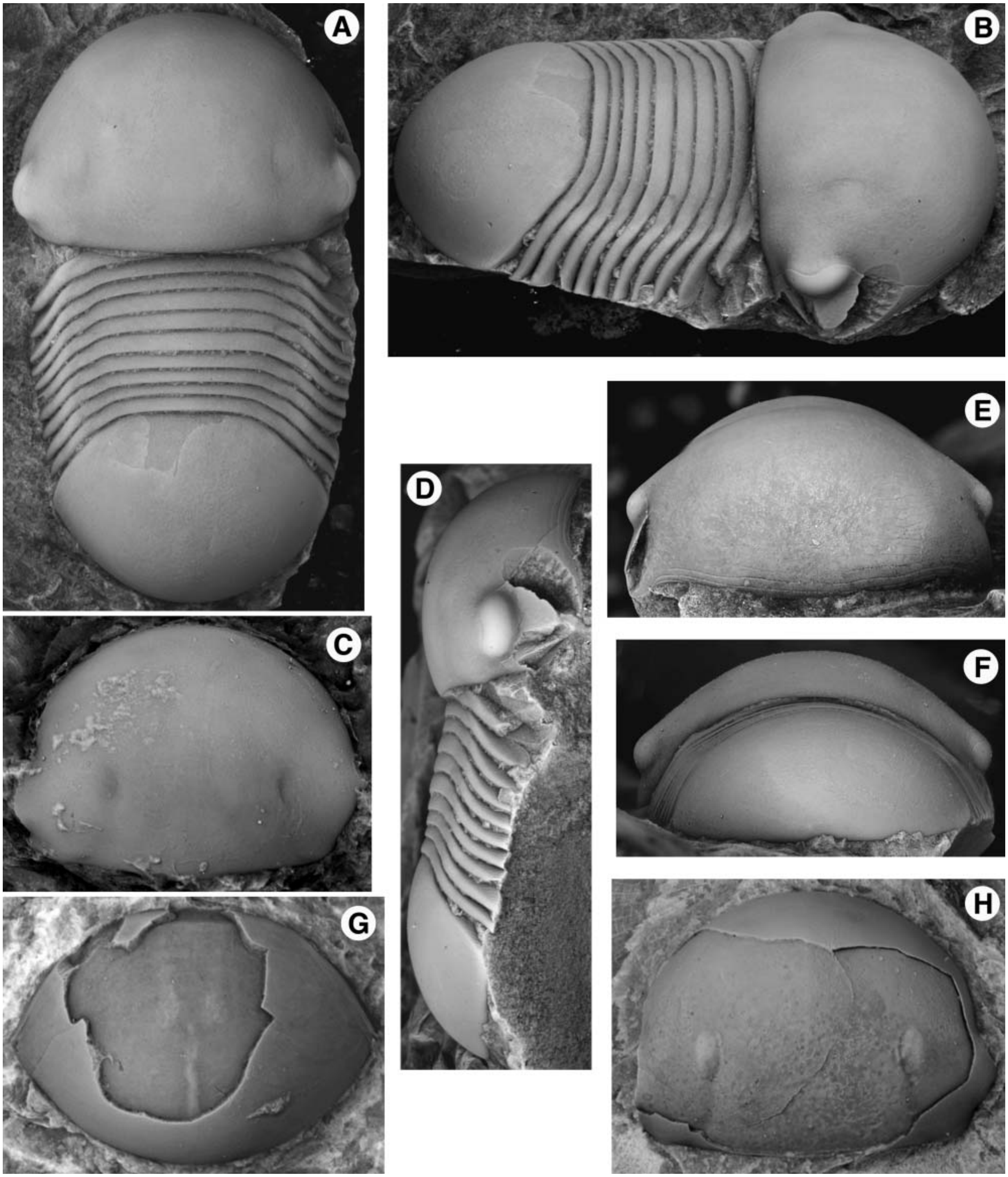

Figure 15. **A**–**F,** *Bumastoides porrectus* (Raymond, 1925). **A, B, D**–**F,** holotype, dorsal exoskeleton (MCZ 101147); Upper Ordovician, Denley Formation (Trenton Group), Trenton Falls, Oneida County, New York, × 2.5 (Raymond 1925, pl. 8, figs 7, 8); **A,** dorsal view; **B,** oblique lateral view; **D,** lateral view; **E,** anterior view; **F,** posterior view. **C, H,** Upper Ordovician, Guttenberg Formation (Decorah Group), Guttenberg and McGregor, Iowa and Fennimore West, Wisconsin; **C,** testate cranidium (MCZ 107234), × 2.6, dorsal view (DeMott 1987, pl. 6, figs 24–26); **H,** exfoliated cranidium (MCZ 107235), × 3, dorsal view (DeMott 1987, pl. 6, figs 27, 28). **G,** *Bumastoides* cf. *porrectus* (Raymond, 1925), Upper Ordovician, Guttenberg Formation (Decorah Group), partially exfoliated pygidium (MCZ 107236), × 2.6, dorsal view (DeMott 1987, pl. 6, figs 29–31).

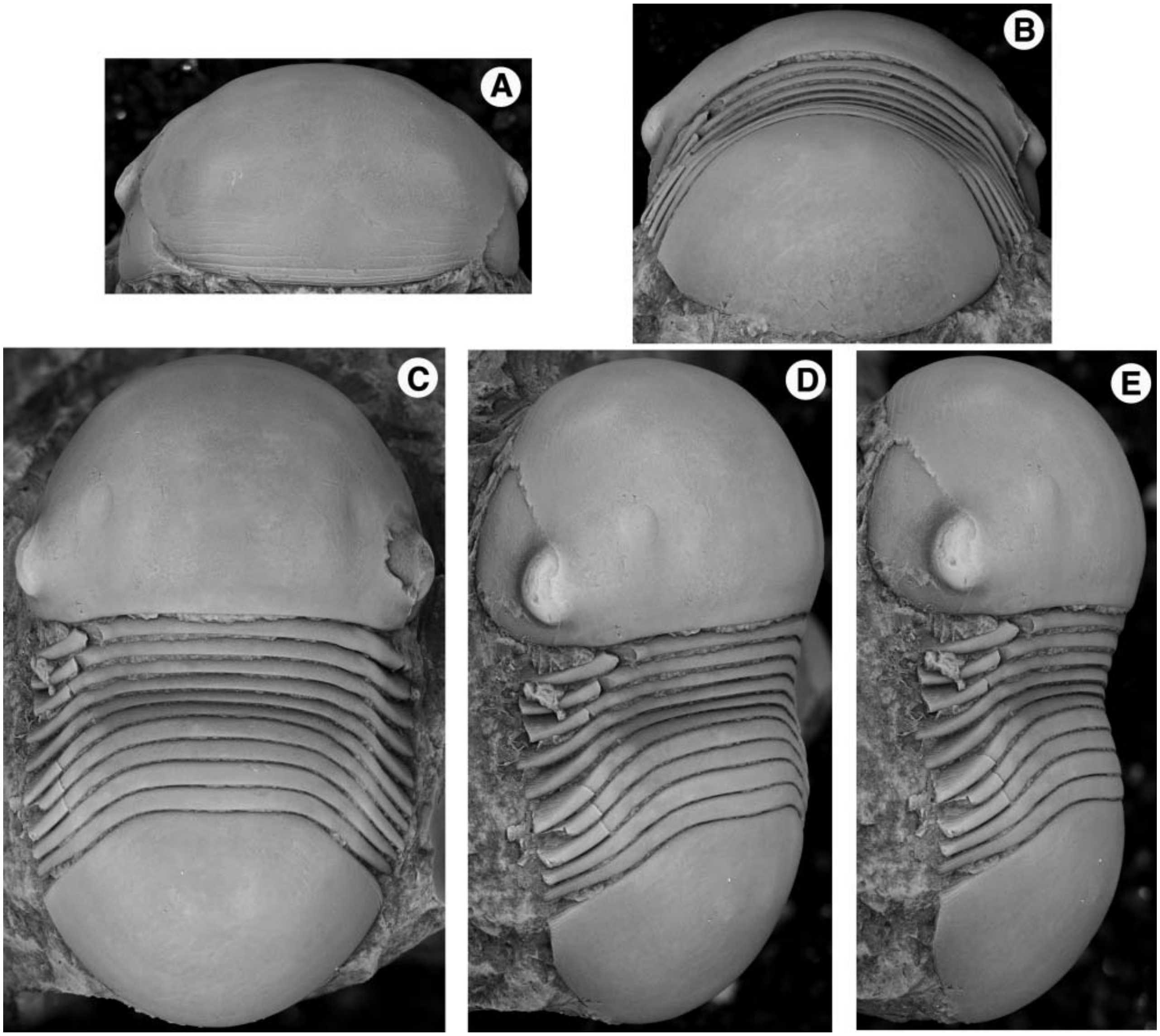

Figure 16. *Bumastoides porrectus* Raymond, 1925 (originally identified by Clarke 1897, fig. 32 as *Bumastus trentonensis*), dorsal exoskeleton (NYSM 4158); Upper Ordovician, Trenton Group, Trenton Falls, Oneida County, New York, × 2 (Clarke 1897, fig. 32); **A,** anterior view; **B,** posterior view; **C,** dorsal view; **D,** oblique lateral view; **E,** lateral view.

B. *porrectus* and *B*. *tenuirugosus* into this taxon, and speculated that species with distinctive pygidia like *B*. *aplatus* might also belong in it because their cranidia were similar to *Bumastoides*. We show here that these species differ in an important cranidial feature (character 1), and a wide variety of pygidial characters, and are best placed in *Stenopareia* (or at the very least excluded from *Bumastoides*). Ludvigsen & Chatterton (1980) elevated *Bumastoides* to full generic status, and placed it in the Illaeninae based on the presence of a forward turning rostral flange in *B*. *lenzi*. This placement was supported by Whittington (1997a) because *Bumastoides* also shares a wide variety of other features with illaenids: a down-curving doublure with the anterior edge lying below the ventral ridge, a virtually nonfulcrate thorax, narrow pleurae and a wide thoracic axis.

Besides the effacement of the *Bumastoides* exoskeleton, one of the largest barriers to the construction of accurate phylogenetic reconstructions has been the inconsistent assessment of the number of thoracic segments by some authors (see Remarks of *B*. *milleri* below for examples). Material with anywhere from 8 to 10 thoracic segments have been placed into the same species because of the lack of identifying features. There is no evidence that the number of thoracic segments varies in holaspids, so the number of segments should be considered diagnostic in material that is obviously morphologically mature.

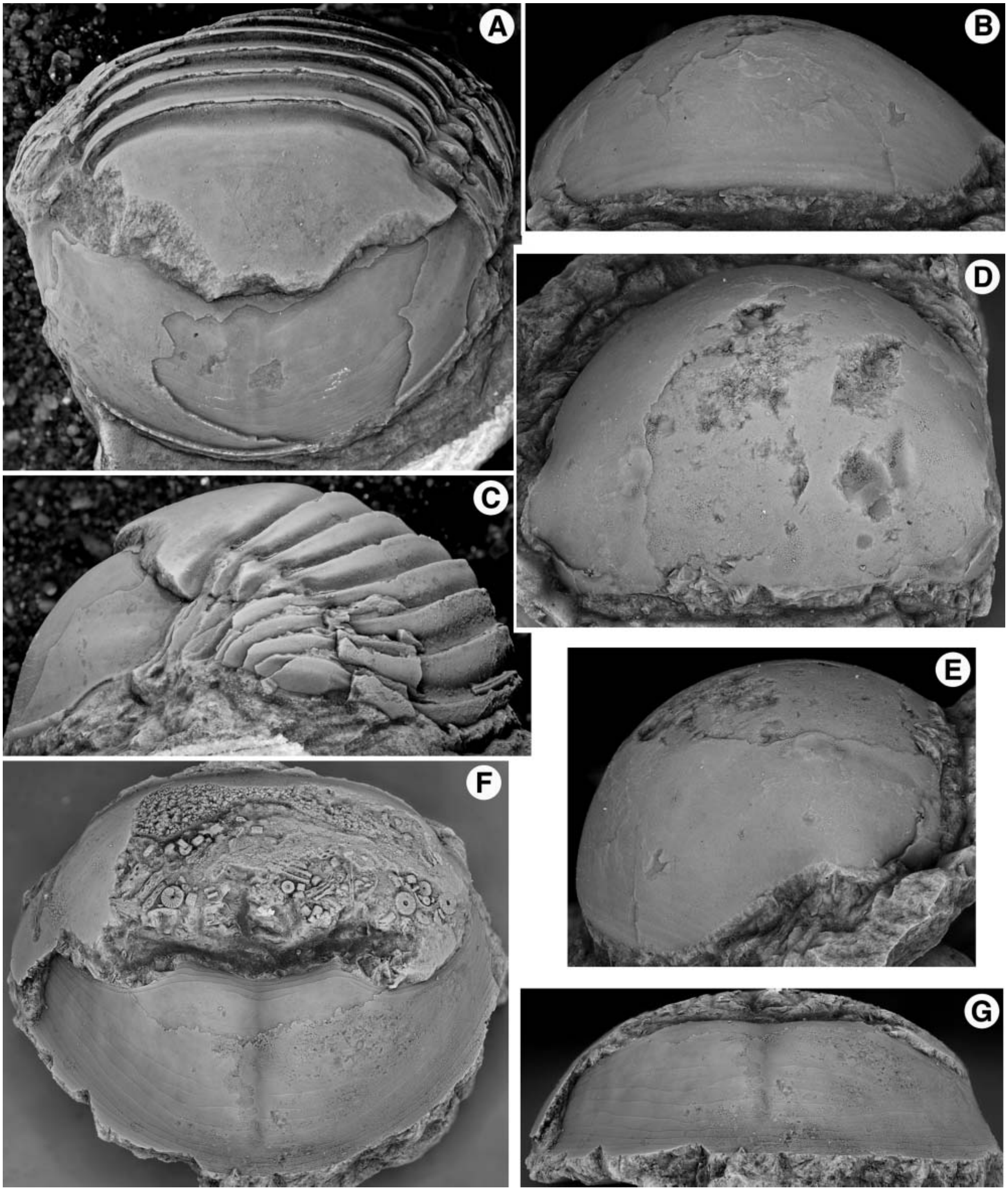

Figure 17. *Bumastoides tenuirugosus* Troedsson, 1928, Upper Ordovician, Selkirk Member of the Red River Formation, Garson, southern Manitoba. **A, C,** thoracopygon (OU 12483); **A,** posterior view, × 1; **C,** lateral view, × 1.2. **B, D, E,** partially exfoliated cranidium (OU 12495), × 2.3; **B,** anterior view; **D,** dorsal view; **E,** lateral view. **F, G,** exfoliated pygidium (OU 12496), × 2; **F,** dorsal view; **G,** posterior view.

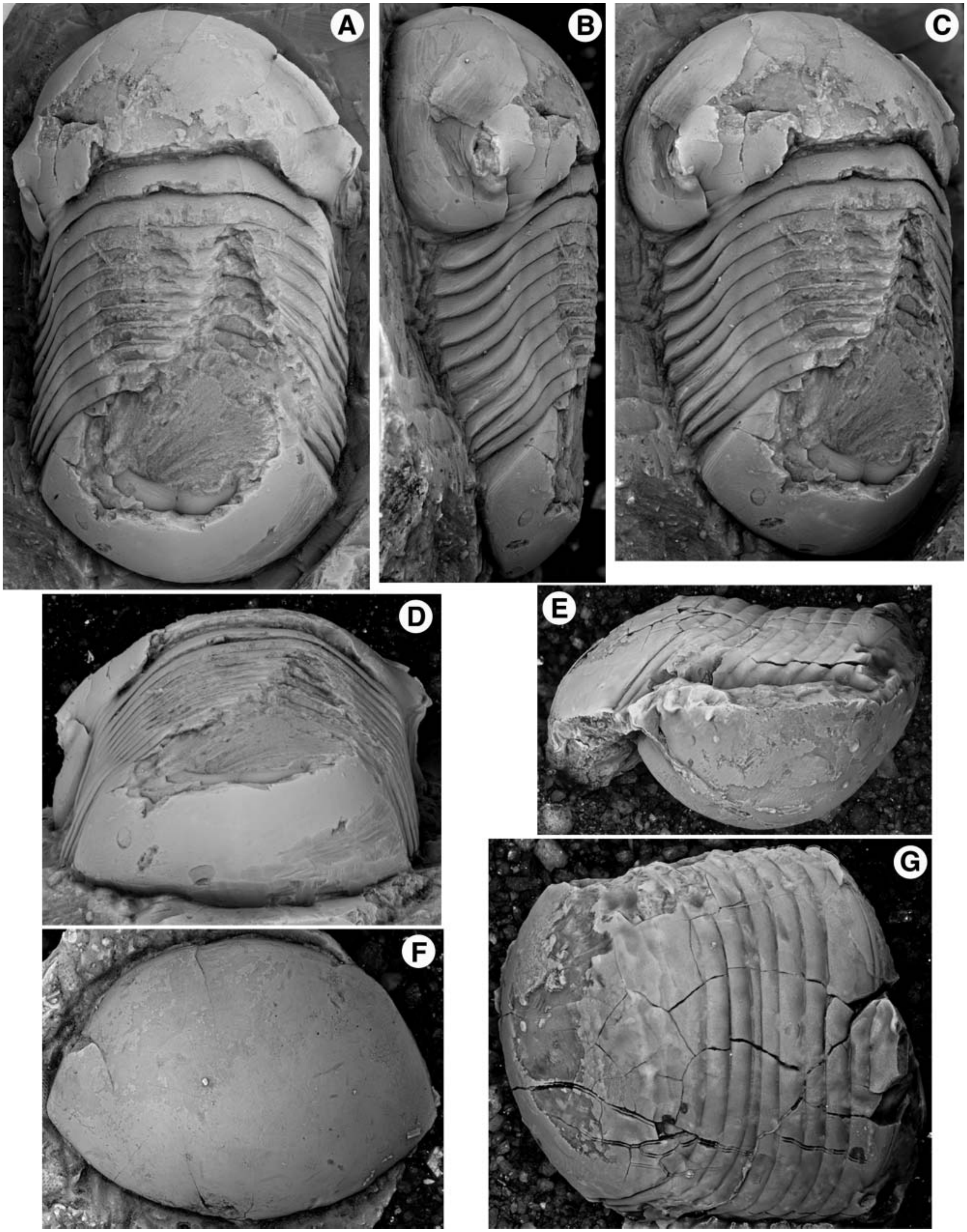

Figure 18. *Bumastoides graffhami* sp. nov., Upper Ordovician, Bromide Formation (Simpson Group), Arbuckle Mountains region, south-central Oklahoma. **A**–**D,** holotype, dorsal exoskeleton (OU 5204), × 1.8 (Shaw 1974, pl. 4, figs. 19–20, 23); **A,** dorsal view; **B,** lateral view; **C,** oblique lateral view, × 2: **D,** posterior view. **E, G,** thoracopygon (OU 12497), × 1; **E,** lateral view, × 1.3; **G,** dorsal view. **F,** testate pygidium (OU 12498), × 1.6, dorsal view.

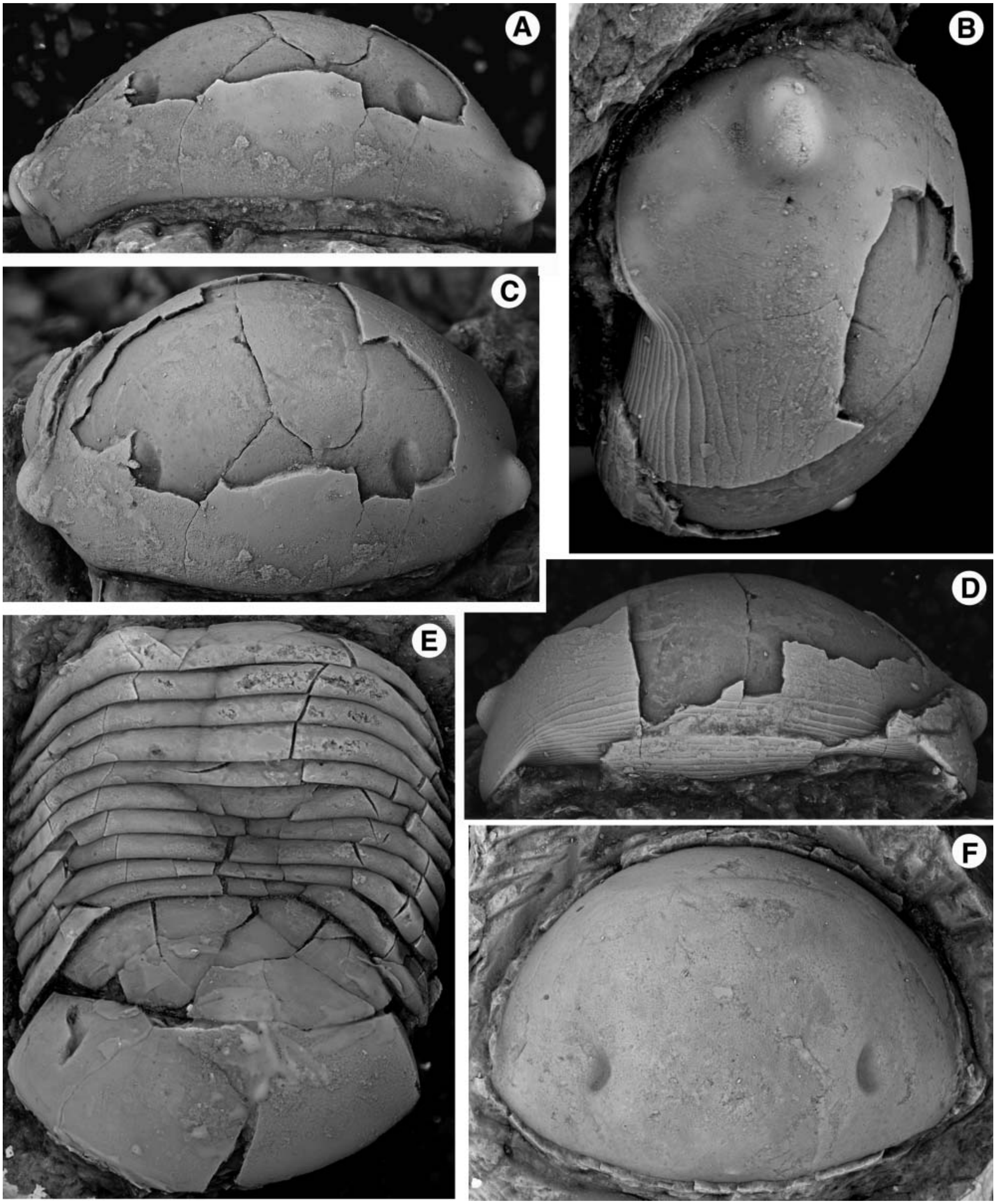

Figure 19. *Bumastoides graffhami* sp. nov., Upper Ordovician, Bromide Formation (Simpson Group), Arbuckle Mountains region, south-central Oklahoma. **A**–**D,** partially exfoliated cranidium (OU 12499), × 2; **A,** posterior view; **B,** lateral view; **C,** dorsal view; **D,** anterior view, × 3. **E,** thoracopygon (OU 12500), × 1.5, dorsal view. **F,** exfoliated cranidium (OU 12501), × 2, dorsal view.

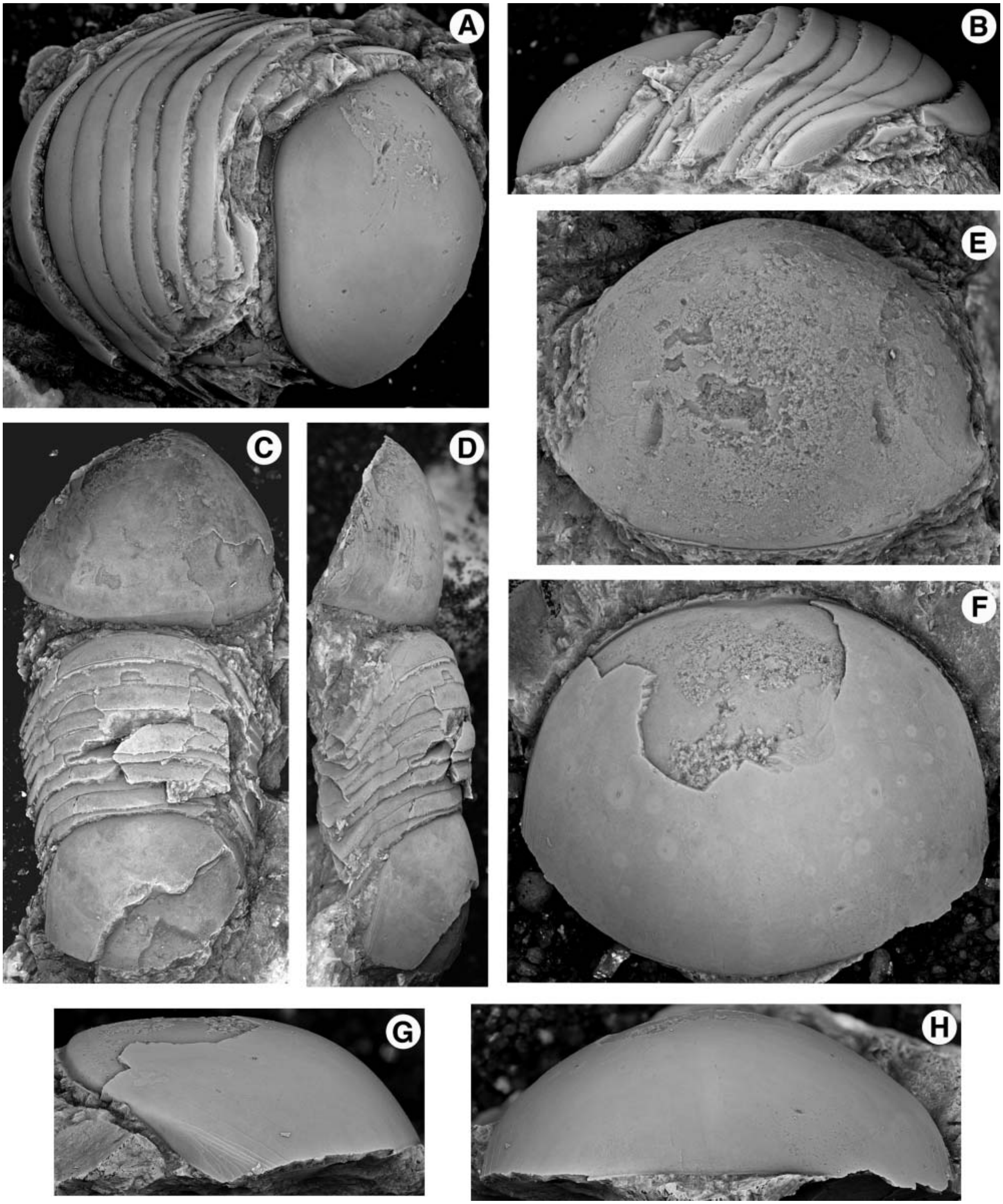

Figure 20. *Bumastoides moundensis* sp. nov., Upper Ordovician, Effna Formation, Smyth County, south-western Virginia. **A, B,** thoracopygon (OU 12503), × 1; **A,** dorsal view; **B,** lateral view. **C, D,** holotype, exfoliated dorsal exoskeleton (OU 12502), × 1; **C,** dorsal view; **D,** lateral view. **E,** exfoliated cranidium (OU 12504), × 1.6, dorsal view. **F**–**H,** testate pygidium (OU 12505), × 1.5; **F,** dorsal view; **G,** lateral view; **H,** posterior view.

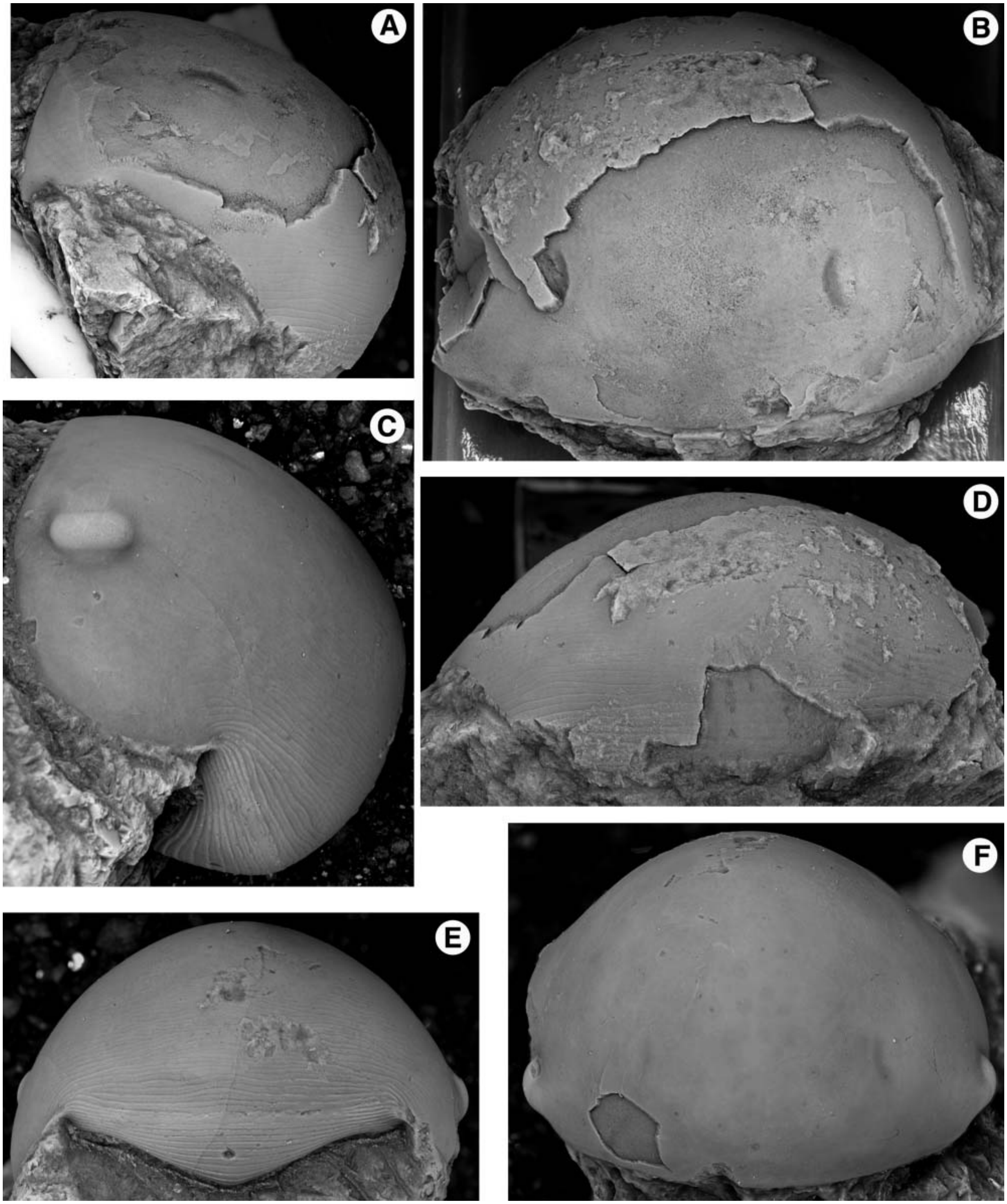

Figure 21. *Bumastoides moundensis* sp. nov. **A, B, D,** exfoliated cranidium (OU 12506); Upper Ordovician, Botetourt Limestone, Bland County, Virginia, × 1.5; **A,** lateral view; **B,** dorsal view; **D,** anterior view. **C, E, F,** testate cranidium (OU 12507); Upper Ordovician, Effna Formation, Smyth County, south-western Virginia, × 2; **C,** lateral view, × 1.5: **E,** anterior view; **F,** dorsal view.

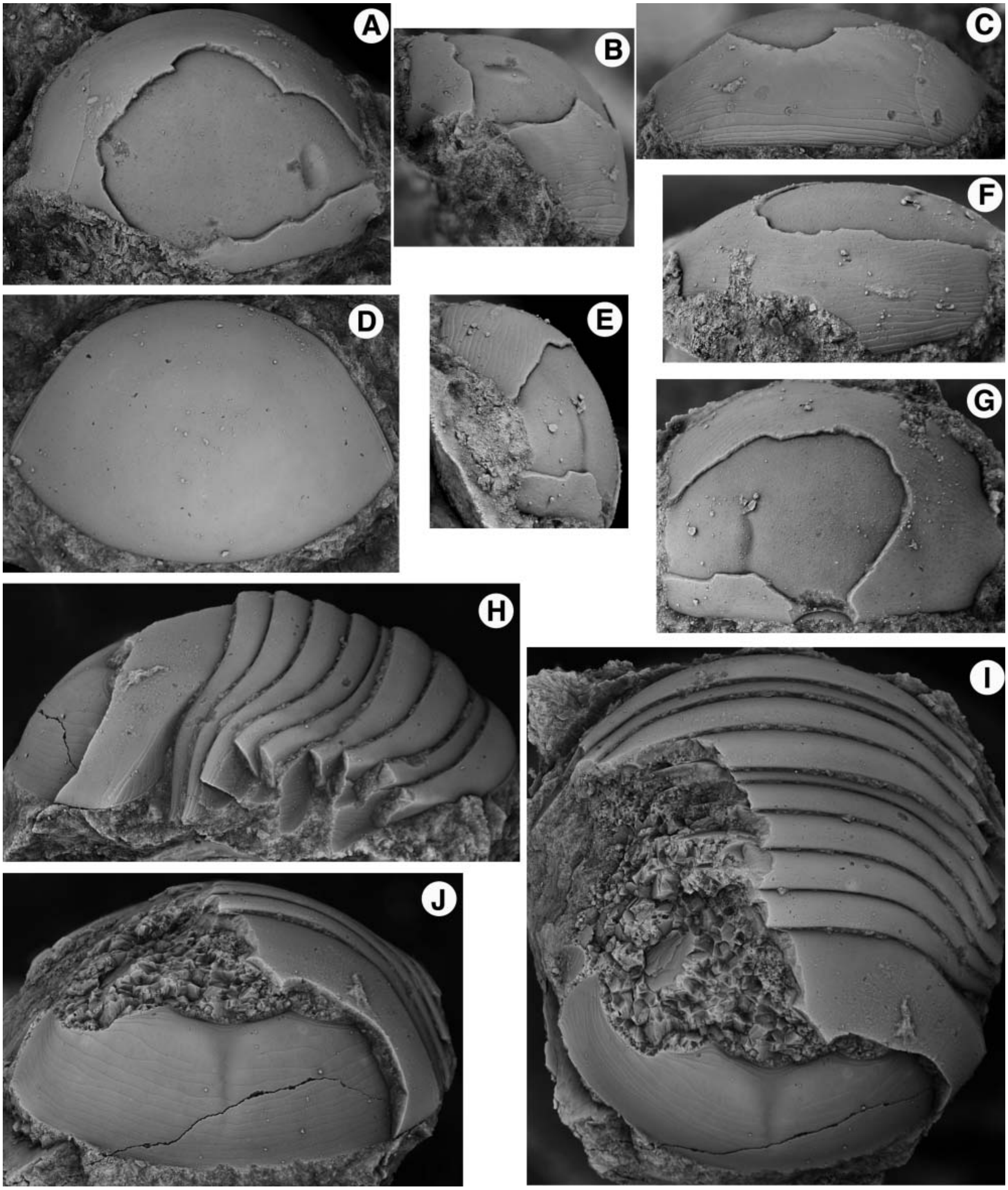

Figure 22. *Bumastoides kimmswickensis* sp. nov., Upper Ordovician, Kimmswick Limestone, Jefferson County, Missouri. **A**–**C,** partially exfoliated cranidium (OU 12509), × 2.8; **A,** dorsal view; **B,** lateral view; **C,** anterior view. **D,** pygidium (OU 12511), × 4.1, dorsal view. **E**–**G,** partially exfoliated cranidium (OU 12510), × 5; **E,** lateral view; **F,** anterior view; **G,** dorsal view. **H**–**J,** holotype, thoracopygon (OU 12508), × 3; **H,** lateral view; **I,** dorsal view; **J,** posterior view.

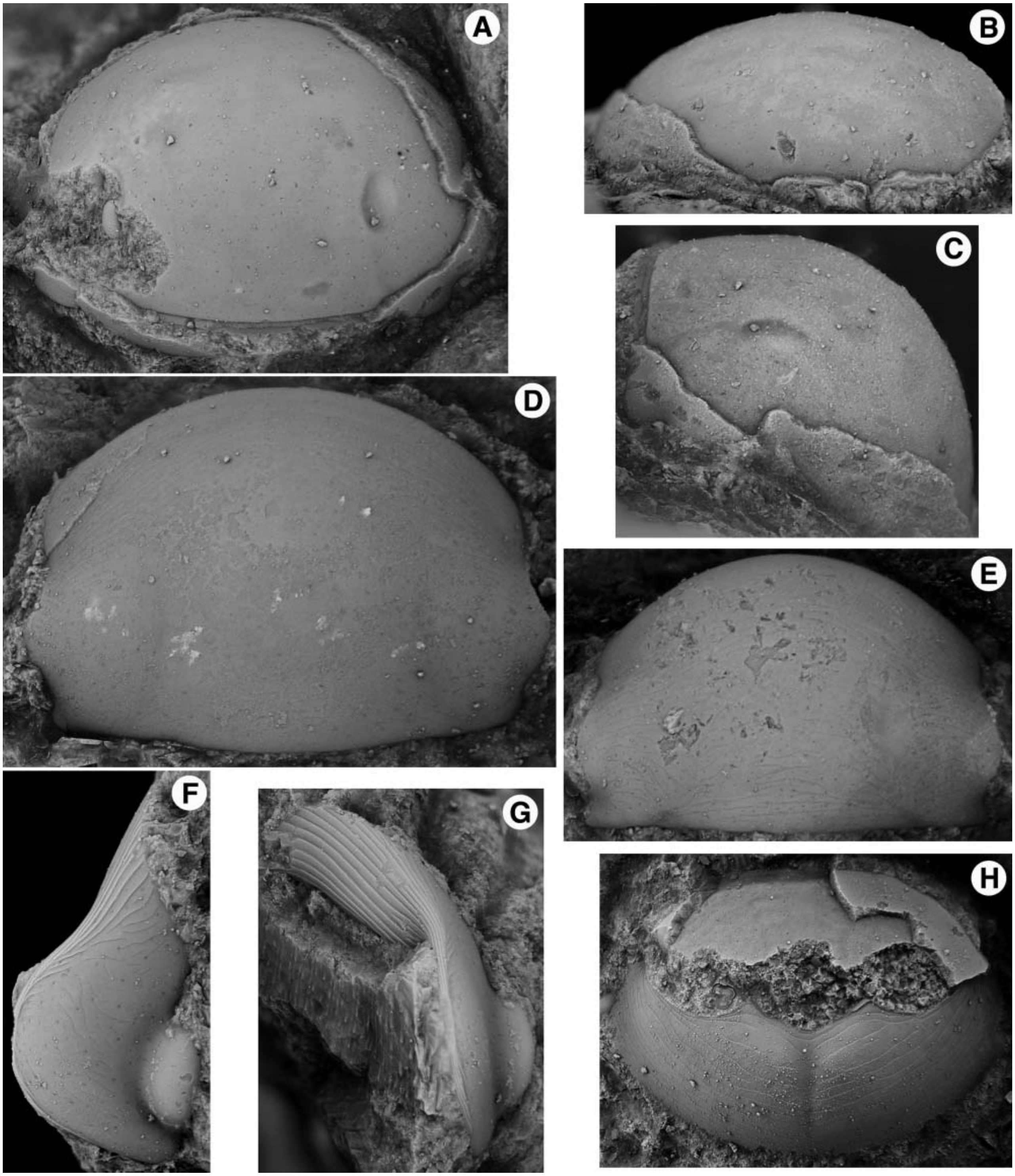

Figure 23. *Bumastoides kimmswickensis* sp. nov., Upper Ordovician, Kimmswick Limestone, Jefferson County, Missouri. **A**–**C,** exfoliated cranidium (OU 12512), × 4; **A,** dorsal view; **B,** anterior view; **C,** lateral view. **D,** testate cranidium (OU12513), × 6, dorsal view. **E,** testate cranidium (OU 12514), × 8, dorsal view. **F, G,** librigena (OU 12515), × 8; **F,** dorsal view; **G,** lateral view. **H,** exfoliated pygidium (OU 12516), × 4, dorsal view.

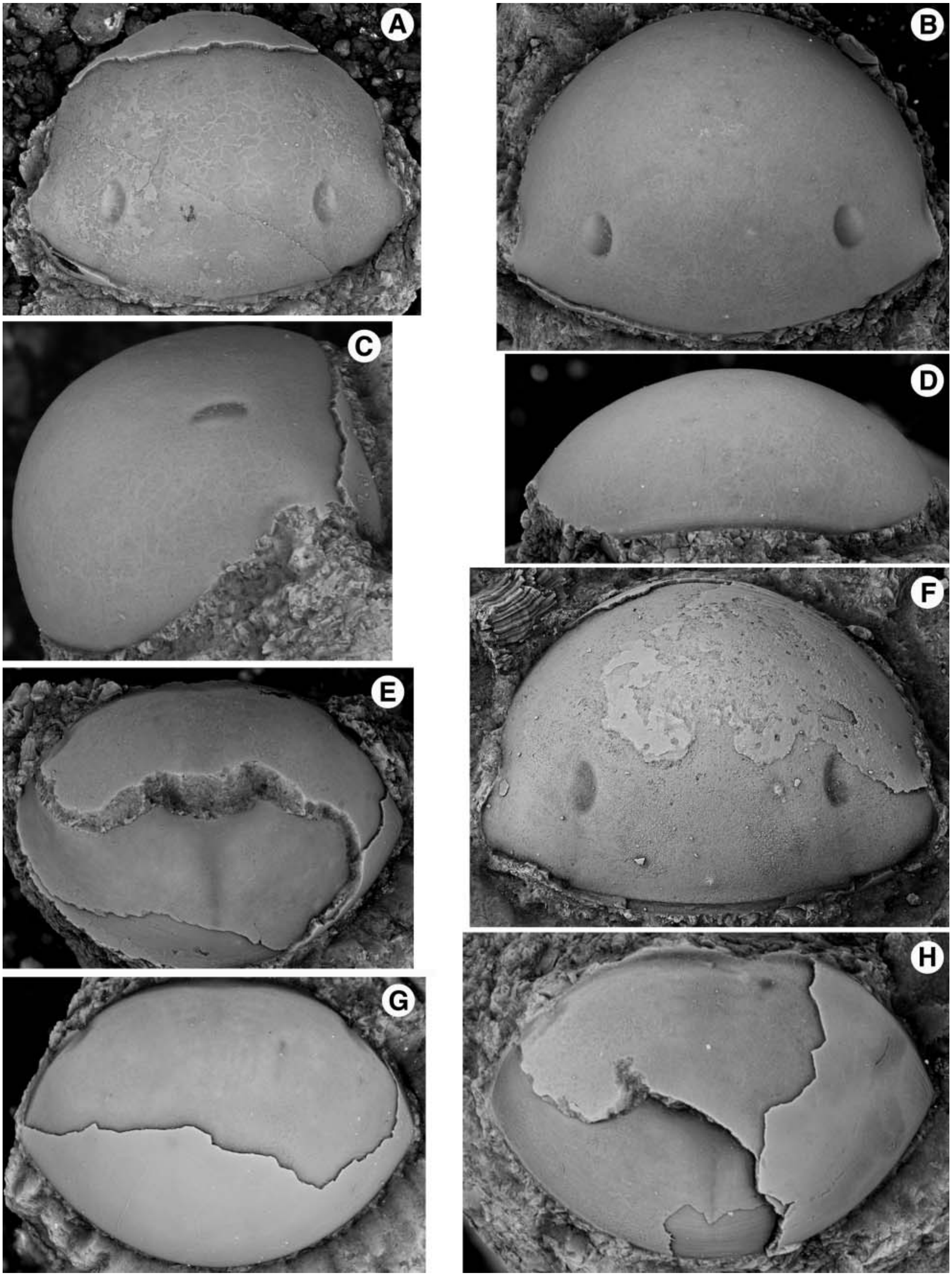
A
B
C
D
E
F
G
H

Ludvigsen & Chatterton (1980) and Chatterton (1980) demonstrated that illaenid trilobites could vary dramatically during their holaspid ontogeny (but not in the number of thoracic segments). Coupled with the lack of morphology in the group, it is clear that extreme rigour is necessary to delineate new species of *Bumastoides*.

Bumastoides milleri (Billings, 1859)
(Figs 6, 7)

1859 *Illaenus milleri* Billings: 375, fig. 10
1877 *Illaenus milleri* Billings; Walcott: 71.
1908 *Bumastus milleri* (Billings); Raymond & Narraway: 254, pl. 61, figs 3–5, 9, 10.
? 1927 *Bumastus milleri* (Billings); Walter: 222, pl. 17, fig. 2.
1954 *Bumastoides milleri* (Billings); Whittington: 224, pl. 62, figs 16–18, 20, 25, 26, 29.
1957 *Bumastus trentonensis* Fisher: 16, pl. 6, fig. 9.
1987 *Bumastoides milleri* (Billings); DeMott: 91, pl. 6, figs 20–23.
1997b *Bumastoides milleri* (Billings); Whittington: 12, fig. 9, 1–4.
non 2002 *Bumastoides milleri* (Billings); Whiteley *et al*.: 211, pl. 6.

Diagnosis. Median tubercle present and circular (character 3, state 1), lunette predominantly crescentic (character 4, state 0), nine thoracic segments (character 8, state 0), low length to width ratio of pygidia (51–58%) (character 16, state 0).

Material. Figured material includes four incomplete individuals (holotype, GSC 1319b, Fig. 6A–D; NYSM 10757, Fig. 7A, B, E, F; SUI 125988, Fig. 7C, G; and SUI 125975, Fig. 7D, H), one incomplete cranidium (MCZ 145734, Fig. 6E–G). Unfigured material includes one thoracopygon (MCZ 107232, DeMott 1987, pl. 6, figs 2020, 21), one nearly complete individual (MCZ107233, DeMott 1987, pl. 6, fig. 22, 23), and 10 other partial specimens (SUI 125976-79, 125981-82, 125985-87, 125989).

Occurrence. Upper Ordovician (Sandbian–Katian) of the Selby Formation and 'Rockland Formations' (lower Trenton Group), New York and Ontario, the Platteville Group (Iowa, Wisconsin and Illinois), and the Maquoketa Formation of Iowa.

Description. Cranidium occupies 36–38% of total exoskeletal length; elliptical, length 66–70% of width across palpebral lobes; inflated, longitudinal and transverse profiles strongly convex, anterior part of the cranidium curving downwards strongly. Anterior margin convex forwards, posterior margin slightly convex backwards, flattened medially. Axial furrows weak, terminating just posterior of lunettes. Lunettes just forward of palpebral lobe, comprise 18–23% of cranidial length (exsag.), each equal to 6–7% of cranidial width opposite palpebral lobes, crescentic, deeply impressed adaxially then shallowing abaxially; expressed on both external surface (Fig. 6F) and internal mould (Fig. 7B) Eyes large, crescentic, situated close to posterior margin, account for 31–35% of cranidial length in lateral view. Palpebral lobes semicircular, each equal to 22–25% of cranidial length and 4–5% of width, palpebral furrow extremely weak, primarily defined by change in slope at fixigena, curved slightly inwards. Posterior branch of facial suture extends backwards and outwards to the posterior margin, posterolateral projection subtriangular, sharply terminating at a point behind the eye. Anterior branches converge forward and downward along curved paths, joining rostral suture at a point approximately in front of lunette. Librigena subsemicircular with rounded genal angle, dorsal surface smooth except for terrace lines which extend over sutural margin onto posterior margin of librigena. Exoskeletal surface smooth posteriorly, slightly undulating closely packed terrace lines present only abaxially, becoming more widely spaced, prominent, and medially complete towards anterior margin. Widely spaced pits present on cranidial internal mould. Circular median tubercle present on dorsal surface, close to posterior margin (Fig. 7A, B).

Thorax of nine segments; strongly convex (tr.), longitudinal profile nearly flat. Axial furrows very weak, defined only by slight change in pleural angle at fulcrum. Axis wide, evenly arched (tr.), subrectangular in outine, comprising approximately 79–80% of thoracic width. Axial rings subrectangular, narrowing (sag.) very slightly backwards. Pleura without furrows, slightly narrower (sag.) than axial rings, directed primarily outwards and downwards (minimally fulcrate), terminations rounded. Articulating facets rounded subtriangular, with eight to nine terrace lines that initially nearly parallel each other, than converge upwards, extend to just below the axial furrow, well-defined border.

Pygidium wide (tr.) and short (sag.), accounts for 28–32% of total exoskeletal length; subtrapezoidal with rounded anterior corners, sharp posterior corners, and well-rounded posterior margin, length equal to 51–58% of maximum width, longitudinal profile initially convex backwards lightly, then strongly convex backwards towards posterior end, convex (tr.) abaxially, flat medially. Axis

←

Figure 24. *Bumastoides* cf. *milleri* (Billings, 1859), Upper Ordovician, Viola Springs Formation (Viola Group), near Fittstown, south-central Oklahoma. **A,** exfoliated cranidium (OU 12517), × 2, dorsal view. **B**–**D,** exfoliated cranidium (OU 12037), × 2; **B,** dorsal view; **C,** lateral view; **D,** anterior view. **E,** exfoliated pygidium (OU 12519), × 2, dorsal view. **F,** exfoliated cranidium (OU 12518), × 2.5, dorsal view. **G,** partially exfoliated pygidium, (OU 12039), × 2, dorsal view. **H,** partially exfoliated pygidium (OU 12520), × 3, dorsal view.

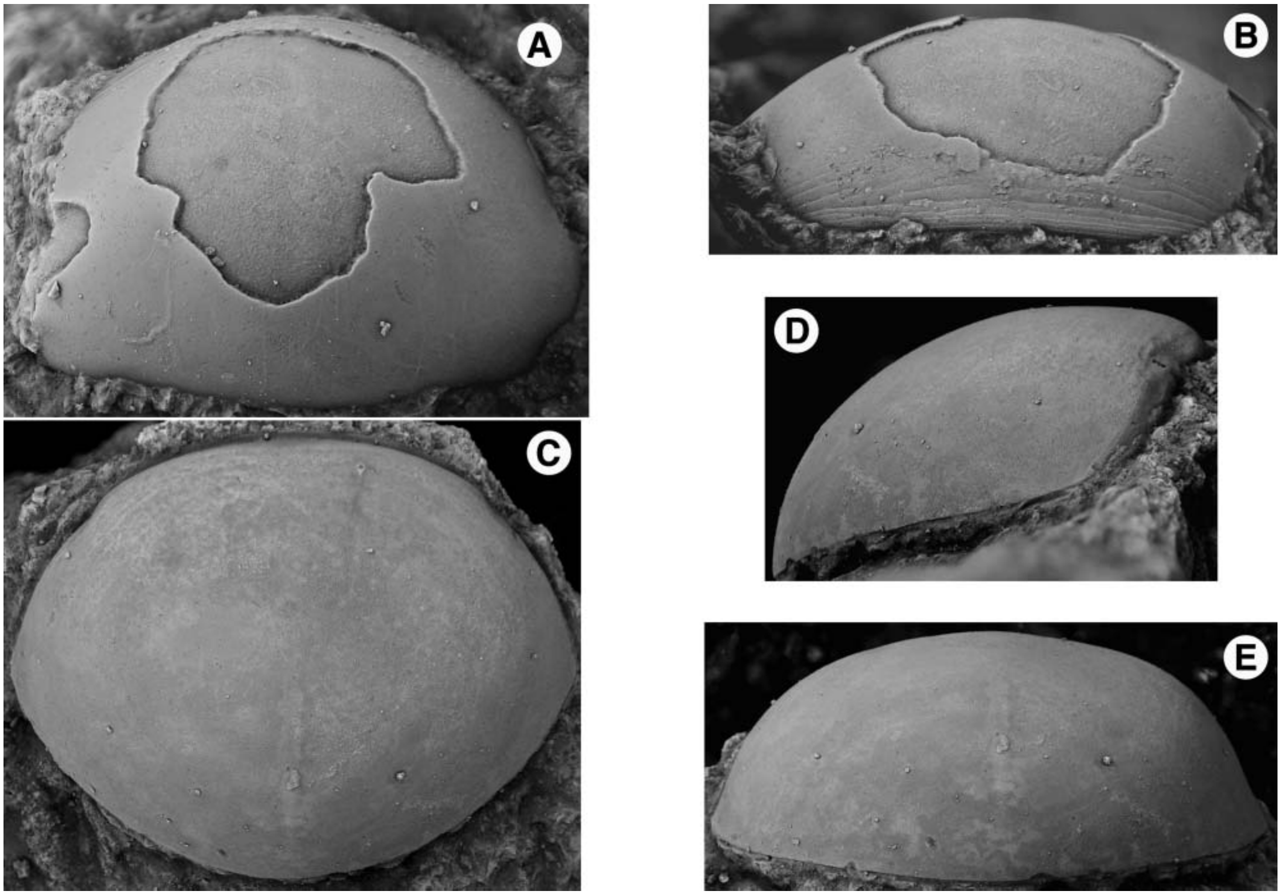

Figure 25. *Bumastoides* cf. *milleri* (Billings, 1859), Upper Ordovician, Viola Springs Formation (Viola Group), near Fittstown, south-central Oklahoma. **A, B,** mostly testate cranidium (OU 12521), × 4.2; **A,** dorsal view; **B,** posterior view. **C**–**E,** exfoliated pygidium (OU 12522), × 2; **C,** dorsal view; **E,** posterior view, × 2.5; **D,** lateral view.

undifferentiated. Dorsal inner margin of pygidial doublure appears bicuspid and curved backward, terrace lines extend inward and slightly downward, dorsal most terrace lines mirror angle of inner margin. Articulating facet subsemicircular with well-defined border, rounded ventral margin, six undulating terrace lines converge upwards, extends dorsally to axial furrow. Dorsal exoskeleton smooth except for three straight terrace lines that follow lateral margins, and three undulating terrace lines that extend inward and upward from lateral margins. Widely spaced pits present on pygidial internal mould.

Remarks. *Bumastoides milleri* has been used as a catch-all for *Bumastoides*-type trilobites since it was first described by Billings (1859). Clarke (1897) and Whittington (1954) assigned holaspid material with anywhere from eight to 10 thoracic segments to *B. milleri*. Walter (1927) assumed a cranidium from the Platteville Limestone in Iowa was *B. milleri*, even though it was damaged and indistinct. Whiteley *et al.* (2002, p. 211, pl. 6) assigned a specimen with 10 thoracic segments to *B. milleri*. As advocated by DeMott (1987), and from the type material from Ontario, *B. milleri* should be restricted to species with nine thoracic segments. Species with eight or 10 segments show consistent character assemblages that separate them from *B. milleri* (see other diagnoses).

Clarke (1897) considered *Bumatoides milleri* to be a synonym of *Illaenus trentonensis* Emmons, 1842. The location of the original *I. trentonensis* material is not known, but the small illustration (Emmons 1842, p. 390, fig. 3) shows a trilobite with well-incised axial furrows, eight thoracic segments, a subtriangular pygidium, and a rather flattened cranidial profile. An assignment of this species to *Bumastoides* is doubtful at best (see also Raymond 1925). Later hypotypes (Clarke 1897; Fisher 1957) of '*B. trentonensis*' can confidently be assigned to other Trenton species of *Bumastoides* (*B. milleri*, NYSM 10757, Fig. 7A, B, E, F; *B. porrectus*, NYSM 4158, Fig. 16A–E).

Bumastoides billingsi (Raymond & Narraway, 1908)
(Figs 8, 9)

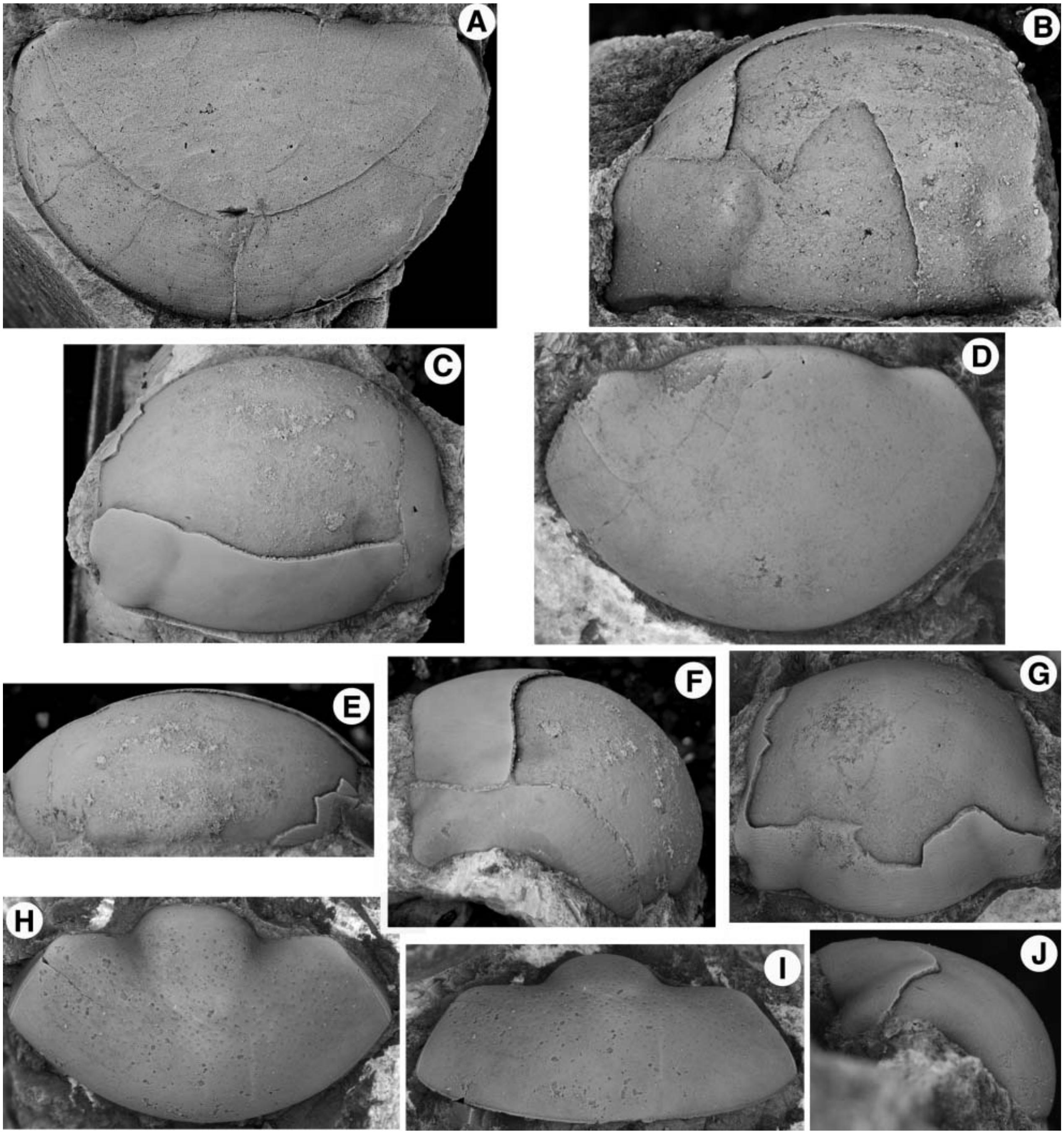

Figure 26. **A, B,** '*Stenopareia*' *rivulus* (Ingham & Tripp, 1991), Upper Ordovician, Doularg Formation (Albany Group), south-west Scotland. **A,** exfoliated pygidium (GLAHM A8313), × 1.5, dorsal view (Ingham & Tripp 1991, fig. 10f). **B,** holotype, exfoliated cranidium (LAHM A8302), × 3, dorsal view (Ingham & Tripp 1991, fig. 10a-b). **C**–**F,** '*Stenopareia*' *aplatus* (Raymond, 1925), Middle Ordovician, lower Chazy Group, Isle La Motte, Vermont. **C, E, F,** holotype, partially exfoliated cranidium (MCZ 101150), × 2 (Raymond 1925, pl. 8, fig. 3); **C**, dorsal view; **E,** anterior view, × 2.5; **F,** lateral view, × 2.3. **D,** testate pygidium (MCZ 101151), × 2.5, dorsal view (Raymond 1925, pl. 8, fig. 4). **G**–**J,** '*Stenopareia*' *gardensis* (Shaw, 1968), Middle Ordovician, Day Point Formation (Chazy Group), near Chazy, New York. **G, J,** holotype, partially exfoliated cranidium, (NYSM 12456), × 4 (Shaw 1968, pl. 16, figs 12, 15, 17); **G,** dorsal view; **J,** lateral view. **H, I,** testate pygidium, (NYSM 12457), × 3 (Shaw 1968, pl. 16, figs 13, 16); **H,** dorsal view; **I,** posterior view.

1908 *Bumastus billingsi* Raymond & Narraway: 253, pl. 62, figs 1, 2.

1913 *Bumastus billingsi* Raymond & Narraway; Raymond: 34, pl. 3, fig. 12.

1930 *Bumastus billingsi* Raymond & Narraway; Bradley: 254, pl. 28, figs 1–7.

1979 *Bumastoides billingsi* (Raymond & Narraway); Ludvigsen: 47, fig. 28C, D.

Diagnosis. Predominant shape of lunette is elliptical (character 4, state 1), path of the cranidial axial furrow is straight (character 5, state 0), 10 thoracic segments (character 8, state 2), large paired muscle scars present on pygidium (character 11, state 1), ratio of pygidial length to width is high (76–83%) (character 16, state 3), axial furrow expressed as notches flanking centre of the pygidial anterior margin (character 17, state 0).

Material. Figured material includes two exfoliated, nearly complete individuals (plastotype CM 5472, Fig. 8A–E, see also Ludvigsen 1979, fig. 28C, D for images of the actual specimen; UC 10776, Fig. 9F, I–J), one exfoliated cranidium (UC 20700a, Fig. 9A–C), and two exfoliated pygidia (UC 20710a, Fig. 9D, E; UC 20710b, Fig. 9G, H). Unfigured material includes one librigena (UC 5858a), four incomplete pygidia (UC5858b-d; UC20710c), and two exfoliated cranidia (UC5858e-f).

Occurrence. Upper Ordovician (Katian) of the Trenton Group, Hull Quebec, and the 'Kimmswick Limestone' (Dunleith Formation) of Missouri and Illinois.

Description. Cranidium occupies approximately 34% of total exoskeletal length, semicircular, length 67–74% of width across palpebral lobes; inflated, longitudinal and transverse profile strongly convex, anterior part of cranidium curving downwards strongly. Anterior margin strongly convex forwards, posterior margin gently convex backwards. Axial furrows straight, approximately 25% of maximum lunette width, terminating at adaxial side of lunette. Lunettes just forward of palpebral lobe, comprise 17–21% of cranidial length (exsag.), each equal to 8% of cranidial width opposite palpebral lobes, elliptical, deeply impressed only as a narrow adaxial band, otherwise uniform impression throughout. Eyes small, crescentic, situated close to posterior margin, accounts for 23–26% of cranidial length in lateral view. Palpebral lobes apparently semicircular. Anterior branches of facial suture converge forward and downward along curved paths. Anterior margin of rostral plate gently bowed, rostral plate apparently subtriangular. Librigena subsemicircular with strongly rounded genal angle, border well-defined, barely perceptible loosely spaced pitting on dorsal surface, terrace lines developed at a point anterior and ventral of palpebral lobes. Widely spaced pitting present on cranidial internal mould, median tubercle absent.

Thorax of 10 segments; strongly convex (tr.), longitudinal profile flat. Axial furrows defined only by slight change in pleural angle at fulcrum. Axis wide, evenly arched (tr.), subrectangular. Axial rings subrectangular, gradually narrowing (sag.) posteriorly. Pleura without furrows, slightly narrower (sag.) than axial rings, directed outwards and downwards (minimally fulcrate), terminations bluntly rounded. Thoracic dorsal exoskeleton smooth.

Pygidium accounts for 35% of total exoskeletal length; subtrapezoidal, anterior corners and posterior margin well rounded, length equal to 76–83% of maximum width, longitudinal profile initially flat, then convex towards the posterior end, gently convex (tr.). Axis expressed as a slight protrusion medially, slight depressions laterally flanking axis. Anterior ventral ridge pronounced, following curvature of the anterior margin. Doublure inner margin dicuspid, median depression on doublure wide, terminates just above posterior margin. Paired subrectangular muscle scars, evenly distributed pits, and median ridge expressed on internal mould.

Remarks. Raymond & Narraway (1908) described *Bumastoides billingsi* as a new species, citing its large size, stronger cranidial dorsal furrows, wider thoracic axis, and stronger lunettes as the primary differences between it and *B. milleri*. They also suggested that *B. billingsi* could be synonymous with Emmon's (1842) larger specimen of *Bumastus trentonensis* (Emmons, 1842, p. 390, fig. 1). Like the smaller specimen (Emmons 1842, p. 390, fig. 3, see Remarks under *B. milleri*) this specimen almost certainly does not belong to *Bumastoides*. The elongated pygidium and well-incised axial furrows that diverge beyond the lunettes strongly suggest this material is best assigned to *Failleana* Chatterton & Ludvigsen, 1976.

Bradley (1930) described material from the Kimmswick Limestone (Fig. 9) that we consider conspecific with the material from Quebec. He noted the similarity with *B. holei*, a sister-taxon relationship present in 3/8 of our MPTs. Both are of generally very large size, have deep, elliptical lunettes, a wide thoracic axis, and well-defined, paired pygidial muscle scars. *B. billingsi* differs from *B. holei* in the length/width ratio of the pygidium (70–74% in the latter, 76–83% in the former), the residual axis expression at the pygidial anterior border, and the density of cranidial internal mould pitting.

Bumastoides bellevillensis (Raymond & Narraway, 1908)
(Fig. 10)

1908 *Bumastus bellevillensis* Raymond & Narraway: 253, pl. 61, figs 6, 7.

Diagnosis. Median cranidial tubercle present (character 3, state 1), eight thoracic segments (character 8, state 1), median pygidal depression on doublure effaced posteriorly (character 13, state 2); median ridge on cranidial internal mould.

Material. One incomplete entire individual (holotype CM 1900, Fig. 10A–E).

Occurrence. Upper Ordovician (Katian) of the Trenton Group (almost certainly Verulam Formation; Ludvigsen 1979, fig. 3), Belleville, Ontario.

Description. Cranidium comprises 36% of total exoskeletal length; elliptical, length 66% of width at palpebral lobes; inflated, longitudinal and transverse profile strongly convex, anterior part of cranidium curving downwards strongly. Anterior margin convex forwards, posterior margin gently convex backwards. Median cranidial ridge present on internal mould, extends from just above anterior margin to a point near lunette base. Axial furrows narrow, converging gently forward, terminating at adaxial side of lunette, width approximately 20% of maximum lunette width. Lunettes just forward of palpebral lobe, occupying 21% of cranidial length (exsag.) each equal to 8% of width across palpebral lobes, deeply impressed adaxially, shallowing abaxially. Eyes crescentic, located close to posterior margin, account for 32% of cranidial length in lateral view. Palpebral lobes semicircular, each equal to 21% of cranidial length and 5% of cranidial width, palpebral furrow extremely weak, defined largely by change in slope at fixigena. Posterior branch of facial suture extends straight backwards to posterior margin (posterolateral projection absent). Anterior branches converge forward and downward along gently curved paths, joining rostral suture at a point in front of lunette. Anterior margin of rostral plate nearly transverse. Librigena apparently subsemicircular with rounded genal angle, dorsal surface smooth, well defined terrace lines present on rounded lateral and ventral margins of librigena. Tightly packed, transverse terrace lines on rostral plate. Pitting on cranidial internal mould widely spaced and evenly distributed. Circular posterior median tubercle present on cranidial internal mould.

Thorax of eight segments; strongly convex (tr.), longitudinal profile nearly flat. Axial furrows very weak, bowed outwards near mid-length of thorax. Axis wide, evenly arched (tr.), subrectangular. Axial rings subrectangular, narrowing (sag.) slightly backwards. Pleura without furrows, directed strongly downwards, slightly backwards and outwards at fulcrum. Articulating facets broad, slightly overlapping each other; subtriangular, extend upwards to axial furrow, six terrace lines converge upwards. Dorsal surface smooth.

Pygidium occupies 33% of total exoskeletal length; subtrapezoidal, with gently rounded anterior corners, and well-rounded posterior margin, length equal to 66% of maximum width, longitudinal profile initially flat, then convex backwards towards the posterior end, convex (tr.) abaxially, nearly flat medially, axis undifferentiated. Dorsal inner margin of doublure curved backwards and bicuspid, median depression present only anteriorly. Evenly spaced, slightly undulating terrace lines transverse across doublure, near inner margin terrace lines extend dorsally along cusps, effaced medially.

Remarks. *Bumastoides bellevillensis* is easily distinguishable from other species because it has three autapomorphies: a sagittal ridge on the cranidum, eight thoracic segments, and a depression on the dorsal surface of doublure that is only expressed anteriorly.

Bumastoides beckeri (Slocom, 1913)
(Figs 11, 12)

1913 *Bumastus beckeri* Slocom: 54, pl. 14, figs 1–4.
1927 *Bumastus milleri* Walter: 220, pl. 18, figs 10, 11.

Diagnosis. Continuous terrace lines cover entire cranidial exoskeleton (character 7, state 2), thorax of 10 segments (character 8, state 2), concentric terrace lines on pygidium present (character 14, state 1), undulatory terrace lines directed inwards from pygidial lateral margins present (character 15, state 0); transverse terrace lines present on the first four segments of the thorax.

Material. Figured material includes a nearly complete enrolled specimen (holotype UC 41154, Fig. 11A–E), a nearly complete individual (SUI 125973, Fig. 12A–F), a partially exfoliated individual (SUI 125984, Fig. 12G, H) and an incomplete thoracopygon (P 16708, Fig. 11F, G).

Occurrence. Upper Ordovician (Hirnantian) of the Maquoketa Formation, Fayette County, Iowa.

Description. Cranidium accounts for 32–34% of total exoskeletal length; semicircular, length 70% of width across palpebral lobes; inflated, longitudinal and transverse profiles convex, anterior part of cranidium curving downwards strongly. Anterior margin convex forwards, posterior slightly convex backwards. Axial furrows completely effaced, lunettes just forward of palpebral lobe, elliptical, equal impression throughout, occupying 29% of cranidial length (exsag.), each lunette equal to 4% of cranidial width across palpebral lobes. Eyes small, crescentic, situated close to posterior margin, occupy 28–30% of cranidial length in lateral view. Palpebral lobes semicircular, each comprises 3–4% of cranidial width, equal to 13% of cranidial length, palpebral furrow only defined by change in slope at fixigena. Posterior branch of facial suture extends backwards and outwards forming a small posterolateral projection. Anterior branches converge forward and downward along gently curved paths, intersection with rostral suture not preserved. Librigena subsemicircular, with well-rounded genal angle and well-defined border. Dorsal surface covered in continuous, transverse, slightly undulatory terrace lines (including librigena), with slight hiatuses near lunette and postocular area; barely perceptible pitting present between terrace lines. Posterior median tubercle absent.

Thorax of 10 segments; strongly convex (tr.), axial furrows weak, bowed outwards near thoracic mid-length. Axis wide, subrectangular, evenly arched (tr.), comprising 79–81% of thoracic width. Axial rings subrectangular, narrowing slightly in length (sag.) backwards, four to five terrace lines present on first three segments, two ridges on fourth segment. Pleura without furrows, slightly narrower than axial rings, directed outwards and downwards (minimally fulcrate), terminations transverse, with well-defined border. Articulating facets subtriangular, slightly overlapping, broad, extend to just below axial furrow, nine to 10 terrace lines converge upwards. Aside from terrace lines, thoracic dorsal exoskeletal surface smooth.

Pygidium occupies 31–32% of total exoskeletal length; subtrapezoidal with rounded anterior corners and well-rounded posterior margin, length equal to 61–63% of maximum width, longitudinal profile initially flat, abruptly convex backwards towards posterior end, strongly convex (tr.) abaxially, weakly convex medially (tr.). Axis undifferentiated. Articulating facet subtriangular, extending to just below the axial furrow. Three widely spaced concentric terrace lines on dorsal surface mirror pygidial outline, terminating near posterior margin. Undulating terrace lines extend inward from lateral margins, effaced medially.

Remarks. Slocom (1913) considered *Bumastoides beckeri* to be closely allied with *B. billingsi* based on its gross morphology. *Bumastoides beckeri* is more closely related to *B. kimmswickensis* (see Remarks below for a comparison), a species not known by Slocom. They are sister taxa, united by their shared possession of terrace lines over the majority of the cranidial exoskeleton. New material from the Maquoketa of Fayette County, Iowa (Fig. 12), is conspecific with the holotype.

Bumastoides holei (Foerste, 1920)
(Figs 13, 14)

1920 *Bumastus holei* Foerste: 214, pl. 21, fig. 15a, b, pl. 22, figs a, b.
1925 *Bumastus holei* Foerste; Raymond: 213, pl. 8, figs 5, 6.
1999 *Bumastoides holei* (Foerste); Brett *et al*.: 294, pl. 7, fig. 4.
2002 *Bumastoides holei* (Foerste); Whiteley *et al*.: 209, pls 4, 5.

Diagnosis. Path of the posterior branch of the facial suture is straight backwards (character 2, state 0), median tubercle present near posterior margin of cranidium (character 3, state 1), predominant shape of lunette is elliptical (character 4, state 1), pitting on cranidial internal mould densely distributed (character 6, state 2), paired pygidial muscle scars visible (character 11, state 1), concentric terrace lines present on pygidial exoskeleton (character 14, state 1); thoracic and pygidial surface granulose.

Material. Figured material includes two exfoliated but otherwise nearly complete individuals (MCZ 144798, Figs 13E, F, 14A–C; plesiotype MCZ 101148, Fig. 13A–D), and one complete individual (MCZ 115909, Fig. 14D–H). Unfigured material includes two incomplete whole individuals (MCZ 144799; 145650), and one exfoliated cranidium with partial thorax (NYSM E998).

Occurrence. Upper Ordovician (Katian) of the Rust Formation (Trenton Group), Trenton Falls, New York and the Kimmswick Limestone of Ralls County, Missouri.

Description. Cranidium accounts for 35–36% of total exoskeletal length; semicircular, length 68–69% of width across palpebral lobes; strongly inflated, longitudinal and transverse profiles convex, anterior part of cranidium curving downwards strongly. Anterior margin convex forwards, posterior margin nearly transverse. Axial furrows weak, converging slightly inwards, terminating on adaxial side of lunette, width approximately 40% of maximum lunette width. Lunettes large, just forward of palpebral lobes, comprise 26–28% of cranidial length (exsag.), each equal to 11–12% of cranidial width across palpebral lobes, elliptical, deeply impressed adaxially, otherwise equal impression throughout. Eyes small, approximately equal in length to lunette, crescentic, situated close to posterior margin, occupies 25–28% of cranidial length in lateral view. Posterior branch of facial suture extends straight backwards (posterolateral projection absent) to posterior margin. Anterior branches initially divergent, then converging forward and downward along gently curved paths, apparently joining rostral suture at a point forward of lunette. Librigena subsemicircular, with well-rounded genal angle. Dorsal surface smooth except for thin, undulating, evenly spaced terrace lines on anterior portion of cranidium, internal mould of cranidia heavily punctate, evenly distributed small pits over entire surface. Circular posterior median tubercle present on cranidial internal mould.

Thorax of 10 segments; strongly convex (tr.), longitudinal profile flat. Axial furrows weak, slightly bowed outwards near mid-length of thorax. Axis wide, subrectangular, evenly arched (tr.), comprising 74–76% of thoracic width. Axial rings subrectangular, narrowing (sag.) slightly backwards. Pleura without furrows, slightly narrower than axial rings, directed outwards and downwards (minimally fulcrate), terminations transverse. Articulating facets broad, non-overlapping, subtriangular, extending to just below axial furrow, seven to nine terrace lines converge upwards. Thoracic dorsal exoskeletal surface covered in very fine granules of approximately even size.

Pygidium accounts for 33–35% of total exoskeletal length; subtrapezoidal with rounded anterior corners and well-rounded posterior margin, length equal to 70–74% of maximum width, longitudinal profile initially flat, gently convex backwards towards posterior end, strongly convex (tr.) abaxially, weakly convex medially. Axis undifferentiated. Depression present medially on doublure, extending to posterior margin. Paired subrectangular muscle scars visible on internal mould. Articulating facet subsemicircular, extending to anterior corner, six terrace lines converge upwards. Six weak, evenly spaced concentric terrace lines on the dorsal surface mimic the pygidial outline, terminating near posterior margin, effaced medially. Granules on exoskeleton similar in shape and distribution to thorax. Pitting on internal mould of same size and distribution as crandia.

Remarks. The original material (a cranidium and associated pygidia) described by Foerste (1920) is from the Kimmswick Limestone, though the location of the type material is currently unknown (Brett *et al.* 1999). Raymond (1925) redescribed the species based on material from the Trenton Formation collected by C. D. Walcott, some of which is re-illustrated here. He noted the close similarity between *Bumastoides holei* and *B. billingsi*, citing the possession of the cranidial median tubercle, fainter dorsal furrows, and the strongly punctate appearance of the internal cast as the primary differences. We add to those differences the granulose texture of the surface (covaries with the pitting on the internal mould, but seems absent on the cranidial surface), and the lack of axis expression at the anterior border. Brett *et al*. (1999) and Whiteley *et al.* (2002) illustrated more of the Trenton material (MCZ 115909, Fig. 14D–H), but did not describe it.

Bumastoides porrectus (Raymond, 1925) (Figs 15, 16)

1897 *Bumastus trentonensis* Clarke: 718, fig. 32.
1925 *Bumastus porrectus* Raymond: 213, pl. 8, figs 7, 8.
1947 *Bumastus porrectus* Raymond; Wilson: 35, pl. 7, figs 7–9.
1987 *Bumastoides porrectus* (Raymond); DeMott: 91, pl. 6, figs 24–28, 30, 31.
1999 *Bumastoides porrectus* (Raymond); Brett et al.: 294, pl. 7, fig. 5.
2002 *Bumastoides porrectus* (Raymond); Whiteley *et al*.: 212, pl. 7.

Diagnosis. Posterior median tubercle faint, but present (character 3, state 1), 10 thoracic segments (character 8, state 2), pygidial concentric terrace lines absent (character 14, state 0), undulatory terrace lines on pygidia absent (character 15, state 0).

Material. Figured material includes two complete individuals (holotype MCZ 101147, Fig. 15A, B, D–F; NYSM 4158, Fig. 16A–E), one complete cranidium (MCZ 107234, Fig. 15C), one exfoliated cranidium (MCZ 107235, Fig. 15H), and one partially exfoliated pygidium (MCZ 107236, Fig. 15G).

Occurrence. Upper Ordovician (Katian) of the Denley Formation (Trenton Group), Trenton Falls, New York and the Guttenberg Formation (Decorah Group), Iowa and Wisconsin.

Description. Cranidium occupies 37% of total exoskeletal length; semicircular, length 64–70% of width across palpebral lobes; inflated, longitudinal and transverse profile strongly convex. Anterior margin well rounded, convex forward, posterior margin very slightly convex backwards. Axial furrows very weak, converging slightly inwards, terminating on adaxial side of lunette, width approximately 75% of maximum lunette width. Lunettes just forward of palpebral lobe, comprise 21–25% of cranidial length (exsag.), each equal to 7% of cranidial width opposite palpebral lobes, elliptical, impression relatively even throughout. Eyes crescentic, situated directly in front of posterior margin, occupy 32–33% of cranidial length in lateral view. Palpebral lobes semicircular, each equal to 16–19% of cranidial length and 4–5% of width; palpebral furrow extremely weak, defined largely by change in slope at fixigena, curved slightly inwards. Posterior branch of facial suture extends backwards and outwards to posterior margin, outlining a small, triangular, posterolateral projection which sharply terminates behind the eye. Anterior branches initially subparallel forward, then converging forward and downward on slightly curved paths, apparently terminating at the rostral suture at a point forward and between lunette and palpebral lobe. Librigena narrow (tr.), subsemicircular, genal angle well rounded. Posterior and lateral exoskeletal surface smooth; shallow, discontinuous, undulating terrace lines developed forward of palpebral lobe, becoming straighter and more complete towards the anterior margin; extending just beyond the edge of librigena. Very small circular posterior median tubercle present on cranidial internal mould, barely perceptible on exoskeletal surface.

Thorax of 10 segments; strongly convex (tr.), longitudinal profile flat. Axial furrows very weak, defined only by slight change in pleural angle at fulcrum, bowed outwards near mid-length of thorax. Axis wide, subrectangular, evenly arched (tr.), occupying 76–81% of thoracic width. Axial rings subrectangular, maintaining equal length on all 10 segments. Pleura without furrows, approximately same length (sag.) as axial rings, directed outwards and downwards (minimally fulcrate), terminations gently rounded. Articulating facets broad, not overlapping, rounded subtriangular, dorsally terminating well before axial furrow, 10 terrace lines converge upwards. Thoracic dorsal exoskeletal surface smooth.

Pygidium accounts for 33–35% of total exoskeletal length; subtrapezoidal with rounded anterior corners and well-rounded posterior margin, length equal to 63–68% of maximum width, longitudinal profile initially flat, then convex backwards towards posterior end, weakly convex (tr.) medially, strongly convex (tr.) abaxially. Axis undifferentiated. Anterior ventral ridge pronounced, following curvature of the anterior pygidial margin. Articulating facet narrow (sag.), subtriangular, five terrace lines converge upwards. Dorsal surface smooth except for thin terrace lines along lateral margins, medially effaced near anterior pygidial margin.

Remarks. Raymond (1925) erected this species partly to accommodate an exoskeleton that Clarke (1897, NYSM 4158, Fig. 16A–E) identified as *Bumastus trentonesis* but which clearly was not conspecific with the types of *B. trentonensis* Emmons, 1842 (see Remarks under *B. milleri*). The holotype of *B. porrectus* (MCZ 101147, Fig. 15A, B, D–F) and Clarke's specimen come from the upper Trenton Group at Trenton Falls, New York State, and are clearly the same species. Raymond (1925) cited the "almost total absence" of dorsal furrows from the cranidium as the primary difference between *B. porrectus* and *B. milleri*. Distinguishing between completely effaced and very faint dorsal furrows (e.g. splitting character 1, state 1, into separate bins) is nearly impossible in *Bumastoides*, especially given the varying exposure to weathering between specimens. We think it better to distinguish *B. porrectus* from morphologically similar species (e.g. *B. milleri*; *B. holei*) based on more discrete characteristics such as the number of thoracic axial rings, and absence of sculpture.

DeMott (1987) described and figured new *Bumastoides porrectus* material from the Decorah Group of Wisconsin (Fig. 15C, G–H). We tentatively accept these as conspecific, except for the pygidia (*Bumastoides* cf. *porrectus*, Fig. 15G), which was found at a different locality from the cranidia, and has a more rounded outline than other *B. porrectus* pygidia. DeMott (1987) stated that the median cranidial tubercle was absent in all specimens of *B. porrectus*. Material he illustrated (MCZ 107235, Fig. 15H) has been exfoliated in the intervening years, and shows the tubercle. Furthermore, the holotype shows the tubercle through the exoskeleton under very high magnification. Rather than lacking this feature, it seems that the tubercle is simply less conspicuous than other species. In general, *B. porrectus* possess more subdued sculptural features across the entire exoskeleton, so the difficulty recognizing the median tubercle is not surprising. Brett *et al*. (1999) and Whiteley *et al*. (2002) re-illustrated the holotype, but did not redescribe it.

Bumastoides tenuirugosus (Troedsson, 1928)
(Fig. 17)

1928 *Bumastus tenuirugosus* Troedsson: 43, pl. 15, figs 1–10.
1983 *Bumastoides tenuirugosus* (Troedsson); Westrop & Ludvigsen: 39, pl. 4, figs 1, 2, 5, 7, 8, pl. 5, figs 1–6.

Diagnosis. Path of the axial furrow straight (character 5, state 0), pitting on the cranidial internal mould absent (character 6, state 0), terrace lines present on the entire cranidial exoskeleton (character 7, state 2), thorax of 10 segments (character 8, state 2), concentric terrace lines present on pygidial exoskeleton (character 14, state 1).

Material. Figured material includes one exfoliated thoracopygon (OU 12483, Fig. 17A, C), an incomplete cranidium (OU 12495, Fig. 17B, D, E) and an exfoliated pygidium (OU 12496, Fig. 17F, G). Unfigured material includes an incomplete cranidium.

Occurrence. Upper Ordovician (Katian) Cape Calhoun Formation of northern Greenland, and the Upper Ordovician (Katian) Selkirk Member of the Red River Formation, Garson, southern Manitoba.

Description. See Westrop & Ludvigsen (1983).

Remarks. Though *Bumastoides tenuirgusosus* has no definitive sister-taxon relationship with any other species (Fig. 4), it is most similar to *B. billingsi* in having straight cranidial axial furrows (though they are more deeply incised in the latter) and strong, elliptical lunettes. *B. tenuirgusosus* shares complete terrace lines (character 7; state 2) with the US midwestern species *B. beckeri* and *B. kimmswickensis*, but the MPTs do not indicate that this character is a synapomorphy that would unite all three taxa.

Raymond (1916) suggested that the number of thoracic segments could vary within a single species of *Bumastus* (*Bumastoides*). Troedsson (1928) took issue with this statement and while noting some degree of ontogenetic variation in *B. tenuirugosus*, indicated that even the smallest individuals of *B. tenuirugosus* have 10 thoracic segments.

Westrop & Ludvigsen (1983) described specimens of *Bumastoides tenuirugosus* from the Selkirk Member of the Red River Formation that is conspecific with the Cape Calhoun material. The sclerites illustrated here are also from the Selkirk Member at Garson, and are considered conspecific with all other specimens of *B. tenuirugosus*. Westrop & Ludvigsen (1983) noted the wide range of variation in the lunette definition and cranidial length/width ratio of the Selkirk material. These differences are likely due to preservation and ontogenetic variation (Westrop & Ludvigsen 1983), and all the material probably belongs to just the one species.

Bumastoides lenzi Chatterton & Ludvigsen, 1976

1976 *Bumastoides lenzi* Chatterton & Ludvigsen: 35, pl. 4, figs 40–42, pl. 5, figs 1–31.

Diagnosis. Posterior median tubercle absent (character 3, state 0), lunette predominantly crescentic (character 4, state 0), pitting on cranidial internal mould absent (character 6, state 1), concentric terrace lines absent on pygidium (character 14, state 0); cranidium subquadrate.

Occurrence. Upper Ordovician (Sandbian) of the Esbataottine Formation, of the South Nahanni River area of the District of Mackenzie, Canada.

Remarks. See *Bumastoides solangeae* below.

Bumastoides solangeae Hunda et al., 2003

2003 *Bumastoides solangeae* Hunda *et al.:* 11, pl. 1, figs 1–26.

Diagnosis. Median tubercle on cranidium absent (character 3, state 0), pygidium rounded subtrapezoidal (character 12, state 1), median dorsal depression (ventral ridge) on pygidial doublure absent (character 13, state 0); librigena subtriangular, subangular genal angles, cranidium subcircular.

Occurrence. Upper Ordovician (Hirnantian) of the Whittaker Formation, Mackenzie Mountains, Canada.

Remarks. *Bumastoides solangeae* is the only Hirnantian species known besides *B. beckeri*. The material from the Whittaker Formation is most similar to *B. lenzi*, but they differ in cranidial outline, librigena outline, and the absence of the axial furrow and median depression on the doublure of the former. The two species are not sister taxa in any of the MPTs, but they always occupy successive nodes at the base of the *Bumastoides* clade.

B. solangeae shares a subtriangular librigena with *B. kimmswickensis*, but this character was not coded due to the lack of well-preserved isolated librigena in most material.

'Bumastoides' tricuspidatus Edgecombe *et al.,* 2006

2006 Bumastoides tricuspidatus Edgecombe *et al.:* 375, figs 2–4.

Occurrence. Upper Ordovician (Sandbian) of the Ida Bay Limestone, Gordon Group, Ida Bay, southern Tasmania.

Remarks. *Bumastoides tricuspidatus* is a potentially important species because it is not Laurentian, and has a series of features not shared with the rest of the genus. A dicuspid doublure and subtrapezoidal to rounded subtrapezoidal pygidium are clear synapomorphies of *Bumastoides* (Fig. 5A). In contrast, *B. tricuspidatus* has a median projection on the inner margin of the doublure (tricuspid), and an elongate, subtriangular pygidium. The strongly pitted dorsal exoskeleton is also uncharacteristic of other *Bumastoides* species.

This species was excluded from our analysis because the material is very fragmentary, and many taxonomically useful features are not preserved: the lunettes, number of thoracic axial rings, cranidial median tubercle, etc. Further work (and better material) is necessary to determine the position of this species within *Bumastoides*, or if it should be the basis of a new illaenid genus entirely.

Bumastoides graffhami sp. nov.
(Figs 18, 19)

1974 *Bumastoides* cf. *B. milleri* Shaw: 20, pl. 4, figs 19, 20, 23.

Diagnosis. Axial furrow completely effaced (character 1, state 1), median tubercle on cranidium elliptical (character 3, state 2), 10 thoracic segments (character 8, state 2), undulatory terrace lines present on pygidia (Fig. 18B) (character 15, state 0).

Derivation of name. Named after Allen Graffham, who collected the holotype material (Shaw 1974, p. 17).

Material. Figured material includes one complete but damaged specimen (holotype OU 5204, Fig. 18A–D), one incomplete enrolled individual (OU 12497, Fig. 18E, G), one complete pygidium (OU 12498, Fig. 18F), one partially exfoliated cranidium (OU 12499, Fig. 19A–D), one thoracopygon (OU 12500, Fig. 19E) and one completely exfoliated cranidium (OU 12501, Fig. 19F). All figured material besides the holotype is designated here as paratypes. Unfigured material includes seven partial cranidia and three partial pygidia.

Occurrence. Upper Ordovician (Sandbian) of the lower Pooleville Member of the Bromide Formation, Arbuckle Mountains region of Oklahoma. Localities include Hwy 177, TQ and DRa.

Description. Cranidium occupies 30% of total exoskeletal length; elliptical, length 63–69% of width at palpebral lobe; inflated, longitudinal and transverse profile strongly convex, anterior part of cranidium curving downwards strongly. Anterior margin convex forwards, posterior margin convex backwards, flattened medially. Axial furrows completely effaced. Lunettes just forward of palpebral lobe, comprise 17–20% of cranidial length (exsag.), each equal to 6% of cranidial width opposite palpebral lobes, crescentic, deeply impressed adaxially then shallowing abaxially. Eyes crescentic, situated close to posterior margin, account for 21% of cranidial length in lateral view. Palpebral lobes semicircular, each equal to 17% of cranidial length and 5% of width; palpebral furrow extremely weak, defined largely by change in slope at fixigena, curved slightly inwards. Posterior branch of facial suture extends straight backwards to posterior margin (posterolateral projection absent). Anterior branches converge forward and downward along gently curved paths, joining rostral suture at a point approximately in front of lunette. Anterior margin of rostral plate transverse. Librigena subsemicircular with rounded genal angle, dorsal surface smooth except faint terrace lines near sutural margin, rounded lateral margin rounded with well-defined, tightly packed terrace lines. Widely spaced pits present on posterior half of cranidium, visible on internal moulds and exoskeleton, but absent anterior of palpebral lobes. Exoskeletal surface otherwise smooth posteriorly, slightly undulating, widely spaced terrace lines develop anterior of palpebral lobes, becoming tighter packed and more prominent towards anterior margin. Elongated posterior median tubercle present on cranidial internal mould.

Thorax of 10 segments; strongly convex (tr.), longitudinal profile nearly flat. Axial furrows weak, bowed outwards near mid-length of thorax. Axis wide, evenly arched (tr.), subrectangular, comprising 78–79% of thoracic width. Axial rings subrectangular, maintaining equal length on all 10 segments. Pleura without furrows, approximately same length (sag.) as axial rings, directed outwards and downwards (minimally fulcrate), terminations nearly transverse. Articulating facets broad, overlapping each other; subtriangular, extend almost to axial furrow, eight to 10 closely spaced chevron shaped terrace lines converge upwards. Articulating half-ring apparently long (tr.), extending laterally to axial furrow. Dorsal thoracic exoskeletal surface smooth.

Pygidium occupies 34% of total exoskeletal length; subtrapezoidal, with rounded anterior corners and well-rounded posterior margin, length equal to 63–70% of maximum width, longitudinal profile initially flat, then convex backwards towards posterior end, convex (tr.) abaxially, flat medially. Axis undifferentiated. Dorsal inner margin of pygidial doublure incompletely preserved but apparently curved backwards and dicuspid, depression present medially, transverse terrace lines mirror margin of doublure. Articulating facet subtriangular, extending upward to thoracic axial furrow, terrace lines less pronounced than on lateral margins. Four straight terrace lines follow the lateral margins, becoming fainter adaxially. Thin, undulating terrace lines extend inward and upward from lateral margins, effaced medially.

Remarks. *Bumastoides graffhami* is morphologically very similar to *B. milleri*, and they are sister taxa in all eight MPTs. Shaw (1974) did not name a new species for the Oklahoma material, and instead used open nomenclature. Our revised diagnosis restricts *B. milleri* to exoskeletons with nine thoracic segments, so a new name is needed for the Oklahoma specimens with 10 segments. *Bumastoides graffhami* also possesses an elliptical cranidial tubercle (Fig. 19F), which further distinguishes it from *B. milleri*, which has a circular tubercle. *B. graffhami* is separated from the other 10-segmented species (e.g. *B. porrectus*, *B. holei*, *B. billingsi*) in having undulatory terrace lines on the pygidium, completely effaced axial furrows, a lack of pygidial muscle scars, and the aforementioned elliptical cranidial tubercle.

Bumastoides moundensis sp. nov.
(Figs 20, 21)

Diagnosis. Median tubercle on cranidium absent (character 3, state 0), lunettes predominantly crescentic (character 4, state 0), pitting on cranidial internal mould densely distributed (character 6, state 2), 10 thoracic segments (character 8, state 2), pygidium rounded subtrapezoidal (character 12, state 1), concentric terrace lines present on pygidium (character 14, state 1), ratio of maximum pygidial length to width high (78–82%) (character 16, state 3); glabella strongly inflated, orientation of lunette and eye not parallel (Fig. 21C).

Derivation of name. After the Effna carbonate mud-mounds, in which this species is particularly abundant.

Material. Figured material includes one damaged and exfoliated, but otherwise complete individual (holotype OU 12502, Fig. 20C, D), one thoracopygon (OU 12503, Fig. 20A, B), two exfoliated cranidia (OU 12504, Fig. 20E; OU 12506, Fig. 21A, B, D), one partial pygidium (OU 12505, Fig. 20F–H) and one complete cranidium (OU 12507, Fig. 21C, E, F). All figured material other than the holotype is designated here as paratypes. Unfigured material includes a large number of partial cranidia and pygidia.

Occurrence. Upper Ordovician (lower Sandbian) of the Effna Formation, Valley and Ridge region of Virginia. Localities include Interstate 77 and Porterfield Quarry (PQ).

Description. Cranidium occupies approximately 37% of total exoskeletal length; circular, length 73–76% of width at palpebral lobe, inflated, longitudinal and transverse profile strongly convex, glabella overhanging anterior border. Anterior margin convex forwards, posterior margin convex backwards, flattened medially. Axial furrows very weak, converging gently forwards, terminating on adaxial side of lunette. Lunettes just forward of palpebral lobe, narrow (tr.), crescentic, impression abruptly shallowing abaxially, occupying 14% of cranidial length (exsag.), each lunette equal to 3–4% of cranidial width across palpebral lobes. Eyes crescentic, situated close to posterior margin, comprise 23–25% of cranidial length in lateral view. Palpebral lobes small, semicircular, each occupies 3% of cranidial width, equal to 7% of cranidial length; palpebral furrow weak, bowed inwards. Posterior branch of facial suture extends backwards and outwards behind the eye, extending to posterior margin, outlines a small triangular posterolateral projection, which sharply terminates behind eye. Anterior branches converge forward and downward on slightly curved paths, apparently terminating at rostral suture at a point in front of lunette. Rostral suture transverse, rostral plate rounded subtrapezoidal, deeply incised, terrace lines become progressively more chevron shaped ventrally. Librigena subsemicircular with rounded genal angle, dorsal surface smooth, some terrace lines developed near sutural margins, convex lateral margin with tightly packed terrace lines. Dorsal exoskeleton smooth until terrace lines develop at a point anterior of palpebral lobes, becoming progressively tighter and more pronounced towards anterior margin. Evenly spaced, uniformly sized pits present in internal moulds, apparently covering entire cranidium. Median tubercle absent.

Thorax of 10 segments; strongly convex (tr.), longitudinal profile flat. Axial furrows weak and wide, directed backwards nearly subparallel. Axis wide, subrectangular, evenly arched (tr.), comprising 74% of thoracic width. Axial rings subrectangular, transverse medially, curved slightly backwards at axial furrow, approximately equal in length (sag.). Pleura without furrows, approximately same length (sag.) as axial rings, directed outwards and downwards (minimally fulcrate), terminations nearly transverse. Articulating facets overlapping, broad, clearly defined, rounded subtriangular, extend almost to axial furrow, 10 to 12 branching terrace lines converge upwards and towards pleural margins. Thoracic dorsal exoskeletal surface smooth.

Pygidium occupies 31% of total exoskeletal length; subcircular (rounded subtrapezoidal), anterior corners and posterior margin well rounded, length equal to 78–82% of maximum width, longitudinal profile initially gently convex backwards, then strongly convex towards posterior end, gently convex (tr.). Axis undifferentiated. Anterior ventral ridge pronounced, following curvature of anterior pygidial margin. Three pronounced terrace lines directed along lateral margins, terminating before anterior margin. Four weak, widely spaced concentric terrace lines on dorsal surface mirror pygidial outline, terminating near posterior margin. Evenly distributed pits of one size are present near posterior and anterior margins on internal moulds.

Remarks. *Bumastoides moundensis* does not have a sister taxon in any of the eight MPTs. It always occupies the node immediately above the northern Canadian species (node 6 on the strict consensus, Fig. 4), and is basal to the rest of *Bumastoides*. It differs from all other species in the degree of its glabellar inflation, and the non-parallel orientation of the lunettes and eye (likely due in part to the glabellar inflation). In terms of its overall shape, *B. moundensis* is most similar to *B. tenuirugosus* because of the rounded appearance of the pygidium, wide axis, and the cephalic outline. Besides its autapomorphies, the former differs in its lack of terrace lines on the entire cranidium, the absence of the cranidial tubercle, and the crescentic lunettes.

Raymond (1925) described three species of *Bumastus* from the Effna (referred to by him as the Holston). *Bumastus dispassus* is probably best placed in *Failleana* (see Raymond 1925, pl. 7, fig. 6) because the axial furrows appear to diverge forward of the eyes, and the pygidium is elongated. *Bumastus lioderma* is known only from a damaged, partial cranidium, which is less inflated than in *Bumastoides moundensis*, and the strong, elliptical lunettes are different from the narrow, crescentic lunettes of the latter. Finally, *B. longiops* is morphologically very similar to *B. aplatus*, and based on the pygidium, almost certainly belongs to the group of species assigned here to *Stenopareia* (see *Stenopareia* remarks below).

Bumastoides kimmswickensis sp. nov.
(Figs 22, 23)

Diagnosis. Median tubercle on cranidium present (character 3, state 0), discontinuous terrace lines present on entire cranidial exoskeletal surface (character 7, state 2), nine thoracic segments (character 8; state 0), concentric terrace lines on pygidium absent (character 14, state 0), undulatory terrace lines on pygidium absent (character 15, state 1); librigena subtriangular.

Derivation of name. After the ‘Kimmswick Limestone’ as defined in pioneering studies of the Ordovician of Missouri (e.g. Bradley 1930).

Material. Figured material includes one thoracopygon (holotype OU 12508, Fig. 22H–J), three exfoliated cranidia (OU 12509, Fig. 22A–C; OU 12510, Fig. 22E–G; OU 12512, Fig. 23A–C), two nearly complete cranidia (OU 12513, Fig. 23D; OU 12514, Fig. 23E), one complete pygidium (OU 12511, Fig. 22D), one exfoliated pygidium (OU 12516, Fig. 23H) and one complete librigena (OU 12515, Fig. 23F, G). All figured material besides the holotype is designated here as paratypes. Unfigured material includes a large number of partial cranidia, pygidia, and librigena.

Occurrence. Upper Ordovician (Katian) of the lower Kimmswick Limestone, Jefferson County, Missouri, Hwy M locality.

Description. Cranidium semicircular, length 68–73% of width at palpebral lobes, inflated, longitudinal profile very convex (nearly vertical), transverse profile somewhat convex. Anterior margin convex forwards, posterior margin slightly convex backwards, flattened medially. Axial furrows very weak, converging gently forwards, terminating on adaxial side of lunette. Lunettes just forward of palpebral lobe, narrow (tr.), elliptical, impression gradually shallowing abaxially, occupying 22–25% of cranidial length (exsag.), each lunette equal to 8% of cranidial width across palpebral lobes. Eyes crescentic, situated close to posterior margin. Palpebral lobes long (sag.), semicircular, each accounts for 5% of cranidial width, equal to 19–22% of cranidial length; palpebral furrow effaced. Posterior branch of facial suture extends backwards then sharply outwards behind the eye, extending to posterior margin, outlines a triangular posterolateral projection, which sharply terminates behind eye. Anterior branches converge forward and downward on slightly curved paths, apparently terminating at rostral suture at a point in front of lunette. Librigena wide (tr.), subtriangular with rounded but slightly angulate genal angle, dorsal surface covered in widely spaced, evenly sized pits. Well-developed straight terrace lines packed tightly on rounded lateral margin of librigena, more widely spaced on doublure, undulatory terrace lines migrate inward from lateral margin towards sutural margin. Dorsal exoskeleton covered in widely spaced pits of one size, undulatory terrace lines present on entire cranidium except in a band between lunettes. Terrace lines migrating inward from lateral margins appear to deflect around lunettes, joining transverse terrace lines at posterior and anterior margins. Terrace lines generally discontinuous becoming more complete, well-incised, and transverse near anterior margin. Evenly spaced, uniformly sized pits present on internal moulds, covering entire cranidium. Posterior median tubercle circular, prominent on internal mould.

Thorax of nine segments; strongly convex (tr.), longitudinal profile flat. Axial furrows barely perceptible, only defined by very slight change in pleural angle. Axis wide, subrectangular, evenly arched (tr.). Axial rings subrectangular, transverse medially, curved slightly backwards at axial furrow, approximately equal in length (sag.). Pleura without furrows, approximately same length (sag.) as axial rings, directed outwards and downwards, slightly backwards (minimally fulcrate), terminations incomplete. Articulating facets incomplete, but dorsal extent is well below axial furrow, eight to nine terrace lines converge upwards. Thoracic dorsal exoskeletal surface smooth.

Pygidium subtrapezoidal, anterior corners and posterior margin well rounded, posterior corners sharp, length equal to 69–72% of maximum width, longitudinal profile initially gently convex backwards, then strongly convex towards posterior end, gently convex (tr.). Axis undifferentiated. One terrace ridge present along lateral margins, terminating before anterior margin, otherwise dorsal exoskeleton completely smooth. Articulating facet subtriangular, extending to just below axial furrow, six terrace lines converge upwards, border prominent. Inner margin of doublure discuspid, anteriormost ridge follows path of inner margin, terrace lines slightly undulatory and transverse, medial depression wider anteriorly, narrows posteriorly, terminating just before posterior margin.

Remarks. *Bumastoides kimmswickensis* differs from other species found in the Kimmswick Limestone (*B. billingsi*, *B. holei*) in having one fewer thoracic segment, terrace lines covering the majority of the cranidium, and in the shape of the librigena. In all eight MPTs *B. kimmswickensis* is the sister taxon of *B. beckeri* from the Maquoketa Formation of Iowa, united by their shared possession of terrace lines covering the cranidium. The details of the terrace lines are slightly different however, as *B. beckeri* retains transverse terrace lines between the lunettes, whereas in *B. kimmswickensis* they are very faint. The latter also has one fewer thoracic segment, a smoother pygidial exoskeleton, and generally more discontinuous terrace lines.

The smallest individuals of *B. kimmswickensis* (Figs 22E–G, 23D, E) illustrate the range of morphological change in illaenid trilobites during holaspid ontogeny (Chatterton 1980; Ludvigsen & Chatterton 1980) observed in *Bumastoides* by Westrop & Ludvigsen (1983). In early holaspids, the lunettes are slightly narrower, the axial furrows are deeper, the terrace lines are stronger, and the glabella is less inflated. These changes are clear when viewing progressively larger specimens: Figs 22A–C, × 2.8; 23A–C, × 4; 22E–G, × 5; 23D, × 6; 23E, × 8. An ontogenetic interpretation of this variation is supported by the presence of only a single pygidium type (e.g. Fig. 22D) associated with *B. kimmswickensis* cranidia. As noted by Chatterton & Ludvigsen (2004), conservatism should be used when delineating new species of illaenids that change dramatically during holaspid ontogeny. In *Stenopareia grandis*, they found smaller individuals had stronger terrace lines, a more forward genal angle, and a rounder pygidium. In agreement with Chatterton & Ludvigsen (2004), we found no larger specimens with similar morphology to the smaller individuals, and conclude that there is allometric shape change from early to late holaspids in this material. This issue is further complicated by the inability of FMC to detect discrete states in continuous shape changes in *Bumastoides*. Extreme caution should be used by workers attempting to identify new species of *Bumastoides* based on limited samples, minor differences in shape, or only with early holaspid material.

***Bumastoides* cf. *milleri* (Billings, 1859)**
(Figs 24, 25)

Material. Figured material includes one mostly testate cranidium (OU 12521, Fig. 25A, B), three exfoliated cranidia (OU 12517, Fig. 24A; OU 12037, Fig. 24B–D; OU 12518, Fig. 24F) and four pygidia in different stages of exfoliation (OU 12039, Fig. 24G; OU 12519, Fig. 24E; OU 12520, Fig. 24H; OU 12522, Fig. 25C–E). Unfigured material includes a large number of partial pygidia and cranidia.

Occurrence. Upper Ordovician (Katian) of the Viola Springs Formation (Viola Group), Highway 99 section, near Fittstown, south-central Oklahoma (see Amati & Westrop 2006, figs 3, 7).

Remarks. The Viola Springs material is nearly identical to *Bumastoides milleri* material from the Trenton. The pygidium is relatively short (sag.) and wide (tr.) with sharp posterior corners, the medial cranidial tubercle is circular and prominent, and the general shape of the cranidia is similar. Even given these similarities, we think it best to use open nomenclature on this material until a complete exoskeleton is discovered because the number of thoracic segments is also an important diagnostic character of *Bumastoides* species.

Genus ***Stenopareia*** Holm, 1886

Remarks. Chatterton & Ludvigsen (1976) and Westrop & Ludvigsen (1983) both agreed that *Stenopareia aplatus* and *S. gardensis* should be moved out of *Bumastoides* based on the transverse anterior margin (semicircular) of the pygidium, and possibly the depth of the axial furrow. The results of our analysis support these claims, and also apply to *S. rivulus* (*S. globosus* had been revised previously by Westrop & Ludvigsen 1983). In *Bumastoides* the cranidial axial furrow is weakly incised and the glabella is not expressed by a change in slope of the glabella (in mature holaspids), whereas the opposite is true of *Stenopareia*. The latter also has a semicircular outline of the pygidium (character 12) and shorter length of the pygidial doublure (character 19). *Stenopareia* species also always retain residual expression of the pygidial axis (character 17), though in *Bumastoides*, some species (*B. billingsi*) still show some minor expression of axial furrow on the pygidium. So this character should be useful in diagnosing species of *Stenopariea*, but is of limited use in *Bumastoides*. The number of cusps on the inner margin of the pygidial doublure (character 10) is useful as a diagnostic character of *Bumastoides* (if *B. tricuspidatus* Edgecombe *et al.* 2006 is excluded from the genus) as all species with complete material are dicuspid, but is not likely to be useful in distinguishing between the two genera. The number of cusps is highly variable within *Stenopareia*, with anywhere from zero to two cusps claimed (e.g. compare *S. linnarssoni*, Jaanusson 1954, fig. 10F with *S. avus*, Jaanusson 1954, fig. 10E.). As shown by Bruton & Owen (1988, p. 252), the original description of the *S. linnarssoni* doublure in Warburg (1925) was incorrect, and it does have a single cusp. We think it is more likely these issues indicate the need for a systematic revision of *Stenopareia*, rather than demonstrating a wide variety of doublure morphologies within the genus.

Diagnoses are not provided for the species transferred provisionally to *Stenopareia* as this is best done in a revision of *Stenopareia* that includes all nominal species. Curtis & Lane (1997) provided the most recent diagnosis of *Stenopareia*, but it is so vague that it does not exclude other species of Illaenidae: "cephalon strongly convex longitudinally, pygidium smaller and flatter. Cranidial axial furrow shallow, only present behind shallow lateral muscle impression. Eyes small, and placed far back. Hypostome subquadrate with small triangular anterior wings. Thorax with 9 segments. Anterior sagittal margin of pygidial doublure modified, usually into cusps. Exoskeletal surface with terrace ridges; doublural surfaces with prominent terrace ridges". This work provides criteria to distinguish between *Bumastoides* and *Stenopareia*, but the latter is still in need of a detailed revision.

'Stenopareia' aplatus (Raymond, 1925)
(Fig. 26C–F)

1925 *Bumastus aplatus* Raymond: 119, pl. 8, figs 3, 4.
1968 *Bumastoides aplatus* (Raymond); Shaw: 43, pl. 16, fig. 19, pl. 17, figs 1–14.

Material. Figured material include one cranidium without librigena (holotype MCZ 101150, Fig. 26C, E, F) and one complete pygidium (paratype MCZ 101151, Fig. 26D).

Occurrence. Middle Ordovician (Darriwilian) of the Day Point and Crown Point Formations (Chazy Group), Isle La Motte, Vermont, Champlain Valley of New York, and the lower Lenoir Limestone, Bluff City, Tennessee.

Remarks. Whittington (1954) questioned the placement of *Stenopareia aplatus* in *Bumastoides* based on the transverse anterior margin. Shaw (1968) stated that this assignment was fairly certain based on its flattened axis and pygidium, and smooth exoskeleton. We now know that many species of *Bumastoides* have highly sculptured surfaces, and that axial furrow of *S. aplatus* is incised much deeper than in species of *Bumastoides*.

'Stenopareia' gardensis (Shaw, 1968)
(Fig. 26G–J)

1968 *Bumastoides gardensis* Shaw: 44, pl. 16, figs 12–18.

Material. Figured material includes one exfoliated cranidium (holotype NYSM 12456, Fig. 26G, J) and one complete pygidium (paratype NYSM 12457, Fig. 26H, I).

Occurrence. Middle Ordovician (Darriwilian) of the Day Point Formation (Chazy Group), Isle La Motte, Vermont, Chazy and Valcour Island, New York.

Remarks. Shaw (1968) noted that the cranidium of *Stenopareia gardensis* was similar to *S. aplatus*. He also stated that the pygidial features (raised axis, low length to width ratio), besides the doublure, were more similar to *Nanillaenus* Jaanusson, 1954. Amati & Westrop (2004) synonymized *Thaleops* and *Nanillaenus* based on the presence of a long, high angle pygidial articulating facet. The facet of *S. gardensis* is not at a high enough angle to be placed in *Thaleops* as defined by Amati & Westrop (2004). Further, the cranidial morphology precludes the possibility that this material belongs to other *Thaleops* species in the Day Point Formation (*T. punctatus*, Raymond, 1905; *T. raymondi*, Shaw, 1968). We think these issues should be explored more, but provisionally place *S. gardensis* in *Stenopareia* as was suggested by Chatterton & Ludvigsen (1976) and Westrop & Ludvigsen (1983).

'*Stenopareia*' *rivulus* (Ingham & Tripp, 1991)
(Fig. 26A, B)

1991 *Bumastoides rivulus* Ingham & Tripp: 42, fig. 10a–f.

Material. Figured material includes a damaged, exfoliated cranidium (holotype GLAHM A8302, Fig. 26B) and an exfoliated pygidium (paratype GLAHM A8313, Fig. 26A).

Occurrence. Upper Ordovician (Sandbian) of the Jubilation Member, Doularg Formation, (Albany Group), Girvan district, south-west Scotland.

Remarks. Ingham & Tripp (1991) were uncertain regarding their placement of *S. rivulus* in *Bumastoides*, and that hesitation seems correct, as both the pygidium and cranidium of this species more strongly resemble *Stenopareia*, and it was resolved outside the *Bumastoides* clade in all of the MPTs. The pygidium of *B. scoticus* (GLAHM A5860a, Tripp 1965, fig. 31a) is semicircular, with a narrow (sag.) doublure, strongly resembling *S. rivulus*. This species should also be placed in *Stenopareia sensu lato.*

Acknowledgements

This research was funded by NSF grant EAR-0819715 to S. Westrop and L. Amati. A. Thomas, K. Carlucci and R. Burkhalter assisted in fieldwork, and R. Burkhalter provided technical support in the lab. F. Read provided helpful locality information in Virginia. Loans of type material were arranged by P. Mayer at the Field Museum, Ed Landing at the New York State Museum, Neil Clark at the Hunterian Museum, Tiffany Adrain at the University of Iowa, Jessica Cundiff at the Museum of Comparative Zoology, Albert Kollar at the Carnegie Museum, and Jean Dougherty at the Geological Survey of Canada. Thanks to Alan Owen and an anonymous reviewer for their insightful comments that greatly improved the manuscript.

References

Akaike, H. 1974. A new look at the statistical model identification. *Automatic Control, IEEE Transactions*, **19**, 716–723.

Amati, L. & **Westrop, S. R.** 2004. A systematic revision of *Thaleops* (Trilobita: Illaenidae) with new species from the middle and late Ordovician of Oklahoma and New York. *Journal of Systematic Palaeontology*, **2**, 207–256.

Amati, L. & **Westrop, S. R.** 2006. Sedimentary facies and trilobite biofacies along an Ordovician shelf to basin gradient, Viola Group, South-Central Oklahoma. *Palaios*, **21**, 516–529.

Amsden, T. W. & **Sweet, W. C.** 1983. Upper Bromide Formation and Viola Group (Middle and Upper Ordovician) in Eastern Oklahoma. *Oklahoma Geological Survey Bulletin*, **132**, 1–76.

Billings, E. 1859. Descriptions of some new species of trilobites from the Lower and Middle Silurian rocks of Canada. *Canadian Naturalist & Geologist*, **4**, 367–383.

Bradley, J. H. 1925. Stratigraphy of the Kimmswick Limestone of Missouri and Illinois. *Journal of Geology*, **33**, 49–74.

Bradley, J. H. 1930. Fauna of the Kimmswick Limestone of Missouri and Illinois. *Walker Museum, University of Chicago Contributions*, **2**, 219–290.

Bremer, K. 1994. Branch support and tree stability. *Cladistics*, **10**, 295–304.

Brett, C. E., **Whiteley, T. E.**, **Allison, P. A.** & **Yochelson, E.** 1999. The Walcott-Rust Quarry: a Middle Ordovician Konservat-Lagerstatten. *Journal of Paleontology*, **73**, 288–305.

Bruton, D. L. & **Owen, A. W.** 1988. The Norwegian Upper Ordovician illaenid trilobites. *Norsk Geologisk Tidsskrift*, **68**, 241–258.

Carlucci, J. R., **Westrop, S.** & **Amati, L.** 2010. Tetralichine trilobites from the Upper Ordovician of Oklahoma and Virginia, and phylogenetic systematics of the Tetralichini. *Journal of Paleontology*, **84**, 1099–1120.

Chatterton, B. D. E. 1980. Ontogenetic studies of Middle Ordovician trilobites from the Esbataottine Formation, Mackenzie Mountains, Canada. *Palaeontographica, Abteilungen A*, **171**, 1–74.

Chatterton, B. D. E. & **Ludvigsen, R.** 1976. Silicified Middle Ordovician trilobites from the South Nahanni River area, District of Mackenzie, Canada. *Palaeontographica*, **154**, 1–106.

Chatterton, B. D. E. & **Ludvigsen, R.** 2004. Early Silurian trilobites of Anticosti Island, Quebec, Canada. *Palaeontographica Canadiana*, **22**, 1–264.

Clarke, J. M. 1897. The Lower Silurian trilobites of Minnesota. *Minnesota Geology and Natural History Survey*, **3**, 694–759.

Cooper, B. N. & **Cooper, G. A.** 1946. Lower Middle Ordovician stratigraphy of the Shenandoah Valley, Virginia. *Bulletin of the Geological Society of America*, **57**, 35–114.

Cooper, G. A. 1956. Early Middle Ordovician of the United States. Pp. 171–194 in M. G. Bassett (ed.) *The Ordovician System*. University of Wales Press and National Museum of Wales, Cardiff.

Curtis, N. J. & **Lane, P. D.** 1997. The Llandovery trilobites of England and Wales, Part 1. *Monographs of the Palaeontographical Society*, **605**, 1–50.

DeMott, L. L. 1987. Platteville and Decorah trilobites from Illinois and Wisconsin. Pp. 63–98 in R. E. Sloan, F. C. Shaw & R. P. Tripp (eds) *Minnesota Geological Survey, Report of Investigations*, 35, 63–98.

DeQueiroz, K. 2007. Toward an integrated system of clade names. *Systematic Biology*, **56**, 956–974.

DeQueiroz, K. & **Gauthier, J.** 1990. Phylogeny as a central principle in taxonomy: phylogenetic definitions of taxon names. *Systematic Zoology*, **39**, 307–322.

Edgecombe, G. D., **Banks, M. R.** & **Banks, D. M.** 2006. *Bumastoides* (Trilobita: Illaenidae) from the Upper Ordovician of Tasmania. *Memoirs of the Association of Australasian Palaeontologists*, **32**, 375–381.

Emmons, E. 1842. *Geology of New York part II, comprising the survey of the second geological district*. W & A White & J. Visscher, Albany, 437 pp.

Fay, R. O., **Graffham, A. A.** & **Sprinkle, J.** 1982. Appendix: measured sections and collecting localities. Pp. 335–369 in J. Sprinkle (ed.) *Echinoderm faunas from the Bromide Formation (Middle Ordovician) of Oklahoma*. University of Kansas Paleontological Contributions Monograph.

Fisher, D. W. 1957. Mohawkian (Middle Ordovician) biostratigraphy of the Wells outlier, Hamilton County, New York. *New York State Museum Bulletin*, **359**, 1–33.

Foerste, A. F. 1920. The Kimmswick and Plattin Limestones of northeastern Missouri. *Denison University Bulletin, Journal of Scientific Laboratories*, **19**, 175–224.

Goloboff, P. 1993. Estimating character weights during tree search. *Cladistics*, **9**, 83–91.

Goloboff, P. A., **Farris, J. S.**, **Kallersjo, M.**, **Oxelman, B.**, **Ramirez, M. J.** & **Szumik, C. A.** 2005. Improvements to resampling measures of group support. *Cladistics*, **19**, 324–332.

Goloboff, P. A., **Mattoni, C. I.** & **Quinteros, A. S.** 2006. Continuous characters analyzed as such. *Cladistics*, **22**, 589–601.

Goloboff, P., **Farris, J.** & **Nixon, K.** 2008. TNT, a free program for phylogenetic analysis. *Cladistics*, **24**, 774–786.

Harris, R. W. 1957. Ostracoda of the Simpson Group. *Oklahoma Geological Survey Bulletin*, **75**, 1–333.

Hawle, I. & **Corda, A. J. C.** 1847. *Prodrom einer monographie der bohmischen Trilobiten. Abhandlungen Koeniglichen Boehmischen Gesellschaft der Wissenschaften*. J. G. Clave, Prague, 176 pp.

Holm, G. 1882. De Svenska artena af Trilobitslägtet *Illaenus* (Dalman). *Bihang till Konglungen Svenska Vetenskaps-Akademiens Handlingar*, **7**, 1–148.

Holm, G. 1886. Revision der ostbalischen silurschen Trilobiten, Abt. III, Illaeniden. *Mémoires de Impériale des Sciences de St Pétersbourg*, **33**(8), 1–173.

Hunda, B. R., **Chatterton, B. D. E.** & **Ludvigsen, R.** 2003. Silicified Late Ordovician trilobites from the Mackenzie Mountans Northwest Territories, Canada. *Palaeontographica Canadiana*, **21**, 1–87.

Ingham, J. K. & **Tripp, R. P.** 1991. The trilobite fauna of the Middle Ordovician Doularg Formation of the Girvan District, Scotland, and its paleoenvironmental significance. *Transactions of the Royal Society of Edinburgh: Earth Sciences*, **82**, 27–54.

Jaanusson, V. 1954. Zur Morphologie und Taxonomie der Illaeniden. *Arkiv För Mineralogie Och Geologi*, **1**, 545–583.

Jaanusson, V. 1959. Suborder Illaenina, Pp. O365–O415 in R. C. Moore (ed.) *Treatise on Invertebrate Paleontology, Part O, Arthropoda I*. Geological Society of America and University of Kansas Press, Lawrence.

King, D. T. 1986. Waulsortian-type buildups and resedimented (carbonate-turbidite) facies, early Mississippian Burlington shelf, central Missouri. *Journal of Sedimentary Petrology*, **56**, 471–479.

Kobayashi, T. 1935. The Cambro-Ordovician formations and faunas of South Chosen. Palaeontology Part III. Cambrian faunas of South Chosen with special study on the Cambrian trilobite genera and families. *Journal of the Faculty of Science, Imperial University of Tokyo*, **4**, 49–344.

Kolata, D. R., **Huff, W. D.** & **Bergström, S.M.** 1998. Nature and regional significance of unconformities associated with the Middle Ordovician Hagan K-bentonite complex in the North American midcontinent. *Geological Society of America Bulletin*, **110**, 723–739.

Longman, M. W. 1982a. Depositional setting and regional characteristics. Pp. 6–10 in J. Sprinkle (ed.) *Echinoderm Faunas from the Bromide Formation (Middle Ordovician) of Oklahoma*. The University of Kansas Paleontological Contributions, Monograph 1, Lawrence, Kansas.

Longman, M. W. 1982b. Depositional environments. Pp. 17–30 in J. Sprinkle (ed.) *Echinoderm Faunas from the Bromide Formation (Middle Ordovician) of Oklahoma*. University of Kansas Paleontological Contributions, Monograph 1, Lawrence, Kansas.

Ludvigsen, R. 1979. *Fossils of Ontario part 1: The trilobites*. Royal Ontario Museum Life Sciences Miscellaneous Publications, Toronto, 96 pp.

Ludvigsen, R. & **Chatterton, B. D. E.** 1980. The ontogeny of *Failleana* and the origin of the Bumastinae (Trilobita). *Geological Magazine*, **117**, 471–478.

Maddison, D. & **Maddison, W.** 2005. *MacClade: Analysis of Phylogeny and Character Evolution 4.08*. Sinauer Associates Inc., Sunderland.

Murchison, R. I. 1839. *The Silurian System*. John Murray, London, 768 pp.

Raymond, P. E. 1905. Trilobites of the Chazy Limestone. *Annals of the Carnegie Museum*, **3**, 328–396.

Raymond, P. E. 1913. Notes on some new and old trilobites in the Victoria memorial Museum. *Bulletin of the Victoria Memorial Museum, Geological Survey of Canada*, **1**, 33–39.

Raymond, P. E. 1916. New and old Silurian trilobites from southeastern Wisconsin, with notes on the genera of the Illaenidae. *Harvard College Museum of Comparative Zoology Bulletin*, **60**(1), 1–41.

Raymond, P. E. 1925. Some trilobites of the lower Middle Ordovician of eastern North America. *Bulletin of the Museum of Comparative Zoology*, **67**, 1–180.

Raymond, P. E. & **Narraway, J. E.** 1908. Notes on Ordovician trilobites: Illaenidae from the Black River Limestone near Ottawa, Canada. *Annals of the Carnegie Museum*, **4**, 242–255.

Read, J. F. 1982. Geometry, facies, and development of Middle Ordovician carbonate buildups, Virginia Appalachians. *AAPG Bulletin*, **66**, 189–209.

Read, J. F. 1998. Phanerozoic carbonate ramps from greenhouse, transitional and ice-house worlds: clues from field and modeling studies. Pp. 107–135 in V. P. Wright & T. P. Burchette (eds) *Carbonate Ramps*. Geological Society of London Special Publications, 149.

Ruppel, S. & **Walker, K.** 1977. The ecostratigraphy of the Middle Ordovician of the Southern Appalachians (Kentucky, Tennessee, and Virginia), U.S.A: A field excursion. *Studies in Geology, University of Tennessee Department of Geological Sciences*, **77–1**, 1–171.

Sabol, J. W. 1958. *Geology of the Porterfield Quarry area, Smyth County, Virginia*. Virginia Polytechnic Institute, Blacksburg, 81 pp.

Shaw, F. C. 1968. Early Middle Ordovician Chazy trilobites of New York. *New York State Museum and Science Services Memoir*, **17**, 1–163.

Shaw, F. 1974. Simpson Group (Middle Ordovician) Trilobites of Oklahoma. *Journal of Paleontology Memoir*, **48**(6), 1–54.

Sheets, H. D. 2003. FMCBox-Finite Mixture Coding of continuous morphological characters [updated at http://www3.canisius.edu/∼sheets/moremorph.html] last accessed March 2nd 2011.

Slocom, A. W. 1913. New trilobites from the Maquoketa beds of Fayette County, Iowa. *Field Museum of Natural History Geological Series*, **4**, 43–83.

Strait, D., **Moniz, M.** & **Strait, P.** 1996. Finite Mixture Coding: A new approach to coding continuous characters. *Systematic Biology*, **45**, 67–78.

Strong, E. E. & **Lipscomb, D.** 1999. Character coding and inapplicable data. *Cladistics*, **15**, 363–371.

Swofford, D. L. 2002. PAUP* Phylogentic Analysis Using Parsimony (*and other methods) *Version 4.0b10*. Sinauer Associates, Sunderland.

Templeton, J. S. & **Willman, H. R.** 1963. Champlainian Series (Middle Ordovician) in Illinois. *Illinois State Geological Survey Bulletin*, **89**, 1–259.

Tripp, R. P. 1965. Trilobites from the Albany Division (Ordovician) of the Girvan District, Ayrshire. *Palaeontology*, **8**, 577–603.

Tripp, R. P. 1980. Trilobites from the Ordovician Ardwell Group of the Craighead Inlier, Girvan district, Scotland. *Transactions of the Royal Society of Edinburgh: Earth Sciences*, **71**, 147–157.

Troedsson, G. T. 1928. On the Middle and Upper Ordovician faunas of northern Greenland, part II. *Meddelelser om Grønland*, **72**, 1–198.

Ulrich, E. O. 1911. Revision of the Paleozoic systems. *Geological Society of America Bulletin*, **22**, 281–680.

Walch, J. E. I. 1771. *Die Naturgeschichte der Versteinerungen, Dritter Theil. Zur Erläuterung der Knorrischen Sammlung von Merkwürdigkeiten der Natur*. P. J. FelBecker, Nürnberg, 235 pp.

Walcott, C. D. 1877. Descriptions of new species of fossils from the Chazy and Trenton Limestones. *Annual Report New York State Museum of Natural History*, **31**, 68–71.

Walter, O. T. 1927. Trilobites of Iowa and some related Paleozoic forms. *Iowa Geological Survey Annual Reports 1923 and 1924*, **31**, 1–388.

Warburg, E. 1925. The trilobites of the Leptaena Limestone in Dalarne. *Bulletin of the Geologic Institute of the University of Upsala*, **27**, 1–446.

Westrop, S. R. & **Ludvigsen, R.** 1983. Systematics and paleoecology of Upper Ordovician trilobites from the Selkirk Member of the Red River Formation, Southern Manitoba. *Manitoba Department of Energy and Mines Geological Report*, **GR 82-2**, 1–51.

Whiteley, T., **Kloc, G.** & **Brett, C.** 2002. *Trilobites of New York*. Cornell University Press, Ithaca and London, 203 pp.

Whittington, H. B. 1954. Ordovician trilobites from Stilliman's Fossil Mount. *Geological Society of America Memoir*, **62**, 119–149.

Whittington, H. B. 1997a. Illaenidae (Trilobita): Morphology of thorax, classification, and mode of life. *Journal of Paleontology*, **71**, 878–896.

Whittington, H. B. 1997b. Morphology of the exoskeleton. Pp. 1–86 in R. L. Kaesler (ed.) *Treatise on Invertebrate Paleontology, Part O, Arthropoda 1. Trilobita (revised). Volume 1. Introduction, Order Agnostida, Order Redlichiida*. Geological Society of America and University of Kansas, Lawrence.

Wilson, A. E. 1947. Trilobita of the Ottawa Formation of the Ottawa-St. Lawrence lowland. *Canada Department of Mines and Resources, Geological Survey Bulletin*, **9**, 1–86.